97 p.

[redacted]

[redacted]

CR-52376

[redacted]

GDD

GENERAL DYNAMICS
ASTRONAUTICS

[redacted]

A2136-1 (REV. 6-61)

(NASA CR ---) AE63-0078) OTS: $

Space Science Laboratory

CATALYSIS OF HYDROGEN ATOM RECOMBINATION

Final Report

12 February 1963

(NASA Contract NAS8-2534)

Prepared by B F Myers for H. Girouard,

Approved by J. T. Neu
Senior Staff Scientist

F. M. Graber, and

B F Myers
B. F. Myers 12 Feb. 1963 rejs

Prepared for Lewis Research Center, Cleveland, Ohio by Space Science Laboratory, General Dynamics/Astronautics, San Diego, California

3517604

Space Science Lab.

INDEX

SUMMARY

13061

Support has been obtained for the concept that potent catalysts can be developed for use in arc jet propulsion units; this leads to an expected increase in the propellant specific impulse in such units.

About twenty materials have been tested for their effectiveness in catalyzing the recombination of hydrogen atoms. The experiments have been conducted generally over the temperature range 300-570°K and at pressures of 0.2 to 1.0 mm Hg. For ten materials which underwent an overall, rapid, second order reaction with hydrogen atoms, evidence for catalytic activity has been found. This evidence was obtained by measuring the rate of hydrogen atom disappearance, determining the number of cycles of atom recombination in which each catalyst molecule was involved and from observation of the pressure independence of rate constants. It is a deduction from experiment that potent activity is demonstrated at temperatures greater than 500°K.

Activation energies, pre-exponential and steric factors have been obtained for the rapid overall reactions of hydrogen atoms with ethylene, allene, 1,3-butadiene, benzene, cis-butene-2, acetylene, propylene and vinyl chloride. Extrapolation of the data indicates that one mole percent of the better catalysts can increase the homogeneous rate of atom recombination by five orders of magnitude over the three body hydrogen atom recombination rate.

Particular attention was given to the contribution of surface phenomena; the assumption of a Langmuir type sorption isotherm was consistent with the experimental data and permitted the gas phase and surface reactions to be distinguished.

It is recommended that extension of the work reported here be directed toward developing high temperature means of atom detection and performing detailed product analyses on reaction flow systems. An arc jet heater and nozzle apparatus would also offer considerable advantage in high temperature work.

AUTHOR

I. Introduction

A. Motivation

The performance of supersonic expansion nozzles that depends upon exothermic reactions in the propellant stream usually involves termolecular reactions between simple chemical species. Such termolecular reaction rates are orders of magnitude smaller than bimolecular reaction rates. The homogeneous catalysis of termolecular reactions by foreign gaseous material is an important consideration in chemical, heat transfer nuclear, and electrothermal arc jet propulsion devices that has not yet been adequately investigated.

The performance potential of hydrogen propellant according to thermodynamic considerations is plotted in Figure 1. The solid line represents the performance if chemical equilibrium is maintained when the propellant expands while the dashed lines refer to expansion with composition fixed at the equilibrium condition in the heater (frozen flow). The performance increment is due to hydrogen molecule dissociation in the heater and atom recombination in the nozzle. It increases with decreasing heater pressure until complete dissociation of hydrogen occurs in the heater. If recombination of atoms does not take place in the nozzle, the propellant specific impulse is only a little higher than in the absence of dissociation-recombination phenomena at higher pressure. (See Fig. 1). Therefore, if frozen flow were allowed in the nozzle, a substantially greater quantity of energy and weight of energy source would be required to produce the same performance as obtained with chemical equilibrium flow.

The reacting hydrogen propellant phenomena could be used to obtain a relatively high propellant specific impulse for a given heater temperature. The development required to attain this potential advantage lies in two areas: (1) the design of optimum nozzle contours and (2) the catalysis of hydrogen atom recombination. The second phase of the work was supported by contract NAS 8-2534. However, some nozzle results will be presented here in order to indicate the performance gain that could be attained with catalysts.

The nozzle concept represented in Figure 2 must be understood before the results on catalytic propellants become meaningful. The chemical energy is largely released in the upstream portion of the nozzle. This chemical energy release results in a substantial reduction of the rate of temperature decrease in the nozzle compared to the frozen flow case. In the first portion of the nozzle where conversion of chemical energy is feasible, the extent of hydrogen atom recombination is increased by a larger reaction rate due to catalysis and by the optimum nozzle contour. The chemical energy thereby released maintains a high propellant temperature; the resulting sensible enthalpy must be converted to jet kinetic energy in the second portion of the nozzle. The sensible enthalpy associated with a 15000°K rise in temperature for hydrogen is approximately equivalent to the energy released on recombination of hydrogen atoms per mole. In the case of electrothermal arc jet propulsion devices, the fraction of energy loss due to heat transfer to the nozzle walls tends to be high, and therefore the sensible energy in frozen flow systems is extensively dissipated in a relatively small nozzle. Chemical energy release could markedly increase the nozzle discharge velocity.

The achievable specific impulse with the reacting propellant is a subject for future studies. However, the amount of chemical recombination in a given nozzle length is indicated in Table I. The calculations are based on a one dimensional invicid adiabatic expansion of dissociated hydrogen in a given conical nozzle geometry. These assumptions would not be expected to reduce the calculated amount of chemical conversion in the nozzle. The results show that very little recombination takes place in the absence of a catalyst. However, an optimum effect for a catalyst present in about one percent concentration is predicted to lead to 0.38 pound of atom recombination per pound of propellant in a nozzle that is 8 cm long. The amount of energy associated with this conversion is equivalent to a sensible enthalpy change resulting from a 5700°K rise per mole of hydrogen.

For a fair catalyst, the conversion is approximately one quarter of that for the optimum catalyst; the rate constant for the latter is two orders of magnitude greater than that of the former. However, the use of an expansion ratio of about 30 at the 8 cm point with the fair catalyst would result in a 0.18 pound of atom recombination; this is about twice as large as the conversion obtained by using the fair catalyst under the nozzle conditions specified in Table I. The amount of recombination in the absence of catalyst is very small in the two nozzle geometries.

B. Previous Work

The above results show that hydrogen atom catalytic effects can substantially contribute toward electrothermal arc jet propulsion performance. The basic chemical kinetic information that was available prior to this investigation was scanty. Only a few materials had been studied under a very limited range of conditions. The reasons for the void on hydrogen atom recombination technology were the experimental difficulties and lack of incentive to perform the studies.

The homogeneous catalysis of hydrogen atom recombination has been reported by a few authors (Refs. 1-5). It was found that the recombination of hydrogen atoms could be catalysed with a small concentration of acetylene with only relatively small quantities of hydrogenated products being formed. The recombination of hydrogen atoms was found to be proportional to the first power of the concentrations of hydrogen atoms and of acetylene molecules. The data obtained did not establish the mechanism for the increased rate of hydrogen atom recombination, but the following reaction path was suggested:

$$H + C_2H_2 \rightleftharpoons C_2H_3 \qquad (R1)$$

$$H + C_2H_3 \rightarrow H_2 + C_2H_2 \qquad (R2)$$

The acetylene interacts with the hydrogen atoms to form a sequence of bimolecular collisions which are, according to Figure 3, orders of magnitude more frequent than the termolecular. The ultimate catalytic

effect would be roughly the difference between the two collision frequencies multiplied by the ratio of the catalyst to hydrogen atoms. The ultimate catalyst effect was not achieved with acetylene, and the factors affecting the catalyst efficiency were not identified.

The catalysis of O, I, and N atom recombinations were studied more extensively (Refs. 6-14) but the information on potent catalyst effects is not significantly more advanced than in the case of H-atoms.

Non-equilibrium nozzle flow has been studied by a number of investigators. A recent study (Ref. 20) has been performed that assumes an initial equilibrium distribution of species involved in a carbon-hydrogen system followed by a non-equilibrium expansion of the system. Various numbers of chemical species, chemical reaction models and orders of magnitude of reaction rate constant data were assumed. The study clearly indicated the need for experimental reaction rate data for the species considered. However, it is possible in principle to design a catalyst injection system that will introduce a non-equilibrium system of catalyst before nozzle expansion. Therefore, the scope of an experimental program on catalysis should be restricted to the species considered in the report.

The optimum amount of catalyst that should be added largely depends upon the molecular weight of the material. An increase in catalyst concentration from one-hundredth to one-tenth mole percent could increase the rate of atom recombination by ten-fold, but the molecular weight of the propellant would normally be increased by only a slight amount. However, at one mole percent catalyst concentration for a material having a molecular weight of 16, the molecular weight of the propellant would increase by 7% while a ten mole percent concentration would increase the propellant molecular weight by 70%. Clearly it is important to maintain a catalyst concentration in the range below one mole percent.

C. Scope of the Current Work

For the catalysis of hydrogen atom recombination in the electro-thermal arc jet propulsion units, the discovery of catalysts and of the degree to which they simulate an ultimate catalyst are major concerns. In this study, the gross determination of potent catalysts was stressed; the problems of the activity and stability of catalysts at very high temperature were not included. It should be noted that catalytic action is required downstream from the throat where the temperature is considerably lower than in the heater section. Calculated downstream nozzle temperatures are shown in Table I. In practice, the temperature would be even lower because of heat transfer loss. Also, the behavior of a catalyst species, which is stable to very high temperatures, could be reasonably predicted from the results of the present program. Continuation of this program, however, would require a detailed study of the chemistry involved in catalyst activity and decomposition at very high temperatures in order to develop the reacting hydrogen propellant.

There are several requirements which a material must satisfy in order to be considered an ideal catalyst. In the first place, it must remain chemically unaltered after the recombination of the two hydrogen atoms in which it participated. In this way, the material can be involved in many recombinations while present in small quantity. Secondly, it must take part in a bimolecular process with hydrogen atoms thus providing a large increase in the frequency of potentially effective collisions as demonstrated in Figure 3. Finally, the overall reaction must be very fast indicating that a large number of the collisions were effective.

In the present work, emphasis was placed on the detection of rapid, second order reactions resulting from the addition of potential catalysts to a flow system. These experiments were carried out over a range of temperatures which permitted the evaluation of factors necessary to establish a general relation between the reaction rate constant and the temperature. These factors, the temperature independent preexponential factor A and the activation energy E, are related to the rate constant by the expression

$$k_c = AT^{1/2} e^{-E/RT} \qquad (1)$$

This relationship may be used to estimate the rate constant at temperatures outside the range of measurement for elementary reactions and for more complex systems when certain restrictions are recognized.

If the catalyst is involved in many cycles of recombination, then the ratio of hydrogen atoms disappearing to catalyst molecules added would be quite large. The ratio should clearly exceed that expected on the basis of any reaction mechanism which required only the consumption of reactants. Consequently, the fate of the potential catalyst may be followed by determining this ratio. This method has been used in the present work since the required data can be obtained from the experimental procedure outlined below.

D. Outline of the Report

Following a description of the experimental aspects, there is a general section on procedures and results. The details of these topics have been relegated to the appendix. After the sections containing the discussion and conclusions, several recommendations for further work are set forth. Some of these could have been concurrently followed but they were avoided through a strict adherence to the work statement of the contract.

II. Experimental

The experiments were conducted in the system sketched in Figure 4. It consisted of a pyrex flow tube, 50 cm long and 5.3 cm in diameter. At the hydrogen inlet end was attached a tube of 2.6 cm diameter and 20 cm length. In this section a discharge was maintained in

the hydrogen stream by means of two 2450 MC diathermy units in order to generate hydrogen atoms. Downstream, approximately 20 cm, was an inlet for catalyst addition. The concentration of hydrogen atoms was measured with Wrede gauges inserted in ports further downstream.

A sketch of a Wrede gauge (18,19) is shown in Figure 5. On the bulb are small (~ 15μ diameter), well spaced holes through which hydrogen atoms and molecules diffuse from the main flow stream. The channel length is about 20μ so that little recombination occurs on the channel wall. The platinum catalyst inside the bulb insures that all the hydrogen atoms entering, recombine. As a result, in the steady flow state, molecules and atoms enter the bulb whereas only molecules diffuse out. Because of the recombination inside the bulb, the pressure decreases; the difference in pressure created across the bulb holes is proportional to the hydrogen atom concentration provided the temperature is the same everywhere. By means of the stop-cock, (see Fig. 5) the two pressures may be measured and their difference obtained. The gauges used in the work described below had response times of less than one minute when there were at least six holes on the bulb.

Capillary flowmeters were used to measure gas flow rates and leak values to regulate them. Pressures were generally determined with Pirani gauges; temperatures were measured with thermocouples inserted in glass wells projecting into the gas flow stream. The flow tube was heated by means of a nichrome wire spirally wound on the tube. Passage of the gases through the heated tube brought them rapidly to the desired temperature before reaction.

The upper limit to the temperature range was determined by two factors. First, fewer atoms were generated at the higher temperature. Part of the decreased production was due to faster recombination on the wall since external cooling of the walls in the discharge region resulted in increased atom signals. Secondly, the detection of the atom concentration at the higher temperature was made difficult because of a background signal due to the thermal gradient along the Wrede gauge body. The tip was inserted in the heated gas stream whereas the Pirani gauge was maintained at room temperature. As a consequence of these restrictions, no measurements were made above 570°K.

The upper pressure limit was about 0.7 mm Hg because it was necessary to maintain diffusional flow across the Wrede gauge holes. This follows from the condition that, to have diffusion only, the gas mean free path should be about ten times the diameter of the opening through which gas passes. Nevertheless, some measurements were made at pressures of 1 mm Hg apparently without effecting the results. The lowest pressure at which the microwave discharge could be sustained was 0.15 mm Hg.

III. Procedures and Results

A. Treatment of Data

In conducting the experiments with a variety of reactants, an important contribution from surface reactions was observed. As the concentration of catalyst is an important variable in the experiments, it is necessary to indicate the simultaneous effect of this variation on both the surface and gas phase reactions. Experimentally, the hydrogen atom concentration is measured and the rate of atom disappearance calculated. The general rate expression can be written as

$$\frac{d(H)}{dt} = \left(\frac{d(H)}{dt}\right)_g + \left(\frac{d(H)}{dt}\right)_s \qquad (2)$$

where (H) is the concentration of atoms in moles cm^{-3} and g and s denote the gas and surface reactions, respectively.

In the absence of catalyst, recombination of hydrogen atoms occurs on the surface and is found to be first order in the atom concentration (Ref. 15). In the presence of catalyst additional recombination occurs which depends on the quantity of sorbed catalyst as well as the hydrogen atom concentration. For a first order dependence on both concentrations which is consistent with the results of these studies, equation (2) becomes

$$-\frac{d(H)}{dt} = \left(-\frac{d(H)}{dt}\right)_g + k_{cs}(C_s)(H) + k_s(H) \qquad (3)$$

where k_s in sec^{-1} is the surface rate constant in the absence of catalyst, k_{cs} in $cm^2 mole^{-1} sec^{-1}$, that in the presence of catalyst, and C_s, the concentration of sorbed catalyst in mole cm^{-2}. For a sorption isotherm of the Langmuir form,

$$(C_s) = \frac{(C)(S)}{K + (C)} \tag{4}$$

where (C) is the catalyst concentration in mole cm^{-3}, (S), the number of sorption sites and $K = (C)(S)/(C_s)$, the equilibrium constant for the desorption. When (C) is large compared to K, (C_s) is constant; thus $(d(H)/dt)_s$ is independent of the catalyst concentration and the variation of the latter may be used in evaluating $(d(H)/dt)_g$.

In the absence of any measurable gas phase reaction and when k_s is known, equation (3) and equation (4) gives

$$- \frac{d \ln(H)}{dt} = \frac{k_{cs}(S)(C)}{K + (C)} = \frac{k'(C)}{K + (C)} \tag{5}$$

where k' is in sec^{-1}. As an example of the agreement between experiment and the assumed sorption isotherm, data from the methyl alcohol-hydrogen atom system are plotted in Fig. 6 along with a curve derived from equation (5) by using $k' = 11.4\ sec^{-1}$ and $K = 5.4 \times 10^{-12}$ mole cm^{-3}.

In the presence of a gas phase reaction with an accompanying surface catalyzed reaction, the rate of atom disappearance does not remain constant at large catalyst concentrations as in the methyl alcohol experiment, but continually increases. An example of this is shown in Fig. 7 where data from an ethylene experiment have been plotted according to the equation

$$- \frac{d \ln(H)}{dt} = k_c(C) + \frac{k'(C)}{K + (C)} \tag{6}$$

where k_c is the gas phase rate constant in $cm^3 mole^{-1} sec^{-1}$ and the term $d \ln(H)/dt$ has been corrected for the contribution from k_s. This expression assumes a second order gas phase reaction which is justified

below. According to equation (6), an extrapolation to (C) = 0 from the region of large (C), gives k' as the intercept; hence $k' = 10.5\ sec^{-1}$. From the initial slope, it is estimated that $K = 1.75 \times 10^{-12}$ mole cm^{-3}. Using these values for the constants, the sorption isotherm for ethylene was drawn as a dotted line in Fig. 7. The difference between the experimental and the sorption curve is used to calculate the gas phase reaction rate constant. The same result is achieved directly by evaluating the slope of the experimental curve at large catalyst concentrations.

In all the experiments it was possible to vary the catalyst concentration over a wide range. A typical result is shown in Fig. 7 where a first order dependence on catalyst concentration is demonstrated. On the other hand, due to the considerable destruction of hydrogen atoms by way of surface reactions, no such variation in atom concentration could be made. The dependence on atom concentration was indirectly arrived at by varying the total pressure in some cases. For ethylene and 1,3-butadiene, measurement was carried out in the pressure range, 0.2 mm to 1.0 mm Hg. In both cases the rate constant was invarient within experimental error. Therefore, in general, data were treated according to the rate expression

$$-\frac{d(H)}{dt} = k_c(C)(H) + \frac{k'(C)(H)}{K + (C)} + k_s(H) \qquad (7)$$

B. Diffusion Effects

Two possible corrections to the experimental data arise from back diffusion of the catalyst and forward diffusion of hydrogen atoms. The former correction is important because in measuring atom concentration change, one reference point was the catalyst inlet position. For this effect, the following approximation was made.

If to the hydrogen atom stream, the added reactant is a true catalyst with an inlet concentration (C_o), then its concentration downstream may be taken as (C_o) by neglecting any small concentration of catalyst intermediates. To the rear of the catalyst inlet, however, the concentration will decrease as a result of the competition between

diffusion backward and mass flow forward. In the steady state,

$$J_D + J_M = - D_c \frac{\partial(C)}{\partial X} + (C)\, V = 0 \qquad (8)$$

where J_D and J_M, in units of mole $cm^{-2} sec^{-1}$, are the fluxes for diffusion and mass, respectively, D_c, in $cm^2 sec^{-1}$, the diffusion constant of catalyst in hydrogen and V, in $cm\ sec^{-1}$, the linear flow velocity. The radial concentration of catalyst is assumed to be constant. Solution of equation (8) gives

$$(C) = (C_o)\, e^{- \frac{V l x l}{D_c}} \qquad (9)$$

The distance rearward, x_r, for which the effective catalyst concentration is (C_o), is

$$x_r = \frac{1}{(C_o)} \int_{\infty}^{o} (C)\, dx \qquad (10)$$

and the total time during which hydrogen atoms are mixed with catalyst at concentration (C_o) is $(X + X_r)V^{-1}$. Consequently, the corrected reaction time used in the calculations of rate constants is, after solution of equation (10),

$$t = \frac{x + D_c V^{-1}}{V} \qquad (11)$$

For a given catalyst concentration, the diffusion of hydrogen atoms is fully described by the following equation which is obtained from a material balance for a volume element in a flow tube in which radial diffusion can be neglected.

$$D_H \frac{\partial^2 H}{\partial x^2} - V \frac{\partial (H)}{\partial x} - k(H) = 0 \qquad (12)$$

where $k = k_c(C) + k'(C)/K+(C) + k_s$. Solution of this equation with the following boundary conditions (H) = (Ho) at x = 0 and (H) = 0 at x = ∞, and rearrangement yields

$$k_D = k + \frac{k^2 D}{V^2} \qquad (13)$$

where k_D is the diffusion corrected rate constant. The ratio of the correction term $k^2 D V^{-2}$ to k for typical operating conditions in a gas phase catalytic reaction is

$$\frac{kD}{V^2} = \frac{k_c(C)D}{V^2} \simeq \frac{2\times10^{11}(5\times10^{-11})(1.2\times10^{3})}{(2.5\times10^{2})^2} \simeq 0.19 \qquad (14)$$

In view of the error analysis presented below, this correction has not been applied to the data reported here.

C. Volume Change

Reactions generally proceed at constant or very nearly constant pressure in flow systems. Therefore if a change in volume occurs during the reaction, this must be taken into account. In the present system the pressure could be considered constant and the fractional change in volume described by

$$\frac{V}{V_o} = \frac{V_{o,H}}{Vo} \left\{ 1 - (\nu-1) \frac{(H_2)'}{(H)} \right\} + \frac{V_{o'H2}}{V_o} \qquad (15)$$

where V_o, is the initial volume, V, the volume after reaction, $V_{o'H}$ and $V_{o'H2}$, the volumes corresponding to hydrogen atoms and molecules prior to reaction, ν, the number of moles of H_2 formed from one mole of H, and $(H_2)'$, the concentration of molecules formed by recombination of (H). If $V_{o'H}/V_o$ is taken as 0.05, a typical value, then V/V_o is 0.99; the volume change may thus be neglected without introducing appreciable error.

D. Error Analysis

The analysis of the random error follows. For a catalytic gas phase reaction having a rate expression given by

$$-\frac{d(H)}{dt} = k_c\,(C)\,(H), \tag{16}$$

the rate constant, in the integrated form of equation (16) becomes

$$k_c = k_c(H_o,H,C,t_o,t) = (t-t_o)^{-1}(C)^{-1}\ln H_o H^{-1} \tag{17}$$

from which, assuming the relative errors in H_o and t_o to be the same as those for H and t, respectively, the square of the relative error in k_c can be shown to be

$$\left(\frac{\Delta k_c}{k_c}\right)^2 = \left(\frac{\Delta t}{t}\right)^2 + \left(\frac{\Delta C}{C}\right)^2 + \left(\frac{2\ \Delta H/H}{\ln Ho/H}\right)^2 \tag{18}$$

In this form, t_o has been set at zero. The evaluation of the various terms in equation (18) is described in detail in the appendix for typical flow situations. When this is done $\Delta k_c/k_c$ becomes 0.25. This compares favorable with the value of 0.15 computed directly from experimental data for those cases in which duplicate experiments were performed (see Tables XXVII and XXVIII, LVII and LXI).

The other important quantity derived from the experiments is the activation energy, E. The error in this quantity, to a good approximation is

$$\left(\frac{\Delta \bar{E}}{\bar{E}}\right)^2 \simeq \left\{\left(\frac{\Delta k_{1c}}{k_{1c}}\right)^2 + \left(\frac{\Delta k_{2c}}{k_{2c}}\right)^2\right\}\left\{(\ln k_2/k_1)^{-2}\right\} \tag{19}$$

Substitution of $\Delta k_c/k_c = 0.25$ yields $\Delta\bar{E}/\bar{E} = 0.25$ where $\bar{E}$ is the average activation energy over the temperature range T_1 to T_2 with corresponding rate constants k_1 and k_2.

E. Results

1. Gas Phase Reactions

In Tables II and III are summarized the results of the present investigation. Table II includes all those reactants studied over a temperature range whereas, those listed in Table III were used only at one temperature. When no gas phase reaction was detected, an upper limit to the expected second order reaction rate constant is given. The data from Table II can be used to determine the rate constant k_c at temperature T by means of equation (1); A can be expressed as $PZT^{-1/2}$ where P is the steric factor and Z, the collision frequency. A was derived from experiment and P was calculated from A using the values of the molecular diameters listed in the last column of Table II.

The calculated values of the ratio of hydrogen atoms consumed per molecule of reactant added are given in Table IV. These values are based only on the gas phase reaction. The change in hydrogen atom concentration, as shown in equation (7) is, at large C,

$$\Delta H \simeq k_c(C)(H)\Delta t + k'(H)\Delta t + k_s(H)\Delta t \qquad (20)$$

The fractional loss occurring through the gas phase is

$$\frac{k_c(C)(H)\Delta t}{\Delta H} = \frac{k_c(C)}{k_c(C) + k' + k_s} = f \qquad (21)$$

This loss f, can be obtained to the accuracy required here directly from graphs as shown in Figure 8. The ratio of moles of atoms disappearing to moles of catalyst added is $(H)_r/(C)$ where $(H)_r$ is f times the total number of moles removed at the measuring port. The ratios of Table IV are minimum values; only the largest of these found for a given reactant has been listed. For a longer reaction time than that of the experiment, the ratio found might have been larger. However, with longer reaction times the atom concentration would have been zero under experimental conditions and in that event, additional information not gained. The various ratios cannot be compared because of different reaction times and initial atom concentrations.

2. Surface Reactions

In the case of those catalysts listed in Tables II and III for which E, A or a rate constant limit are not given, it was found that upon addition to the stream of hydrogen atoms, they increased the atom concentration. In the case of ammonia, which was an exception to this observation, only a surface reaction which vanished with increasing temperature was found. For water, boron trifluoride and carbon tetrafluoride, no further change in atom concentration was observed after the initial addition. This behavior was consistent with the sorption of these materials on the flow tube wall where they retarded hydrogen atom surface recombination. Generally, when addition was stopped, the effect persisted. With nitric oxide, on the other hand, increasing the amount added distinctly increased the Wrede gauge signals. This was not further investigated.

IV. Discussion

A. Catalytic Activity

The main evidence for catalytic activity to be found in the results consists in the rapid, second order reactions of those substances listed in Tables II and III and in the values of the ratios of hydrogen atoms consumed to reactant molecule involved.

At room temperature, the rate of the reactions observed is sufficiently large to rule out termolecular collision processes for those elementary reactions involving the disappearance of hydrogen atoms. The second order nature of the reacting systems suggests, but does not unequivocally confirm, a bimolecular collision process. Finally, the most likely reactions involving hydrogen atoms, especially with those reacting materials listed in Table II, are addition or abstraction reactions and these will be bimolecular.

In general, the ratios of atoms consumed to reactant added are sufficiently large to indicate a distinct catalytic effect. For those substances with low ratios at high temperature such as acetylene and propylene, it is possible that sufficient time has not elapsed during the measurement to provide an adequate test. For acetylene, the

lack of hydrogen atoms is definitely an important factor in preventing a reliable analysis.

Whenever measurements could be made at the two ports along the tube which were separated by 10 cm, the ratios calculated at both ports were the same within the estimated error of $\pm$ 3. The measurements were carried out at room temperature for vinyl chloride, fluorobenzene and hexene-1 only. These results indicate that sufficient time was available for the full extent of catalytic action to be detected; consequently, the ratios determined at room temperature were probably a true measure of the catalytic action rather than a minimum. For all substances undergoing a fast, gas phase reaction with hydrogen atoms, the ratio was 5 $\pm$ 3 at room temperature. On the other hand, when the temperature was raised, the ratio increased; for example, in the case of cis-butene-2, it increased linearly with temperature. If this increase had been solely due to a faster reaction rate at the higher temperatures, then the room temperature measurements with longer reaction times should have shown the same effect. If, however, the reaction mechanism was changing to favor a catalytic sequence of elementary reactions, then the observed behavior would obtain. While this is not definitive, it does suggest that a catalysis of hydrogen atom recombination is becoming potent at higher temperatures ($> 500°K$).

B. High Temperature Considerations

Since the experimental temperature limit was 570°K, it is important to consider the extrapolation of data to higher temperatures.

Hydrogen atoms disappear in at least two elementary reactions; it is probable that a composite of reactions is being described by the activation energies, preexponential and steric factors presented. However, there is no evidence from the Arrhenius plot of any marked differences in the effects of the elementary reactions throughout the experimental range of temperature since for most plots, a straight line is obtained without doubt. (See Figs. 30, 32, 33, 34). But this is no assurance that extrapolation of the data to higher temperatures will not overlook a change in reaction mechanism that will markedly alter the predominate values of E and A.

With the above reservations in mind, the relation of the rate constants at higher temperatures may be considered. To a good approximation, the ratio of rate constants for any two materials at an arbitrary temperature above 750°K, is given by the ratio of the A factors. As a result, the order in rate constant magnitudes at high temperature is the same as the order in which gases are listed in Table II. Insofar as catalysts are defined by reaction rate constants, the table also lists the catalysts in order of effectiveness.

The effectiveness of the catalysts may be estimated for conditions close to those prevailing in the downstream portion of an arc jet nozzle. At high temperatures, the collision efficiency approaches a value equal to the steric factor; consequently the ultimate catalytic effect will be less than an order of magnitude greater than that provided by the better catalysts of Table II. On the other hand, one mole percent of the better catalysts will increase the homogeneous atom recombination rate by more than five orders of magnitude as compared to the rate in the absence of catalyst at 1000°K and 10^{-4} atm. This is based on a termolecular rate constant for atom recombination of 2.7×10^{15} $cm^6 mole^{-2} sec^{-1}$ at 1000°K obtained from reference (16) by extrapolation of data; also $k_c = 4.5 \times 10^{12} T^{1/2}$ exp (-3.5/RT) and $(H_o) = 0.6\ (H_2)$. Thus the performance will be approximately that of the optimum catalyst of Table I.

The stability of the catalysts at high temperature is an additional consideration. Even though a catalyst may not be thermodynamically stable at a given high temperature, it may still be an effective catalyst since the important question concerns the extent of decomposition during its residence time in the propulsion device. For example, acetylene, which at moderate temperatures tends to decompose, appeared to be rather stable when heated to 1800°K for time intervals of 2 to 10 m sec (17). In a propulsion unit, the residence time could be less than this depending on the location of the catalyst injection point and catalyst might exist in a non-equilibrium condition during this time. It is also possible that a catalytic material such as benzene, when added to the nozzle, would decompose giving other catalysts such as acetylene, butadiene, etc. The

time for initial decomposition plus that for decomposition of the derived catalysts might be sufficient to ensure effective catalytic activity during the residence time of an injected particle. Finally, there may be an effect on catalyst stability due to its participation in the hydrogen atom recombination cycle, but this is unknown.

C. Steric Factors

The steric factors found in Table II, with the exception of that for ethylene, fall into three groups. Those unsaturated compounds with more than two multiple bonds have steric factors of the order of 0.1. In the second group are those with only one multiple bond having steric factors of the order of 0.05. Vinyl chloride has a P value lower by a factor of about ten than the second group. If the steric factor is considered in terms of the orientation of reactants during effective collisions, then the approximate doubling of P in passing from one to several multiple bonds in the reactant, can be associated with the increased probability of proper orientation of the multiple bond upon collision. On the other hand, there is no evidence, based on the calculated steric factors, for a difference in reactivity of a hydrogen atom with a multiple bond in various structural contexts. There is one further correlation which might, on further investigation, offer a reason for the low steric factor of vinyl chloride. In the second group, propylene has the smallest steric factor, 0.02 and is one above vinyl chloride in order. Upon substituting either a methyl group or a chlorine atom for a hydrogen atom in ethylene, qualitatively the same electron displacement occurs. If this takes place to a greater extent with chlorine, the resulting alteration of the electron density about the multiple bond may decrease the reactivity to the extent that it would account for the observed steric factor differences.

V. Conclusions

Evidence for a catalytic effect by several foreign gases in the recombination of hydrogen atoms has been presented. This effect appears to be greatly enhanced at high temperatures (>500°K).

At high temperatures, for the catalysts tested, the order of effectiveness has been estimated to be ethylene, allene, butadiene, benzene, cis-butene-2, acetylene, propylene and vinyl chloride without consideration of the stability of any material.

VI. Recommendations

The following extensions of the work reported above are recommended.

A. Emphasis should be placed on extending the means of detecting hydrogen atoms to high temperatures (> 600°K) through development of methods using mass spectrometry, spin resonance, optical means and titration techniques.

B. Product analyses should be made over a wide range of temperatures including that interval covered by the present work. The two chief benefits of so doing are:

1. More accurate information on the extent of catalysis.
2. A complete product analysis will permit a reaction mechanism to be constructed. Only on the basis of such work carried out at different temperatures, will maximum insight into the reasons for catalytic effectiveness be gained.

C. The extent of surface reactions at high temperatures should be ascertained by sorption studies, either directly or by an empirical means such as employed in this study.

D. The measurement of the catalysis of hydrogen atom recombination in an electric arc heated, continuous flow nozzle apparatus would circumvent certain problems. High temperature chemical kinetic information could be obtained from nozzle pressure and discharge temperature measurements; analysis of nozzle discharge materials would be useful in determining reaction mechanisms. With large atom fluxes and gas velocities, higher catalyst concentrations could be employed thereby increasing the extent of homogeneous compared to surface reactions.

VII. Appendix

The experimental results obtained in this study are presented in the following tables and figures.

A. Gas Phase Reactions

1. Rate Constants

Tables V to LI and figures 9 to 23 represent experiments in which the catalyst concentration and the temperature were varied. On the average, the maximum catalyst concentration used was less than 0.4 mole % of the total hydrogen present. In the figures, the data have been plotted according to equation (6); where the temperature listed in the accompanying legend is followed by a notation such as 2(A), the corresponding data have been plotted on an abscissa scale expanded by a factor of 2.

To confirm the assumption of an overall second order rate expression, the total pressure was varied in several cases and these results are given in Tables LII to LXI and figures 24 to 27. In Fig. 25, the the rate constants for the reactions of 1,3-butadiene with hydrogen atoms are plotted against the total pressure. The dotted line shown is the least squares straight line. Over a pressure variation by a factor of five, the rate constants corresponding to the curve change by 1.1. Since the experimental error in the rate constant was estimated to be 25%, the least squares variation of about 10% is well within this error and is negligible compared with the change in pressure. In Fig. 27 ethylene data from experiments involving a change in total pressure are shown. In this case, for a doubling of the pressure, the least squares straight line (shown dotted) corresponds to a 20% change in rate constant. This again is within the experimental error and is neglected.

2. Activation Energies

Activation energies have been derived from Arrhenius plots, shown in Figures 28 to 34 which were drawn using rate data summarized in Tables LXII to LXIX. These curves represent a plot of the equation

$$k_c = A' e^{-E_A/RT} \qquad (22)$$

where E_A is the Arrhenius activation energy and is related to E, the activation energy listed in Table II by

$$E = E_A - 0.5R < T > \qquad (23)$$

where $< T >$ is the average temperature for the range used. The pre-exponential factor of equation 22 is equal to $AT^{1/2}$ where A is reported in Table II. From the slope and intercept, E_A and A' were derived, respectively. The steric factors shown in Table II were calculated using the expression

$$P = A'Z^{-1} = A'\left\{\sigma_{C,H}^{2} N \left(\frac{8\pi RT}{\mu}\right)^{1/2}\right\}^{-1} \qquad (24)$$

where $\sigma_{C,H}$ is the effective molecular diameter for the collision complex of catalyst C and hydrogen atom, N, Avogadro's number, R, the gas constant and μ, the reduced mass.

B. Surface Reactions

1. Catalyzed Surface Reactions

a. In Absence of Gas Phase Reactions

Only catalyzed surface reactions were found to occur in those experiments where the reactants were ammonia, carbon monoxide, ethylene oxide, methane and methyl alcohol (See Tables XII to XIV, XXVI, XXXVII, XLI, XLII and Figs. 11, 16, 19, 21 and 22 respectively).

Common to all these reactants was an independence of the atom loss upon reactant concentration when the latter exceeded a particular, small value. This was interpreted as complete coverage of the flow tube surface available for sorption; further increase in the reactant concentration did not alter that fraction involved in the surface reaction and did not change the rate at which hydrogen atoms were recombining.

b. In Presence of Gas Phase Reactions

When a gas phase reaction was also occurring, as with ethylene for example, the surface catalyzed reaction was observed

by decreasing the flow tube diameter one half and increasing the linear flow rate. This was done for some ethylene experiments with the results shown in Tables LXX to LXXI and in Fig. 35. With a decreased tube diameter, the surface to volume ratio increased and surface effects were accentuated; due to faster flow, a shorter reaction time in the measurement interval reduced the gas phase contribution to atom disappearance. Thus the curves of Fig. 35 resemble those for the reactants of Section (a) and are described adequately by equation (5).

2. Surface Reactions in Absence of Added Catalysts

When no catalysts are added, the rate of disappearance of hydrogen atoms remains larger than expected from gas phase recombination. The later can be reasonably estimated solely on the basis of the reaction

$$H + H + H_2 \longrightarrow H_2 + H_2 \qquad (R3)$$

since the hydrogen atom concentration is always small compared to the hydrogen molecule concentration. The consequence of this is that three body recombination involving only hydrogen atoms is rare. The rate expression for R3 becomes

$$-1/2 \ \frac{d\ln(H)}{dt} = k_H(H)(H_2) \qquad (25)$$

where k_H, the rate constant is about $10^{16} cm^6 mole^{-2} sec^{-1}$. Typically with $(H_2 \sim 2 \times 10^{-8} mole\ cm^{-3}$ and $(H) < 0.05\ (H_2)$, $d\ln(H)/dt < 0.4\ sec^{-1}$. This is negligible under the present experimental conditions as is evident in Fig. 1-16.

Thus neglecting volume recombination, the surface rate constant in the absence of catalyst was determined for a number of linear flow rates (LFR); the results are shown in Table LXXVIII. The surface rate constants of column 5 are given by $VX^{-1} \ln H_1 H_2^{-1}$; those in column 6 are calculated according to equation (12), with k' and k_c set equal to zero. The fractional contribution , y, of diffusion to the observed surface rate constant, decreases as the LFR increases; under normal experimental conditions, y is less than the error in the calculated rate constant.

The surface rate constant, k_s, was assumed not to change appreciably when catalysts were added to the flow tube. In the method adopted for calculating the catalyzed gas phase reaction rate constant, as described above, account was thus automatically taken for the "uncatalyzed" surface reaction contribution.

C. Surface Poisons

When boron trifluoride, carbon tetrafluoride, nitric oxide and water were added to the flow tube, the Wrede gauge signals increased. Interpreted in terms of hydrogen atoms, this was equivalent to an increase in atom concentration. For boron trifluoride and carbon tetrafluoride, the measured hydrogen atom concentrations did not change after the initial addition of reactants. Also in the absence of hydrogen atoms no signal changes were observed upon adding these reactants. The observations are consistent with a poisoning of the flow tube wall which hinders hydrogen atom surface recombination. If the surface rate constant is calculated as shown in column 4 of Tables LXXII to LXXIV, it is found that the rate constant has decreased in the presence of the fluorides. It is worth noting that hydrofluoric acid has generally been used to clean the flow tube because qualitative observations have indicated that the atom concentration is thereby increased. It appears likely that fluoride containing compounds will in general act as surface poisons.

With the addition of water, no change in atom concentration was detected at 25°C; but at 224°C, the gauge signals increased. Moreover, the ratio of atom concentrations, $(H_1)/(H_2)$, (see Table LXXVII) decreased as more water was added. This corresponds to a decreasing surface rate constant. At the largest added water concentration, 0.09 mole %, the ratio had decreased to one, within experimental error. This is equivalent to a zero surface rate constant and indicates that any surface recombination was too small to be detected.

With extensive addition of nitric oxide, the gauge signals continued to increase beyond the initial rapid change displayed in other cases; note that $-\,d\ln(H)/dt$ is plotted in Fig. 36. The data are given in Tables LXXV and LXXVI.

D. Surface Sorption

While the initial surface condition of the flow tube was not constant from experiment to experiment, the change was small enough so that sorption data at room temperature may be compared. In Table LXXIX, the surface rate constants for various sorbed species are listed. These data suggest a correlation between the degree of unsaturation of the species and the surface rate constant which might be expected. Conversely, the assumption of a sorbed species participating in a catalyzed surface reaction is strengthened.

E. Error Analysis

The evaluation of the various terms in equation (18) above was arrived at as follows: The relative errors in x, v and D_c were estimated to be 7×10^{-3}, 5.7×10^{-2} and 3.0×10^{-1} respectively. Since

$$\left(\frac{\Delta t}{t}\right)^2 = \left(\frac{x}{tv}\right)^2 \left(\frac{\Delta x}{x}\right)^2 + \left(\frac{d+2D_c V^{-1}}{tV}\right)^2 \left(\frac{\Delta V}{V}\right)^2 + \left(\frac{D_c}{tV^2}\right)^2 \left(\frac{\Delta D_c}{D_c}\right)^2 \qquad (26)$$

the error becomes, using the typical operating conditions of d = 15 cm, t = 40 m sec, V = 250 cm sec^{-1} and D_c = 1500 $cm^2 sec^{-1}$, $(\Delta t/t)^2 = 5.5 \times 10^{-2}$.

The relative error in catalyst concentration is

$$\left(\frac{\Delta C}{C}\right)^2 = 2\left(\frac{\Delta V}{V}\right)^2 + \left(\frac{\Delta P}{P}\right)^2 + \left(\frac{\Delta T}{T}\right)^2 \qquad (27)$$

Since $(\Delta P/P)$ and $(\Delta T/T)$ are 0.014 and 0.01 respectively, $(\Delta C/C)^2 = 6.7 \times 10^{-3}$.

The hydrogen atom concentration as determined by Wrede gauge measurements is $C_1 Sd/P$ where S is the sensitivity of the Pirani element in mm/μa, d, the observed ammeter needle deflection in μa corresponding to the difference in pressure between the flow tube and Wrede gauge, P, the pressure and C_1 a constant. For relative error in S and d of 2.44×10^{-2} and 2.0×10^{-2}, the atom concentration error is

$$\left(\frac{\Delta H}{H}\right)^2 = \left(\frac{\Delta S}{S}\right)^2 + \left(\frac{\Delta d}{d}\right)^2 + \left(\frac{\Delta P}{P}\right)^2 = 12 \times 10^{-4} \qquad (28)$$

The error in the observed rate constant becomes

$$\frac{\Delta k}{k} = (5.5\times10^{-2} + 6.7\times10^{-3} + 3.4\times10^{-3})^{1/2} \sim 0.25 \qquad (29)$$

where the typical value of two for the ratio $(H_o)/(H)$ has been used.

F. Correlation of Wrede Gauge Signals with Mass Spectrometer Signals

The flow tube was connected with a "Gas Analysis Modulated Beam Apparatus", a mass spectrometer developed by the General Atomic Division of General Dynamics. This instrument operates by modulating a beam of particles which enters the vacuum chamber of the apparatus through a small hole in the side of the flow tube. Because the beam of incoming particles is modulated, it can be distinguished from the background noise in the instrument in the manner in which an AC and DC signal may be separated. In this way, particular species in the modulated beam can be detected in spite of their presence in the background in much larger concentrations. Thus the instrument could readily be used to measure directly the strength of the hydrogen atom signal.

The direct measure by both the mass spectrometer and the Wrede gauge of the hydrogen atoms present in the flow tube to which both detectors were directly attached, is shown in Fig. 37. It is clear that a proper linear relation exists between the magnitude of the signals indicated by the two instruments.

G. Sample Calculations

1) Rate constant (see Tables XIX, LXIV and Figure 13, Θ) for p = 0.43 mm and T = 30°C.

$$\frac{d\ \ln(H)}{dt} \simeq \frac{2.3\ \log\ (H)/(H)c}{\Delta t} = \frac{2.3\ \log\ (11.3)/(1.21)}{0.0452} = 49.3\ \text{sec}^{-1}$$

$$\Delta t = \frac{x + DV^{-1}}{V} = \frac{4.5 + 1310/227}{227} = 0.0452\ \text{sec}$$

$$k_c = \frac{\{d\ell n(H)/dt\}_2 - \{d\ell n(H)/dt\}_1}{(C_4H_6)_2 - (C_4H_6)_1} = \frac{49.0 - 38.5}{(13.0-3.0)10^{-11}}$$

$$k_c \simeq 1.1 \times 10^{11} \text{ cm}^3 \text{ mole}^{-1}\text{sec}^{-1}$$

2) Activation energy (See Tables II and LXIV and Figure 10)

$$E_A = \frac{-R}{0.434}\left(\frac{\log k_{c1} - \log k_{c2}}{T_1^{-1} - T_2^{-1}}\right)$$

$$= \frac{-1.99}{0.434}\left(\frac{12.0 - 11.0}{2.14 - 3.29}\right) = 4.0 \text{ kcal mole}^{-1}$$

$$E = E_A - 0.5R \langle T \rangle = 4.0 - 0.5(1.99)(398)10^{-3} = 3.6 \text{ kcal mole}^{-1}$$

3) Preexponential factor (See Tables II and LXIV)

$$\log A' = \frac{0.434\ E_A}{RT_2} + \log k_{c2}$$

$$= \frac{0.434}{1.99}(4.0)(2.14\text{x}10^{-3}) + 12.0 = 13.86$$

$$A' = 9.3 \times 10^{13} \text{ cm}^3 \text{ mole}^{-1}\text{sec}^{-1}$$

$$A = A' \langle T \rangle^{-1/2} = 9.3 \times 10^{13}(3.98\text{x}10^{2})^{-1/2}$$

$$= 4.7 \times 10^{12} \text{ cm}^3 \text{ mole}^{-1}\text{sec}^{-1} \cdot \text{K}^{-1/2}$$

4) Steric factor (See Table I)

$$P = A'Z^{-1} = A' \left\{ \sigma_{C_4H_6,H} N \left(\frac{8\pi RT}{\mu} \right)^{1/2} \right\}^{-1}$$

$$= 9.3\times10^{13} \left\{ 1.72\times10^{15}(6.06\times10^{23}) \left\{ \frac{8\pi(8.32\times10^{7})(398)}{54\ /\ 55} \right\}^{+1/2} \right\}^{-1} \simeq 0.10$$

$$\sigma_{C_4H_6,H} = 1/2(\sigma_{C_4H_6} + \sigma_H) = 1/2(6.3 + 2.0)10^{-8} = 4.2\times10^{-8}\text{cm}$$

5) Catalyst effectiveness at T = 1000°K and P = 10^{-4}atm

$$(H_2) = P(RT)^{-1} = 10^{-4}\{(82)(1000)\}^{-1} = 1.2\times10^{-9}\text{mole cm}^{-3}$$

$$k_c = 4.5\times10^{12}T^{1/2}e^{-3.5/RT} = 1.4\times10^{14}\text{cm}^3\text{mole}^{-1}\text{sec}^{-1}$$

$$k_H = 2.7\times10^{15}\text{cm}^6\text{mole}^{-2}\text{sec}^{-1} \text{ (Ref. 16)}$$

$$\frac{\{d(H)/dt\}_c}{\{d(H)/dt\}_H} = \frac{k_c(H)(C)}{2k_H(H)^2(H_2)} = \frac{k_cM_c}{2k_HM_H(H_2)}$$

where M_c and M_H are the mole fractions of catalyst and hydrogen atoms, respectively. If $M_c = 0.01$ and $M_H = 0.60$, then

$$\frac{\{d(H)/dt\}_c}{\{d(H)/dt\}_H} = \frac{1.4\times10^{14}(0.01)}{2(2.7\times10^{15})(0.60)(1.2\times10^{-9})} = 3.6\times10^{5}$$

VIII References

1. K. F. Bonhoeffer and P. Harteck, Zeits. f. physik Chemie 139 64 (1928).

2. H. v. Wartenberg and G. Schultz, ibid B2 1 (1929).

3. K. H. Geib and E. W. R. Steacie, ibid B29 215 (1935).

4. E. L. Tollefsen and D. J. LeRoy, J. Chem. Phys. 16 1057 (1948).

5. J. R. Dingle and D. J. LeRoy, ibid 18 1632 (1950).

6. F. Kaufman, Proc. Roy Soc., A247 123 (1958).

7. R. Marshall and N. Davidson, J. Chem. Phys. 21 659 (1953).

8. D. L. Bunker and N. Davidson, J. Am Chem. Soc. 80 5085 (1958).

9. R. L. Strong, J. C. W. Chien, P. E. Graf and J. E. Willard, J. Chem. Phys. 26 1287 (1957).

10. D. Britton, N. Davidson, W. Gehman and G. Schott, ibid 25, 804 (1956)

11. H. G. V. Evans, G. R. Freeman and C. A. Winkler, Can J. Chem. 34 1271 (1956).

12. J. T. Herron, J. Chem. Phys. 33 1273 (1960).

13. F. Kaufman and J. R. Kelso, ibid 32 301 (1960).

14. J. T. Herron, J. L. Franklin, P. Bradt and V. H. Diebeler, ibid 30 879 (1959).

15. B. J. Wood and H. Wise, J. Phys. Chem. 66 1049 (1962).

16. E. A. Sutton, J. Chem. Phys. 36 2923 (1962).

17. G. B. Skinner and E. M. Sokoloski, J. Phys. Chem. 64 1028 (1960)

18. E. Wrede, Z. physik 54 53 (1929)

19. J. W. Linnett, M. Green, J. R. Jennings and D. Schofield, Trans. Faraday Soc., 55 2152 (1959).

20. A. Q. Eschenroeder and J. A. Lordi, Cornell Aeronautical Laboratory Report No. AD-1689-A-1 (1962).

IX. List of Symbols

A	pre-exponential factor, $cm^3\ mole^{-1} sec^{-1}\ °K-1/2$
A'	pre-exponential factor, $cm^3\ mole^{-1} sec^{-1}$
C	catalyst
C_1	constant
d	ammeter deflection, μa
D	diffusion constant in hydrogen, $cm^2 sec^{-1}$
E	activation energy, $cal\ mole^{-1}$
E_A	"Arrhenius" activation energy, $cal\ mole^{-1}$
f	fractional loss of hydrogen atoms in gas phase
J_D or M	flux for diffusion or mass, $mole\ cm^{-2} sec^{-1}$
K	equilibrium constant for desorption, $mole\ cm^{-3}$
k	overall, rate constant, sec^{-1}
k'	pseudo surface rate constant, sec^{-1}
k_c	rate constant of gas phase catalyzed reaction, $cm^3 mole^{-1} sec^{-1}$
k_D	diffusion corrected overall rate constant, sec^{-1}
k_{cs}	catalyzed surface reaction rate constant, $cm^2\ mole^{-1} sec^{-1}$
k_H	rate constant of termolecular H atom recombination, $cm^6\ mole^{-2} sec^{-1}$
k_s	surface rate constant, sec^{-1}
N	Avogadro's number
P	steric factor or pressure, mm Hg
R	gas constant, $cal\ mole^{-1}\ °K^{-1}$
S	sorption sites, $mole\ cm^{-2}$; ~sensitivity of Pirani element, mm/μa

t	time, sec
T	temperature, °K
V	linear flow velocity, $cm\ sec^{-1}$ or volume element, cm^3
x	distance, cm
Z	collision frequency, $cm^3\ mole^{-1} sec^{-1}$
σ	collision diameter, cm
μ	reduced mass, gm

Subscripts

c	catalyst
g	gas phase reaction
H	hydrogen atoms
0	initial state
r	gas phase atom loss
s	surface reaction

Other Notation

( )	concentration in mole cm^{-3} or mole cm^{-2}

TABLE I

CATALYSIS OF H-ATOM RECOMBINATION
IN A CONICAL NOZZLE

(Note: one-dimensional, adiabatic, inviscid flow with finite reaction rate)

CATALYTIC EFFECT	CONDITIONS AT ϵ = 100 L = 8 cm			CONDITIONS AT ϵ = 840 L = 25 cm		
	X	T°K	Patm	X	T°K	Patm
NO CATALYST $K = 10^{10}$	0.61	245	0.285 $\times 10^{-3}$	0.61	24	0.102 $\times 10^{-4}$
FAIR CATALYST $K_c = 10^{8}$	0.53	563	0.581 $\times 10^{-3}$	0.52	224	0 263 $\times 10^{-4}$
INCREMENTAL CHANGE-%	14.0	130	104	15	814	158
GOOD CATALYST $K_c = 10^{9}$	0.35	1455	0.121 $\times 10^{-2}$	0.34	703	0.64 $\times 10^{-4}$
INCREMENTAL CHANGE-%	34	158	108	36	214	143
OPTIMUM CATALYST $K_c = 10^{10}$	0.25	2323	0.18 $\times 10^{-2}$	0.21	1508	0.121 $\times 10^{-3}$
INCREMENTAL CHANGE-%	26	60	48	38	115	89

THROAT CONDITIONS

T = 4000°K
P = 1.0 atm
X = Weight Fraction H-Atoms; $X_o = 0.63$
K = liters^2/mole^{2}sec
K_c = liters/mole sec
ϵ = nozzle expansion ratio

TABLE II

Summary of Experimental Data

Catalyst	Temp. Range °K	E k cal mole^{-1}	A cm^3 mole^{-1} sec^{-1} °K$^{-1/2}$	P	Molecular dia/°A
Ethylene	297-564	4.2	2.7×10^{13}	0.88	4.6
Allene	303-458	3.0	4.1×10^{12}	0.11	5.4
1,3-Butadiene	297-498	3.6	4.7×10^{12}	0.10	6.3
Benzene	295-510	1.6	4.8×10^{12}	0.08	6.9
Cis-butene-2	301-432	2.4	1.6×10^{12}	0.04	6.2
Acetylene	295-514	3.0	1.1×10^{12}	0.04	3.3
Propylene	299-522	3.3	7.4×10^{11}	0.02	5.4
Vinyl chloride	299-426	0.9	1.5×10^{11}	0.004	5.8
*Ethane	297-443	--	--	--	--
Nitric oxide	297-394	+	+	+	+
Ammonia	298-442	+	+	+	+
Water	298-497	+	+	+	+

* $k_{T < 443°K} < 3 \times 10^{10}$ cm^3 mole^{-1} sec^{-1}

\+ See discussion in text

TABLE III

Summary of Experimental Data

Catalyst	Temp./°K	k_c/cm^{3}mole^{-1}sec^{-1}
Fluorobenzene	304	2.1×10^{12}
Hexene-1	297	2.4×10^{11}
Trans-butene-2	296	1.4×10^{11}
Ethylene oxide	298	$< 2 \times 10^{10}$
Carbonyl Sulfide	301	2.6×10^{11}
Methane	513	$< 1 \times 10^{11}$
Methyl alcohol	304	$< 1 \times 10^{9}$
Boron trifluoride	301	*
Carbon tetrafluoride	303	*
Carbon monoxide	301	$< 1.5 \times 10^{10}$

* See discussion in text

TABLE IV

Atom Consumption per Catalyst Molecule.

Catalyst	T/°K	P/mm	f	(H)r/(C)
Ethylene	493	0.39	0.76	$\geq$ 20
Allene	361	0.43	0.40	$\geq$ 14
1,3-Butadiene	466	0.43	0.44	$\geq$ 14
Benzene	393	0.45	0.55	$\geq$ 45
Cis-butene-2	432	0.43	0.34	> 30
Acetylene	514	0.39	0.44	$\geq$ 6
Propylene	456	0.26	0.36	$\geq$ 2
Vinyl chloride	348	0.39	0.83	> 7
Fluorobenzene	304	0.39	0.50	> 25
Hexene - 1	298	0.26	0.46	> 21
Trans-butene - 2	296	0.43	0.48	> 7
* Carbonyl sulfide	301	0.43	0.52	$\geq$ 9
	301	0.43	0.37	> 8

*Duplicate experiments

TABLE V

Acetylene Experiments

Reactants: C_2H_2, H
Temperature: 22.5°C
Initial (H_2) 2.36×10^{-8} moles cm^{-3}

Linear Flow Rate: 2.46×10^2 cm sec^{-1}
Total Pressure: 0.435 mm.

Mole % C_2H_2	Mole % H	$\frac{d\ln (H)}{dt}$ / sec^{-1}	$\frac{(C_2H_2)}{10^{-10}}$ moles cm^{-3}
0.0	4.43	0.0	-
0.0224	4.21	1.5	0.053
0.0535	3.90	3.8	0.13
0.103	3.62	5.9	0.24
0.189	3.10	10.4	0.45
0.441	2.34	18.6	1.04
1.08	1.09	41.0	2.55

TABLE VI

Acetylene Experiments

Reactants: C_2H_2, H
Temperature: 73.2°C
Initial (H_2) 2.09×10^{-8} mole cm^{-3}

Linear Flow Rate: 2.98×10^2 cm sec^{-1}
Total Pressure: 0.451 mm

Mole % C_2H_2	Mole % H	$\frac{d\ln (H)}{dt}$ / sec^{-1}	$\frac{(C_2H_2)}{10^{-10}}$ moles cm^{-3}
0.0	2.58	0.0	-
0.00175	2.58	0.0	0.002
0.00736	2.51	1.3	0.015
0.0173	2.34	3.3	0.036
0.0376	2.13	6.5	0.079
0.103	2.13	6.5	0.22
0.263	1.71	14.0	0.55
1.20	0.99	32.6	2.51

TABLE VII

Acetylene Experiments

Reactants: C_2H_2, H — Linear Flow Rate: 3.94×10^2 cm sec^{-1}

Temperature: 167.6°C — Total Pressure: 0.435 mm

Initial (H_2) 1.58×10^{-8} mole cm^{-3}

Mole % C_2H_2	Mole % H	dln (H) /dt / sec^{-1}	(C_2H_2) / 10^{-10} moles cm^{-3}
0.0	1.60	0.0	-
0.0189	1.45	4.1	0.03
0.0465	1.03	17.8	0.073
0.313	0.50	47.1	0.495
1.24	0.15	95.6	1.96

TABLE VIII

Acetylene Experiments

Reactants: C_2H_2 H — Linear Flow Rate: 383 cm sec^{-1}

Temperature: 241°C — Total Pressure: 0.388 mm

Initial (H_2): 1.21×10^{-8} mole cm^{-3}

Mole % C_2H_2	Mole % H_1	dln (H_1) /dt / sec^{-1}	(C_2H_2) / 10^{-12} mole cm^{-3}
0.0	1.91	0.0	-
0.009	0.63	31	1.05
0.0278	0.39	43	3.46
0.126	0.18	64	15.2

TABLE IX

Allene Experiments

Reactants: C_3H_4, H — Linear Flow Rate: 236 cm sec^{-1}

Temperature: 30°C — Total Pressure: 0.43 mm

Initial (H_2): 2.29×10^{-8} mole cm^{-3}

Mole % C_3H_4	Mole % H	d ln (H) /dt / sec^{-1}	(C_3H_4) / 10^{-11} mole cm^{-3}
-	9.50	-	-
0.0334	3.05	25.8	0.77
0.0840	2.50	31.8	1.92
0.162	2.02	36.8	3.71
0.406	1.48	43.0	9.3
0.576	1.17	49.6	13.2

TABLE X

Allene Experiments

Reactants: C_3H_4, H — Linear Flow Rate: 287 cm sec^{-1}

Temperature: 88°C — Total Pressure: 0.43 mm

Initial (H_2): 1.92×10^{-8} mole cm^{-3}

Mole % C_3H_4	Mole % H	d ln (H) /dt / sec^{-1}	(C_3H_4) / 10^{-11} mole cm^{-3}
-	8.76	-	-
0.0136	3.24	26.9	0.26
0.0244	2.33	35.9	0.46
0.128	1.48	48.1	2.46
0.219	1.08	56.7	4.21

TABLE XI

Allene Experiments

Reactants: C_3H_4, H

Temperature: 185°C

Initial (H_2): 1.52×10^{-8} mole cm^{-3}

Linear Flow Rate: 343 cm sec^{-1}

Total Pressure: 0.43 mm

Mole % C_3H_4	Mole % H	$\frac{d \ln (H)/dt}{sec^{-1}}$	$\frac{(C_3H_4)}{10^{-11} \text{ mole } cm^{-3}}$
-	6.90	-	-
0.0388	2.36	32.5	0.60
0.171	1.62	45.9	2.6
0.342	1.04	60.0	5.2

TABLE XII

Ammonia Experiments

Reactants: NH_3, H

Temperature: 24.5°C

Initial (H_2): 2.22×10^{-8} moles cm^{-3}

Linear Flow Rate: 2.30×10^{2} cm sec^{-1}

Total Pressure: 0.412 mm

Mole % NH_3	Mole % H	$\frac{d \ln(H)/dt}{sec^{-1}}$	$\frac{NH_3}{10^{-11} \text{ moles } cm^{-3}}$
0.0	4.72	0.0	0.0
0.0254	4.16	8.9	0.564
0.0778	3.64	17.8	1.73
0.144	3.34	23.7	3.20
0.367	3.50	20.5	8.14

Mole % H estimated error ±0.12

TABLE XIII

Ammonia Experiments

Reactants: NH_3, H

Temperature: 110°C

Initial (H_2): 1.74×10^{-8} moles cm^{-3}

Linear Flow Rate: 2.95×10^2 cm sec^{-1}

Total Pressure: 0.414 mm

Mole % NH_3	Mole % H	$\frac{d \ln (H)/dt}{sec^{-1}}$	$\frac{(NH_3)}{10^{-11} \text{ moles } cm^{-3}}$
0.0	2.89	0.0	0.0
0.0663	2.74	4.5	1.15
0.139	2.49	13.0	2.42
0.218	2.44	14.6	3.80

Mole % H estimated error ± 0.13

TABLE XIV

Ammonia Experiments

Reactants: NH_3, H

Temperature: 169°C

Initial (H_2): 1.51×10^{-8} moles cm^{-3}

Linear Flow Rate: 3.41×10^2 cm sec^{-1}

Total Pressure: 0.414 mm

Mole % NH_3	Mole % H	$\frac{(NH_3)}{10^{-11} \text{ moles } cm^{-3}}$
0.0	2.07	0.0
0.00514	2.05	0.078
0.0419	2.05	0.631
0.121	2.32	1.82

Mole % H estimated error ± 0.40

TABLE XV

Benzene Experiments

Reactants: C_6H_6, H
Linear Flow Rate: 2.12×10^2 cm sec^{-1}
Temperature: 22°C
Total Pressure: 0.435 mm
Initial (H_2): 2.35×10^{-8} moles cm^{-3}

Mole % C_6H_6	Mole % H	d ln (H)/dt / sec^{-1}	(C_6H_6) / 10^{-12} moles cm^{-3}
0.0	7.85	0.0	-
0.00077	6.03	9.1	0.180
0.0025	5.20	14.3	0.579
0.0165	4.08	22.8	3.88
0.0376	3.55	27.6	8.84
0.0650	2.71	36.9	15.3
0.0720	2.45	40.5	16.5

TABLE XVI

Benzene Experiments

Reactants: C_6H_6,H
Linear Flow Rates: 2.94×10^2 cm sec^{-1}
Temperature: 120°C
Total Pressure: 0.43 mm
Initial (H_2): 1.76×10^{-8} moles cm^{-3}

Mole % C_6H_6	Mole % H	d ln (H) /dt / sec^{-1}	(C_6H_6) / 10^{-12} moles cm^{-3}
0.0	8.19	0.0	-
0.00455	5.78	17.3	0.800
0.00654	5.93	16.6	1.15
0.0165	4.61	27.6	2.90
0.0464	5.23	22.2	8.15
0.0612	3.14	44.6	10.8

TABLE XVII

Benzene Experiments

Reactants: C_6H_6, H Linear Flow Rate: 397 cm sec^{-1}

Temperature: 237°C Total Pressure: 0.388 mm

Initial (H_2): 1.22×10^{-8} mole cm^{-3}

Mole % C_6H_6	Mole % H	d ln (H)/dt sec^{-1}	(C_6H_6) 10^{-13} mole cm^{-3}
0.0	2.78	0.0	-
0.00071	1.51	27.4	0.87
0.0013	0.93	49.1	1.52
0.0067	0.58	70.4	8.14

TABLE XVIII

1, 3-Butadiene Experiments

Reactions: C_4H_6, H Linear Flow Rate: 241 cm sec^{-1}

Temperature: 30°C Total Pressure: 0.43 mm

Initial (H_2): 2.29×10^{-8} mole cm^{-3}

Mole % C_4H_6	Mole % H	d ln (H)/dt sec^{-1}	(C_4H_6) 10^{-11} mole cm^{-3}
-	13.0	-	-
.0462	3.25	33.6	1.06
.126	2.58	39.2	2.88
.234	1.85	47.3	5.13
.265	2.06	44.5	6.06
.268	1.40	54.0	6.14
1.37	0.69	71.2	31.4

TABLE XIX

1, 3-Butadiene Experiments

Reactants: C_4H_6, H
Temperature: 30°C
Initial (H_2): 2.29×10^{-8} mole cm^{-3}
Linear Flow Rate: 227 cm sec^{-1}
Total Pressure: 0.43 mm

Mole % C_4H_6	Mole % H	d ln (H) /dt / sec^{-1}	(C_4H_6) / 10^{-11} mole cm^{-3}
-	11.3	-	-
.0044	3.97	23.8	0.10
.0054	4.14	22.2	0.12
.0099	3.60	25.2	0.23
.0280	2.93	29.8	0.64
.0416	2.43	33.9	0.96
.0820	2.12	36.9	1.88
.206	1.82	40.3	4.72
.327	1.48	44.9	7.5
.473	1.44	45.6	10.8
.580	1.21	49.3	13.3

TABLE XX

1, 3-Butadiene Experiments

Reactants: C_4H_6, H

Temperature: 98°C

Initial (H_2): 1.92×10^{-8} mole cm^{-3}

Linear Flow Rate: 282 cm sec^{-1}

Total Pressure: 0.44 mm

Mole % C_4H_6	Mole % H	d ln (H)/dt / sec^{-1}	(C_4H_6) / 10^{-11} mole cm^{-3}
-	10.3	-	-
0.0212	3.06	31.6	0.41
0.0474	2.32	38.9	0.91
0.106	1.80	45.5	2.04
0.259	1.25	54.8	4.97

TABLE XXI

1, 3-Butadiene Experiments

Reactants: C_4H_6, H

Temperature: 193°C

Initial (H_2): 1.49×10^{-8} mole cm-3

Linear Flow Rate: 378 cm sec^{-1}

Total Pressure: 0.43 mm

Mole % C_4H_6	Mole % H	d ln (H)/dt / sec^{-1}	(C_4H_6) / 10^{-11} mole cm^{-13}
-	6.65	-	-
0.0123	1.96	39.4	0.18
0.0137	2.36	33.3	0.20
0.0179	1.69	43.9	0.27
0.038	1.55	46.7	0.57
0.0747	1.11	57.5	1.11
0.194	0.57	79.1	2.90

TABLE XXII

Cis-butene-2 Experiments

Reactants: C_4H_8, H — Linear Flow Rate: 222 cm sec^{-1}

Temperature: 28°C — Total Pressure: 0.392 mm

Initial (H_2): 2.09×10^{-8} mole cm^{-3}

Mole % C_4H_8	Mole % H	d ln(H)/dt sec^{-1}	(C_4H_8) 10^{-12} mole cm^{-3}
-	2.90	-	-
0.0039	1.80	9.9	0.81
0.0131	1.74	10.5	2.24
0.0223	1.31	15.8	4.66
0.0553	1.19	18.2	11.6
0.0615	1.14	19.3	12.9
0.219	0.70	29.3	45.7

TABLE XXIII

Cis-butene-2 Experiments

Reactants: C_4H_8, H — Linear Flow Rates 254 cm sec^{-1}

Temperature: 74°C — Total Pressure: 0.432 mm

Initial (H_2): 1.99×10^{-8} mole cm^{-3}

Mole % C_4H_8	Mole % H	d ln(H)/dt sec^{-1}	(C_4H_8) 10^{-11} mole cm^{-3}
-	7.74	-	-
0.0011	4.45	12.7	0.023
0.0050	3.40	19.0	0.100
0.0056	3.75	16.8	0.115
0.0071	3.16	20.6	0.141
0.0093	1.99	31.4	0.185
0.0102	2.87	23.0	0.203
0.0292	1.41	39.3	0.581
0.102	0.94	48.8	2.03
0.218	0.59	59.7	4.34

TABLE XXIV

Cis-butene-2 Experiments

Reactants: C_4H_8, H — Linear Flow Rate: 323 cm sec^{-1}

Temperature: 159°C — Total Pressure: 0.432

Initial (H_2): 1.60×10^{-8} mole cm^{-3}

Mole % C_4H_8	Mole % H	d ln(H)/dt sec^{-1}	(C_4H_8) 10^{-12} mole cm^{-3}
--	8.45	-	
0.0011	4.93	13.6	0.18
0.0018	4.05	18.5	0.28
0.0154	3.16	24.6	2.46
0.0226	2.70	28.7	3.62
0.0750	1.88	37.8	12.0

TABLE XXV

Trans-butene-2 Experiments

Reactants: C_4H_8,H — Linear Flow Rate: 220 cm sec^{-1}

Temperature 23°C — Total Pressure: 0.432 mm

Initial (H_2): 2.34×10^{-8} mole cm^{-3}

Mole % C_4H_8	Mole % H	d ln (H)/dt sec^{-1}	(C_4H_8) 10^{-11} mole cm^{-3}
-	11.1	-	-
0.0246	4.27	20.1	0.58
0.0411	3.45	24.0	0.96
0.0512	3.09	26.3	1.20
0.101	2.69	29.1	2.36
0.194	2.34	32.0	4.54
0.320	2.04	34.8	7.49
0.612	1.78	37.6	14.3
0.466	1.44	42.0	10.9
0.663	1.14	46.7	15.5

TABLE XXVI

Carbon Monoxide Experiments

Reactants: CO, H
Temperature: 28°C
Initial (H_2): 2.3 x 10^8 mole cm^{-3}

Linear Flow Rate: 244 cm sec^{-1}
Total Pressure: 0.43 mm

Mole % CO	Mole % H	d ln(H)/dt / sec^{-1}	(CO) / 10^{-11} mole cm^{-3}
-	8.0	-	-
0.002	7.5	1.6	0.04
0.009	7.0	3.3	0.21
0.034	7.0	3.3	0.79
0.091	7.1	3.1	2.1
0.156	7.0	3.3	3.6

TABLE XXVII

Carbonyl Sulfide Experiments

Reactants: COS, H
Temperature: 28°C
Initial (H_2): 2.3 x 10^8 mole cm^{-3}

Linear Flow Rate: 226 cm sec^{-1}
Total Pressure: 0.43 mm

Mole % COS	Mole % H	d ln(H)/dt / sec^{-1}	(COS) / 10^{-11} mole cm^{-3}
-	10.0	-	-
0.003	7.2	8.0	0.07
0.007	6.5	10.3	0.17
0.019	5.0	16.4	0.44
0.040	3.8	23.0	0.92
0.088	2.6	32.2	2.03
0.138	2.2	36.2	3.17
0.328	1.6	43.0	7.55
0.530	0.94	55.6	12.2

TABLE XXVIII

Carbonyl Sulfide Experiments

Reactants: COS, H
Temperature: $28^{\circ}C$
Initial (H_2): 2.3×10^{-8} mole cm^{-3}

Linear Flow Rate: 239 cm sec^{-1}
Total Pressure: 0.43 mm

Mole % COS	Mole % H	d ln (H)/dt / sec^{-1}	(COS) / 10^{-11} mole cm^{-3}
-	10.3	-	-
0.072	3.3	28.9	1.65
0.124	1.0	58.0	2.85
0.139	1.4	50.0	3.2
0.296	0.81	60.0	6.8
0.459	0.57	74.5	10.6

TABLE XXIX

Carbonyl Sulfide Experiments

Reactants: COS, H
Temperature: $92^{\circ}C$
Initial (H_2): 1.9×10^{-8} mole cm^{-3}

Linear Flow Rate: 279 cm sec^{-1}
Total Pressure: 0.43 mm

Mole % COS	Mole % H	d ln (H)/dt / sec^{-1}	(COS) / 10^{-11} mole cm^{-3}
-	6.8	-	-
0.007	2.0	32.6	0.13
0.020	1.5	41.0	0.38
0.057	1.1	49.8	1.1
0.114	0.54	68.4	2.2

TABLE XXX

Ethane Experiments

Reactants: C_2H_6, H Linear Flow Rate: 2.56×10^2 cm sec^{-1}

Temperature: 24°C Total Pressure: 0.45 mm

Initial (H_2): 2.44×10^{-8} moles cm^{-3}

Mole % C_2H_6	(C_2H_6) 10^{-11} moles cm^{-3}	Mole % H
0.0	-	4.89
0.0446	1.09	4.78
0.0617	1.51	4.75
0.0664	1.62	4.86
0.101	2.46	4.75
0.127	3.11	4.75
0.155	3.78	4.75

The variations in mole % H shown here are not significant because the observed variation is less than the estimated error, ± 0.3, in determining mole % H.

TABLE XXXI

Ethane Experiments

Reactants: C_2H_6, H Linear Flow Rate: 3.95×10^2 cm sec^{-1}

Temperature: 75°C Total Pressure: 0.45 mm

Initial (H_2): 2.08×10^{-8} moles cm^{-3}

Mole% C_2H_6	(C_2H_6) 10^{-12} moles cm^{-3}	Mole % H
0.0	-	3.49
0.0086	1.79	3.77
0.0157	3.28	3.77
0.0312	6.50	3.28
0.0713	14.8	2.79
0.156	32.4	3.35
0.192	40.0	3.32

The variations in mole % H shown here are not significant because the observed variation is generally less than the estimated error, ± 0.6, in determining mole % H.

TABLE XXXII

Ethane Experiments

Reactants: C_2H_6, H — Linear Flow Rate: 3.96×10^2 cm sec^{-1}

Temperature: 170°C — Total Pressure: 0.45 mm

Initial (H_2): 1.58×10^{-8} moles cm^{-3}

Mole % C_2H_6	$\frac{(C_2H_6)}{10^{-12} \text{ moles cm}^{-3}}$	Mole % H
0	-	3.47
0.00117	0.185	3.07
0.00179	0.283	3.34
0.00410	0.648	3.34
0.00835	1.32	3.62
0.0282	4.46	3.62
0.0454	7.19	3.77
0.0784	12.4	3.77
0.173	27.3	3.07

The variations in mole % H shown here are not significant because the observed variation is less than the estimated error, ± 0.4, in determining mole % H.

TABLE XXXIII

Ethylene Experiments

Reactants: C_2H_4, H — Linear Flow Rate: 2.48×10^2 cm sec^{-1}

Temperature: 24°C — Total Pressure: 0.448 mm

Initial (H_2): 2.35×10^{-8} moles cm^{-3}

Mole % C_2H_4	Mole % H	$\frac{d \ln (H)/dt}{sec^{-1}}$	$\frac{(C_2H_4)}{10^{-10} \text{ moles cm}^{-3}}$
0.0	5.84	0.0	-
0.00946	4.77	10.6	0.023
0.0144	3.98	16.2	0.035
0.0376	3.37	21.2	0.091
0.0646	3.20	22.7	0.156
0.148	2.72	27.6	0.356
0.537	1.42	47.4	1.30

TABLE XXXIV

Ethylene Experiments

Reactants: C_2H_4, H Linear Flow Rate: 3.02×10^2 cm sec^{-1}

Temperature: 78.2°C Total Pressure: 0.448 mm

Initial (H_2) 2.05×10^{-8} mole cm^{-3}

Mole % C_2H_4	Mole % H	d ln (H)/dt sec^{-1}	(C_2H_4) 10^{-11} moles cm^{-3}
0.0	3.94	0.0	-
0.00109	3.06	8.8	0.022
0.00233	3.10	8.2	0.047
0.0214	2.71	12.9	0.439
0.130	1.68	29.2	2.66
0.467	0.46	73.5	9.59

TABLE XXXV

Ethylene Experiments

Reactants: C_2H_4, H Linear Flow Rate: 3.92×10^2 cm sec^{-1}

Temperature: 167.0°C Total Pressure: 0.436 mm

Initial (H_2): 1.63×10^{-8} mole cm^{-3}

Mole % C_2H_4	Mole % H	d ln (H) /dt sec^{-1}	(C_2H_4) 10^{-11} moles cm^{-3}
0.0	2.35	0.0	-
0.00936	2.24	2.0	0.153
0.0271	1.05	32.5	0.442
0.0432	1.51	17.9	0.704
0.121	0.671	50.5	1.97
0.233	0.14	113.0	3.80

TABLE XXXVI

Ethylene Experiments

Reactants: C_2H_4, H

Linear Flow Rate: 363 cm sec^{-1}

Temperature: 220°C

Total Pressure: 0.392 mm

Initial (H_2): 1.27×10^{-8} mole cm^{-3}

Mole % C_2H_4	Mole % H_1	d ln (H_1)/dt / sec^{-1}	(C_2H_4) / 10^{-12} mole cm^{-3}
0.0	1.87	0.0	-
0.0011	1.62	3.8	0.14
0.0067	1.44	6.9	0.85
0.0185	1.15	12.9	2.35
0.0204	1.33	9.0	2.59
0.0427	0.72	25.1	5.42

TABLE XXXVII

Ethylene Experiments

Reactants: C_2H_4, H

Linear Flow Rate: 415 cm sec^{-1}

Temperature: 291°C

Total Pressure: 0.392 mm

Initial (H_2): 1.12×10^{-8} mole cm^{-3}

Mole % C_2H_4	Mole % H_1	d ln(H_1)/dt / sec^{-1}	(C_2H_4) / 10^{-12} mole cm^{-3}
0.0	2.84	0.0	0.0
0.0063	1.96	9.4	0.70
0.0414	0.60	39.9	4.64

TABLE XXXVIII

Ethylene Oxide Experiments

Reactants: C_2H_4O, H

Linear Flow Rate: 230 cm sec^{-1}

Temperature: 25°C

Total Pressure: 0.432 mm

Initial (H_2): 2.34×10^{-8} mole cm^{-3}

Mole % C_2H_4O	Mole % H	d ln (H)/dt sec^{-1}	(C_2H_4O) 10^{-11} mole cm^{-3}
--	10.8	--	--
0.0537	5.65	17.1	1.26
0.0694	4.92	21.5	1.62
0.0994	4.33	23.9	2.32
0.278	3.84	26.9	6.50
0.466	4.20	24.7	10.9

TABLE XXXIX

Fluorobenzene Experiments

Reactants: C_6H_5F, H

Linear Flow Rate: 228 cm sec^{-1}

Temperature: 31°C

Total Pressure: 0.386 mm

Initial (H_2): 2.04×10^{-8} mole cm^{-3}

Mole % C_6H_5F	Mole % H_1	d ln $(H_1)/dt$ sec^{-1}	Mole % H_2	d ln$(H_2)/dt$ sec^{-1}	(C_6H_5F) 10^{-12} mole cm^{-3}
0.0	3.25	0.0	2.43	0.0	--
0.0015	2.48	8.1	0.96	12.3	0.31
0.0033	2.07	13.5	0.73	15.9	0.68
0.0104	1.68	19.8	0.42	23.2	2.12
0.0275	1.42	24.8	0.26	29.6	5.61
0.0434	1.07	33.3	0.13	38.8	8.83

The subscript 1 refers to data obtained at the first gauge and 2, to data obtained at the second Wrede gauge port, 9.6 cm downstream.

TABLE XL

Hexene-1 Experiments

Reactants: C_6H_{12}, H

Linear Flow Rate: 189 cm sec^{-1}

Temperature: 24°C

Total Pressure: 0.26 mm

Initial (H_2): 1.40×10^{-8} mole cm^{-3}

Mole % Hexene-1	(C_6H_{12}) 10^{-12} mole cm^{-3}	Mole% H_1	Mole % H_2	kc 10^{11} cm^3 $mole^{-1}$ sec^{-1}
0.0	0.0	5.96	4.82	*
0.0041	0.57	2.12	1.41	*
0.0099	1.39	2.00	1.65	*
0.0379	5.31	1.35	1.06	1.15
0.107	15.0	0.957	0.598	3.60
			average	2.4

TABLE XLI

Methane Experiments

Reactants: CH_4,H

Linear Flow Rate: 414 cm sec^{-1}

Temperature: 240°C

Total Pressure: 0.43 mm

Initial (H_2): 1.35×10^{-8} mole cm^{-3}

Mole % CH_4	Mole % H_1	Mole % H_2	$d\ln(H_1)/dt$ sec^{-1}	$d\ln(H_2)/dt$ sec^{-1}	(CH_4) 10^{-11} mole cm^{-3}
-	6.7	5.3	-	-	-
0.009	5.2	4.3	8.2	4.0	0.12
0.023	4.5	3.4	13.2	7.9	0.31
0.051	4.3	3.6	14.3	7.0	0.69
0.069	4.1	2.9	16.1	11.2	0.93
0.125	4.1	3.0	15.7	10.6	1.69

TABLE XLII

Methyl Alcohol Experiments

Reactants: CH_3OH, H — Linear Flow Rate: 218 cm sec^{-1}

Temperature: 31°C — Total Pressure: 0.43 mm

Initial (H_2): 2.28×10^{-8} mole cm^{-3}

Mole % CH_3OH	Mole % H	$d\ell n(H)/dt$ sec^{-1}	(CH_3OH) 10^{-11} mole cm^{-3}
-	6.8	-	-
0.002	6.4	0.7	0.05
0.004	5.7	1.9	0.09
0.018	4.5	4.7	0.41
0.056	3.6	7.3	1.29
0.124	2.8	9.9	2.83
0.352	2.7	10.4	8.03
0.571	2.5	11.4	13.0
0.80	2.5	11.4	18.3
1.06	2.5	11.4	24.2

TABLE XLIII

Nitrogen Experiments

Reactants: N_2, H — Linear Flow Rate: 222 cm sec^{-1}

Temperature: 25°C — Total Pressure: 0.421 mm

Initial (H_2): 2.26×10^{-8} mole cm^{-3}

Mole % N_2	Mole % H	(N_2) 10^{-11} mole cm^{-3}
-	10.9	-
0.011	10.9	0.25
0.061	10.9	1.38
0.603	10.8	13.6

TABLE XLIV

Nitrogen Experiments

Reactants: N_2, H
Linear Flow Rate: 387 cm sec^{-1}
Temperature: 222°C
Total Pressure: 0.422 mm
Initial (H_2): 1.37×10^{-8} mole cm^{-3}

Mole % N_2	Mole % H	$\frac{(N_2)}{10^{-11}\ \text{mole cm}^{-3}}$
-	4.1	-
0.053	4.1	0.73
0.54	4.1	7.4

TABLE XLV

Propylene Experiments

Reactants: C_3H_6, H
Linear Flow Rate: 188 cm sec^{-1}
Temperature: 26°C
Total Pressure: 0.246 mm
Initial (H_2): 1.43×10^{-8} mole cm^{-3}

Mole % C_3H_6	$\frac{(C_3H_6)}{10^{-11}\ \text{mole cm}^{-3}}$	Mole % H (detector 1)	Mole % H (detector 2)	$(H_1)/(H_2)$
0.0	-	5.10	3.03	1.68
0.0097	0.139	4.45	2.32	1.92
0.0530	0.759	3.80	2.05	1.85
0.154	2.20	3.00	1.69	1.77
0.294	4.21	2.27	1.64	1.38
0.603	8.63	2.02	1.24	1.63
1.31	18.7	1.13	0.71	1.59

TABLE XLVI

Propylene Experiments

Reactants: C_3H_6, H

Linear Flow Rate: 246 cm sec^{-1}

Temperature: 119°C

Total Pressure: 0.264 mm

Initial (H_2): 1.08×10^{-8} mole cm^{-3}

Mole % C_3H_6	(C_3H_6) / 10^{-11} mole cm^{-3}	Mole % H (detector 1)	Mole % H (detector 2)
0.0	-	5.57	4.40
0.0053	0.0574	4.05	3.22
0.0459	0.497	2.11	1.91
0.188	2.04	1.70	0.36

TABLE XLVII

Propylene Experiments

Reactants: C_3H_6, H

Linear Flow Rate: 307 cm sec^{-1}

Temperature: 183°C

Total Pressure: 0.264 mm

Initial (H_2): 9.29×10^{-9} mole cm^{-3}

Mole % C_3H_6	(C_3H_6) / 10^{-11} mole cm^{-3}	Mole % H (detector 1)	Mole % H (detector 2)	k_c / cm^3 $mole^{-1}$ sec^{-1}
0.0	-	4.90	5.37	*
0.0060	0.0556	3.85	3.40	*
0.0094	0.0872	3.08	2.83	*
0.0308	0.286	2.57	1.70	*
0.168	1.56	1.29	1.13	2.64×10^{11}
0.856	8.04	1.03	0.566	2.36×10^{11}
			average	2.50×10^{11}

TABLE XLVIII

Propylene Experiments

Reactants: C_3H_6, H — Linear Flow Rate: 351 cm sec^{-1}

Temperature: 249°C — Total Pressure: 0.264 mm

Initial (H_2): 8.11×10^{-9} mole cm^{-3}

	Mole % C_3H_6	(C_3H_6) / 10^{-11} mole cm^{-3}	Mole % H (detector 1)	Mole % H (detector 2)	k_c / 10^{-11} cm^3 $mole^{-1}$ sec^{-1}
A.	0.0	-	5.65	5.66	*
	0.0080	0.0646	4.62	3.96	*
	0.0232	0.188	3.60	2.83	*
	0.0696	0.565	3.22	2.83	*
	0.1250	2.03	2.57	1.70	*
	1.12	9.09	2.57	0.85	*
	1.76	14.2	2.31	0.85	*
B.		10.00	2.4	0.90	3.2
		5.00	2.5	1.3	4.3
	0.250	2.03	2.6	1.7	5.7
	-	2.00 - 14.2	-	-	4.2

TABLE XLIX

Vinyl Chloride Experiments

Reactants: C_2H_3Cl, H — Linear Flow Rate: 223 cm sec^{-1}

Temperature: 26°C — Total Pressure: 0.388 mm

Initial (H_2): 2.08×10^{-8} mole cm^{-3}

Mole % C_2H_3Cl	Mole % H	d ln(H)/dt / sec^{-1}	(C_2H_3Cl) / 10^{-11} mole cm^{-3}
0.0	4.71	0	-
0.0370	2.58	12.8	0.774
0.0540	1.91	19.2	1.13
0.0712	1.62	22.6	1.48
0.0773	1.23	28.5	1.61
0.116	1.41	25.4	2.42
0.195	1.28	27.6	4.07
0.253	1.04	32.2	5.23
0.338	0.79	38.0	7.06
0.436	0.58	44.4	9.10

TABLE L

Vinyl Chloride Experiments

Reactants: C_2H_3Cl, H

Temperature: 75°C

Initial (H_2): 1.79×10^{-8} mole cm^{-3}

Linear Flow Rate: 260 cm sec^{-1}

Total Pressure: 0.388 mm

Mole % C_2H_3Cl	Mole % H_1	$d \ln(H_1)/dt$ sec^{-1}	Mole % H_2	$d \ln(H_2)/dt$ sec^{-1}	(C_2H_3Cl) 10^{-11} mole cm^{-3}
0.0	3.71	0.0	3.81	0.0	-
0.0135	2.67	8.0	2.32	6.2	0.242
0.0540	2.32	10.9	1.47	11.9	0.965
0.140	1.74	17.5	0.84	18.9	2.50
0.223	1.28	24.7	0.80	19.5	3.99
0.391	0.55	44.3	-	-	7.00

TABLE LI

Vinyl Chloride Experiments

Reactants: C_2H_3Cl, H

Temperature: 153°C

Initial (H_2): 1.46×10^{-8} mole cm^{-3}

Linear Flow Rate: 317 cm sec^{-1}

Total Pressure: 0.388 mm

Mole % C_2H_3	Mole % H	$d \ln(H)/dt$ sec^{-1}	(C_2H_3Cl) 10^{-11} mole cm^{-3}
-	2.78	0.0	-
0.0113	2.32	4.9	0.165
0.0498	1.47	16.7	0.726
0.204	0.90	29.9	2.98
0.315	0.75	34.7	4.60
0.461	0.43	49.5	6.72

TABLE LII

1,3-Butadiene Experiments

Reactants: C_4H_6, H

Linear Flow Rate: 170 cm sec^{-1}

Temperature: 30°C

Total Pressure: 0.226 mm

Initial (H_2): 1.20×10^{-8} mole cm^{-3}

Mole % C_4H_6	Mole % H	d ln (H)/dt sec^{-1}	(C_4H_6) 10^{-11} mole cm^{-3}
-	14.4	-	-
0.0036	4.18	10.9	0.04
0.0043	3.88	11.6	0.05
0.0055	4.18	10.9	0.06
0.0067	3.56	12.4	0.08
0.0276	2.94	14.0	0.33
0.0295	2.94	14.0	0.35
0.0428	2.64	15.0	0.51
0.0436	2.94	14.0	0.52
0.0824	2.02	17.4	0.99
0.0980	1.94	17.8	1.17
0.128	1.94	17.8	1.54
0.150	2.02	17.4	1.80

TABLE LIII

1,3-Butadiene Experiments

Reactants: C_4H_6, H

Linear Flow Rate: 197 cm sec^{-1}

Temperature: 30°C

Total Pressure: 0.31 mm

Initial (H_2): 1.61×10^{-8} mole cm^{-3}

Mole % C_4H_6	Mole % H	d ln (H)/dt sec^{-1}	(C_4H_6) 10^{-11} mole cm^{-3}
-	13.0	-	-
0.0486	2.36	24.2	0.78
0.139	2.38	24.1	2.24
0.245	1.79	28.2	3.94
0.486	1.45	31.1	7.76
0.909	0.99	36.5	14.6

TABLE LIV

1,3-Butadiene Experiments

Reactants: C_4H_6, H

Linear Flow Rate: 275 cm sec^{-1}

Temperature: 30°C

Total Pressure: 0.68 mm

Initial (H_2): 3.60×10^{-8} mole cm^{-3}

Mole % C_4H_6	Mole % H	d ln (H)/dt sec^{-1}	(C_4H_6) 10^{-11} mole cm^{-3}
-	8.92	-	-
0.0632	3.04	39.4	2.28
0.218	2.28	50.0	7.85
1.34	1.71	60.5	48.3
1.55	0.76	90.1	55.8

TABLE LV

1,3-Butadiene Experiments

Reactants: C_4H_6, H Linear Flow Rate: 304 cm sec^{-1}

Temperature: 30°C Total Pressure: 0.99 mm

Initial (H_2): 5.22×10^{-8} mole cm^{-3}

Mole % C_4H_6	Mole % H	d ln (H)/dt sec^{-1}	(C_4H_6) 10^{-11} mole cm^{-3}
-	7.34	-	-
0.0098	3.2	43.0	0.57
0.0916	2.48	53.6	4.78
0.0939	2.48	53.6	4.90
0.478	1.55	76.2	25.0

TABLE LVI

1,3-Butadiene Experiments

Reactants: C_4H_6, H Linear Flow Rate: 104 cm sec^{-1}

Temperature: 30°C Total Pressure: 0.99 mm

Initial (H_2): 5.22×10^{-8} mole cm^{-3}

Mole % C_4H_6	Mole % H	d ln (H)/dt sec^{-1}	(C_4H_6) 10^{-11} mole cm^{-3}
-	8.28	-	-
0.006	3.72	8.35	0.33
0.0103	3.10	10.2	0.53
0.0312	2.48	12.6	1.63
0.0647	2.08	14.5	3.38
0.264	0.93	22.8	13.8

TABLE LVII

1,3-Butadiene Pressure Variation Experiments

Pressure / mm	k_c / 10^{11} cm^3 mole^{-1} sec^{-1}
0.226	-
0.31	0.78
0.43	1.1
0.43	0.91
0.68	0.86
0.99	1.15
0.99	0.86

TABLE LVIII

Ethylene Experiments

Reactants: C_2H_4, H

Linear Flow Rate: 206 cm sec^{-1}

Temperature: 25°C

Total Pressure: 0.304 mm

Initial (H_2): 1.65×10^{-8} mole cm^{-3}

Mole % C_2H_4	Mole % H_1	d ln(H)/dt / sec^{-1}	(C_2H_4) / 10^{-11} mole cm^{-3}
-	4.97	-	-
0.0183	3.48	5.7	0.30
0.0317	3.11	7.5	0.52
0.0773	2.45	11.4	1.28
0.128	1.93	15.2	2.12
0.225	1.62	18.0	3.72
0.348	1.24	22.3	5.75
0.493	0.87	27.9	8.15

TABLE LVIX

Ethylene Experiments

Reactants: C_2H_4, H Linear Flow Rate: 208 cm sec^{-1}

Temperature: 25°C Total Pressure: 0.408 mm

Initial (H_2): 2.18×10^{-8} mole cm^{-3}

Mole % C_2H_4	Mole % H_1	d ln(H)/dt sec^{-1}	(C_2H_4) 10^{-11} mole cm^{-3}
-	5.10	-	-
0.0089	4.80	1.2	0.19
0.0133	4.13	4.0	0.29
0.0241	3.58	6.9	0.53
0.0609	2.55	13.5	1.33
0.220	1.88	19.5	4.80
0.352	1.48	24.2	7.67

TABLE LX

Ethylene Experiments

Reactants: C_2H_4, H Linear Flow Rate: 244 cm sec^{-1}

Temperature: 25°C Total Pressure: 0.561 mm

Initial (H_2): 3.02×10^{-8} mole cm^{-3}

Mole % C_2H_4	Mole % H_1	d ln(H)/dt sec^{-1}	(C_2H_4) 10^{-11} mole cm^{-3}
-	4.06	-	-
0.0070	2.67	12.6	0.21
0.0131	2.20	18.4	0.40
0.0246	1.86	23.5	0.74
0.0460	1.47	30.4	1.39
0.0718	1.36	32.9	2.16
0.131	1.16	35.9	3.96
0.199	1.04	40.7	6.00
0.406	0.81	48.4	12.3

TABLE LXI

Ethylene Experiments

Pressure mm	k_c 10^{11} cm^3 mole^{-1} sec^{-1}
0.304	2.1
0.408	1.7
0.448	2.2
0.561	1.7

TABLE LXII

Acetylene Experiment Rate Constants and Activation Energy

T/°C	T/°K	T^{-1}/°K^{-1}	k_c/cm^3 mole^{-1} sec^{-1}	E_A/k cal	A'/cm^3 mole^{-1} sec^{-1}
22.5	296	3.38×10^{-3}	1.5×10^{11}		
73	346	2.89×10^{-3}	1.2×10^{11}		
167.6	441	2.27×10^{-3}	3.3×10^{11}		
241	514	1.95×10^{-3}	1.79×10^{12}		
				3.4	2.2×10^{13}

TABLE LXIII

Allene Experimental Rate Constants and Activation Energy

$T/^{o}C$	$T/^{o}K$	$T^{-1}/^{o}K^{-1}$	$k_c/cm^3 mole^{-1} sec^{-1}$	$E_A/kcal\ mole^{-1}$	$A'/cm^3 mole^{-1} sec^{-1}$
30	303	3.3×10^{-3}	1.5×10^{11}		
88	361	2.77×10^{-3}	5.3×10^{11}		
185	458	2.18×10^{-3}	6.1×10^{11}		
				~ 3.4	7.9×10^{13}

TABLE LXIV

Experimental Rate Constants and Activation Energies for 1.3-Butadiene

$T/^{o}C$	$T/^{o}K$	$T^{-1}/^{o}K^{-1}$	$k_c/cm^3 mole^{-1} sec^{-1}$	$E_A/kcal\ mole^{-1}$	$A'/cm^3 mole^{-1} sec^{-1}$
30	303	3.3×10^{-3}	0.9×10^{11}		
30	303	3.3×10^{-3}	1.1×10^{11}		
98	371	2.69×10^{-3}	3.1×10^{11}		
193	466	2.14×10^{-3}	1.2×10^{12}		
				4.0	9.3×10^{13}

TABLE LXV

Benzene Experimental Rate Constants and Activation Energy

$T/^{o}C$	$T/^{o}K$	$T^{-1}/^{o}K^{-1}$	$k_c/cm^3 mole^{-1} sec^{-1}$	$E_A/kcal\ mole^{-1}$	$A'/cm^3 mole^{-1} sec^{-1}$
22	295	3.39×10^{-3}	2.7×10^{12}		
120	393	2.55×10^{-3}	6.5×10^{12}		
237	510	1.96×10^{-3}	3.0×10^{13}		
				2.0	9.6×10^{13}

TABLE LXVI

Experimental Rate Constants and Activation Energies for Cis-butene-2

$T/^{o}C$	$T/^{o}K$	$T^{-1}/^{o}K^{-1}$	$k_c/cm^3 mole^{-1} sec^{-1}$	E_A/kcal mole^{-1}	$A'/cm^3 mole^{-1} sec^{-1}$
28	301	3.32×10^{-3}	3.2×10^{11}		
74	347	2.88×10^{-3}	5.5×10^{11}		
159	432	2.32×10^{-3}	1.26×10^{12}		
				2.8	3.1×10^{13}

TABLE LXVII

Ethylene Experimental Rate Constants and Activation Energy

$T/^{o}C$	$T/^{o}K$	$T^{-1}/^{o}K^{-1}$	$k_c cm^3$ mole^{-1}sec^{-1}	E_A/kcal mole^{-1}	$A'/cm^3 mole^{-1} sec^{-1}$
24	297	3.37×10^{-3}	2.17×10^{11}		
78	351	2.84×10^{-3}	6.46×10^{11}		
167	440	2.27×10^{-3}	2.88×10^{12}		
220	493	2.03×10^{-3}	4.1×10^{12}		
291	564	1.73×10^{-3}	1.05×10^{13}		
				4.7	5.6×10^{14}

TABLE LXVIII

Propylene Experimental Rate Constants and Activation Energy

$T/^{o}C$	$T/^{o}K$	$T^{-1}/^{o}K^{-1}$	$k_c/cm^3 mole^{-1} sec^{-1}$	E_A/kcal mole^{-1}	$A'/cm^3 mole^{-1} sec^{-1}$
183	456	2.19×10^{-3}	2.5×10^{11}		
249	522	1.92×10^{-3}	4.2×10^{11}		
				3.7	1.5×10^{13}

TABLE LXIX

Vinyl Chloride Experimental Rate Constants and Activation Energy

$T/^{\circ}C$	$T/^{\circ}K$	$T^{-1}/^{\circ}K^{-1}$	$k_c/cm^3 mole^{-1} sec^{-1}$	$E_A/kcal\ mole^{-1}$	$A'/cm^3 mole^{-1} sec^{-1}$
26	299	3.34×10^{-3}	2.8×10^{11}		
75	348	2.87×10^{-3}	4.3×10^{11}		
153	426	2.35×10^{-3}	5.5×10^{11}		
				1.34	2.8×10^{12}

TABLE LXX

Small Tube Diameter Ethylene Experiment

Reactants: C_2H_4, H

Temperature: $25^{\circ}C$

Initial (H_2): 1.66×10^{-8} mole cm^{-3}

Linear Flow Rate: 714 cm sec^{-1}

Total Pressure: 0.304 mm

Flow Tube Diameter: 2.6 cm

Mole % C_2H_4	Mole % H_1	d ln(H)/dt sec^{-1}	(C_2H_4) 10^{-11} mole cm^{-3}
-	8.94	-	-
0.0027	4.23	77	0.044
0.0073	3.66	91	0.12
0.0178	3.10	109	0.30
0.0422	2.67	124	0.70
0.114	2.44	134	1.89
0.163	2.08	149	2.71
0.220	1.77	165	3.65
0.425	1.74	167	7.05
0.658	1.74	167	10.9

TABLE LXXI

Small Tube Diameter Ethylene Experiment

Reactants: C_2H_4, H — Linear Flow Rate: 849 cm sec^{-1}

Temperature: 25°C — Total Pressure: 0.389 mm

Initial (H_2): 2.1×10^{-8} mole cm^{-3} — Flow Tube Diameter: 2.6 cm

Mole % C_2H_4	Mole % H_1	d ln(H)/dt / sec^{-1}	(C_2H_4) / 10^{-11} mole cm^{-3}
-	6.22	-	-
0.124	3.01	100	2.60
0.155	2.54	124	3.26
0.293	2.16	146	6.15
0.466	2.28	138	9.80
0.666	2.28	138	14.0

TABLE LXXII

Boron Trifluoride Experiments

Reactants: BF_3, H — Linear Flow Rate: 236 cm sec^{-1}

Temperature: 28°C — Total Pressure: 0.43 mm

Initial (H_2): 2.3×10^{-8} mole cm^{-3}

Mole % BF_3	Mole % H_1	Mole % H_2	k_s / sec^{-1}	(BF_3) / 10^{-11} mole cm^{-3}
-	10.3	7.3	8.2	-
0.075	12.2	9.6	5.8	1.7
0.306	-	9.7	-	7.0
1.10	-	9.6	-	25.3
1.81	-	9.7	-	41.6

TABLE LXXIII

Boron Trifluoride Experiments

Reactants: BF_3, H — Linear Flow Rate: 236 cm sec^{-1}

Temperature: 28°C — Total Pressure: 0.43 mm

Initial (H_2): 2.3×10^{-8} mole cm^{-3}

Mole % BF_3	Mole % H_1	Mole % H_2	k_s sec^{-1}	(BF_3) 10^{-11} mole cm^{-3}
-	12.1	9.3	6.3	-
0.013	13.3	11.0	4.5	0.31
0.033	13.4	11.1	4.5	0.76
0.074	13.3	11.2	4.2	1.7
0.010*	0.0	0.0	-	0.22

*Experiment with microwave generator turned off.

TABLE LXXIV

Carbon Tetrafluoride Experiments

Reactants: CF_4, H — Linear Flow Rate: 248 cm sec^{-1}

Temperature: 30°C — Total Pressure: 0.43 mm

Initial (H_2): 2.3×10^{8} mole cm^{-3}

Mole % CF_4	Mole % H_1	Mole % H_2	k_s sec^{-1}	(CF_4) 10^{-11} mole cm^{-3}
-	5.5	4.85	3.1	-
0.034	6.4	-	-	0.78
0.187	6.9	6.2	2.8	4.3
1.09	-	6.3	-	25.1
-	-	6.3	-	-

TABLE LXXV

Nitric Oxide Experiments

Reactants: NO, H — Linear Flow Rate: 2.30×10^{2} cm sec^{-1}

Temperature: $24^{\circ}C$ — Total Pressure: 0.412 mm

Initial (H_2): 2.22×10^{-8} Moles cm^{-3}

Mole % NO	Mole % H	$\frac{d\ln(H)/dt}{sec^{-1}}$	$\frac{(NO)}{10^{-11} \text{ moles cm}^{-3}}$
0.0	2.88	0.0	0.0
0.00345	4.09	-24.0	0.079
0.0269	5.26	-41.4	0.596
0.0634	6.15	-52.1	1.41
0.127	6.05	-51.0	2.82
0.500	7.48	-63.5	11.1
0.0466[a]	0.0	0.0	
0.318[a]	0.0	0.0	

a Experiments for which the microwave discharge was turned off; thus no H atoms were present.

TABLE LXXVI

Nitric Oxide Experiments

Reactants: NO, H — Linear Flow Rate: 3.24×10^{2} cm sec^{-1}

Temperature: $120^{\circ}C$ — Total Pressure: 0.435 mm

Initial (H_2): 1.77×10^{-8} moles cm^{-3}

Mole % NO	Mole % H	$\frac{d\ln(H)/dt}{sec^{-1}}$	$\frac{(NO)}{10^{-11} \text{ moles cm}^{-3}}$
0.0	2.50	0.0	0.0
0.0184	3.26	-25.5	0.326
0.0365	3.75	-39.2	0.646
0.0841	4.30	-52.5	1.49
0.310	5.19	-70.6	5.49

TABLE LXXVII

Water Experiments

(a)

Reactants: H_2O, H Linear Flow Rate: 216 cm sec^{-1}

Temperature: 25°C Total Pressure: 0.422 mm

Initial (H_2): 2.26×10^{-8} mole cm^{-3}

Mole % H_2O	Mole % H_1	Mole % H_2	$\frac{(H_2O)}{10^{-12} \text{ mole cm}^{-3}}$
-	11.0	10.3	-
0.0074	11.0	10.2	1.66
0.0112	11.4	10.8	2.53
0.0174	8.9	10.2	3.93
0.0180	11.6	10.8	4.08
0.0916	10.9	10.1	20.7

(b)

Reactants: H_2O, H Linear Flow Rate: 410 cm sec^{-1}

Temperature: 224°C Total Pressure: 0.422 mm

Initial (H_2): 1.38×10^{-8} mole cm^{-3}

Mole % H_2O	Mole % H_1	Mole % H_2	$\frac{(H_2O)}{10^{-12} \text{ mole cm}^{-3}}$
-	3.3	2.8	-
0.0169	4.6	4.1	2.34
0.0398	6.2	6.2	5.50
0.0876	8.1	8.5	12.1

TABLE LXXVIII

Surface Rate Study Results

Pressure	LFR	Mole %	Mole %	k_s	$(k_s)_d$	y
mm	cm sec^{-1}	H_1	H_2	sec^{-1}	sec^{-1}	
0.371	236	2.55	2.02	5.6	8.0	0.3
0.371	137	3.07	2.20	4.7	9.4	0.5
0.371	64	3.60	2.58	2.2	7.1	0.7
0.371	24	4.35	3.08	0.8	6.2	0.87

The diffusion coefficients for H are taken from Weissman and Mason, J. Chem. Phys. 36,794 (1962).

TABLE LXXIX

Sorbed Species	k'/sec^{-1}
$CH_3 - CH = CH - CH_3$ (trans)	12
$CH_3 - CH = CH - CH_3$ (cis)	14
$CH_2 = CH_2$	16
$CH_2 = CHCl$	18
$CH_2 = CH - CH = CH_2$	31
$CH_2 = C = CH_2$	31
C_6H_6	35

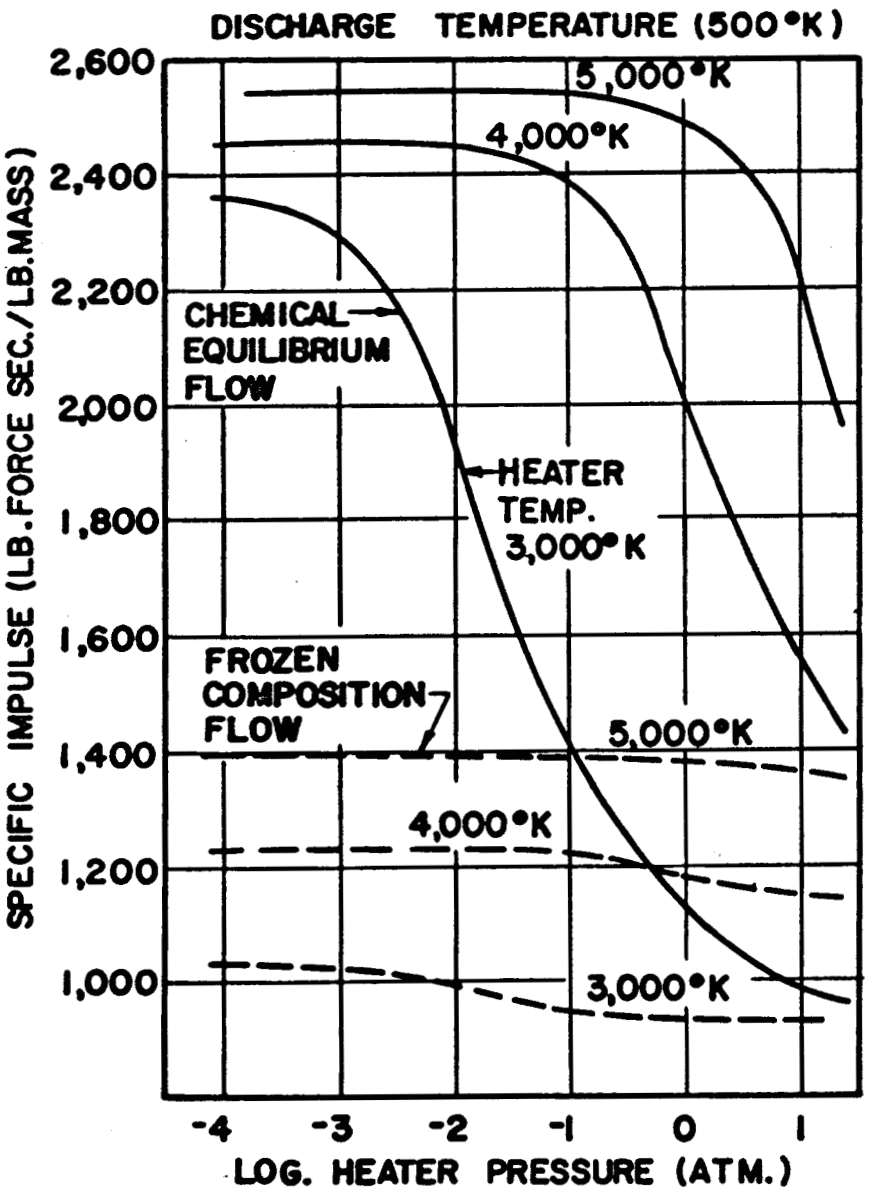

FIG. 1: POTENTIAL HYDROGEN PROPELLANT PERFORMANCE.

FIG. 2: NOZZLE DESIGN CONCEPT

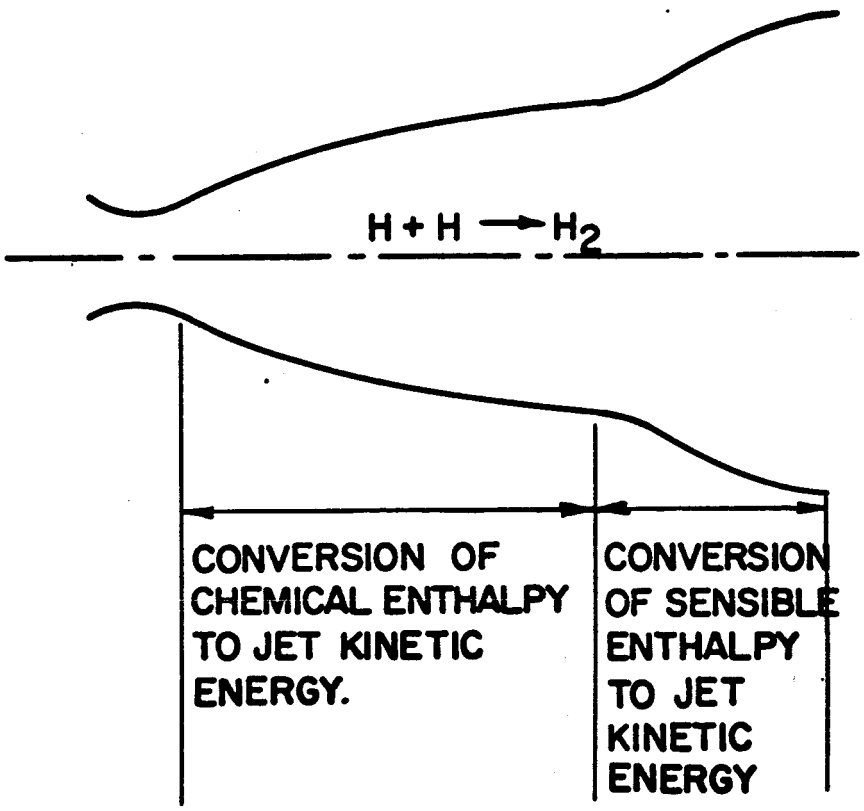

$$I_{SP} = \sqrt{\frac{2J}{g_c}\left[\frac{X(\Delta H_R) + \Delta H_S}{M}\right]}$$

PROPELLANT PERFORMANCE

CHEMICAL ENTHALPY CHANGE $H + H \longrightarrow H_2$ (@ 3000°K) $\quad \frac{\Delta H_R}{M} = 54900$

SENSIBLE ENTHALPY CHANGE $(a\,H + b\,H_2)\,3000°K \rightarrow (a\,H + b\,H_2)\,0$

$$\frac{\Delta H_S}{M} = \begin{bmatrix} 11600\,(a = 0) \\ 14900\,(b = 0) \end{bmatrix}$$

X - WEIGHT FRACTION OF HYDROGEN ATOMS THAT RECOMBINE IN NOZZLE.

ΔH_S - SENSIBLE HEAT CHANGE PER MOLE OF PROPELLANT, CAL / MOLE.

ΔH_R - ENTHALPY OF REACTION PER MOLE OF H_2 FORMED IN NOZZLE, CAL/MOLE.

M - MOLECULAR WEIGHT OF PROPELLANT.

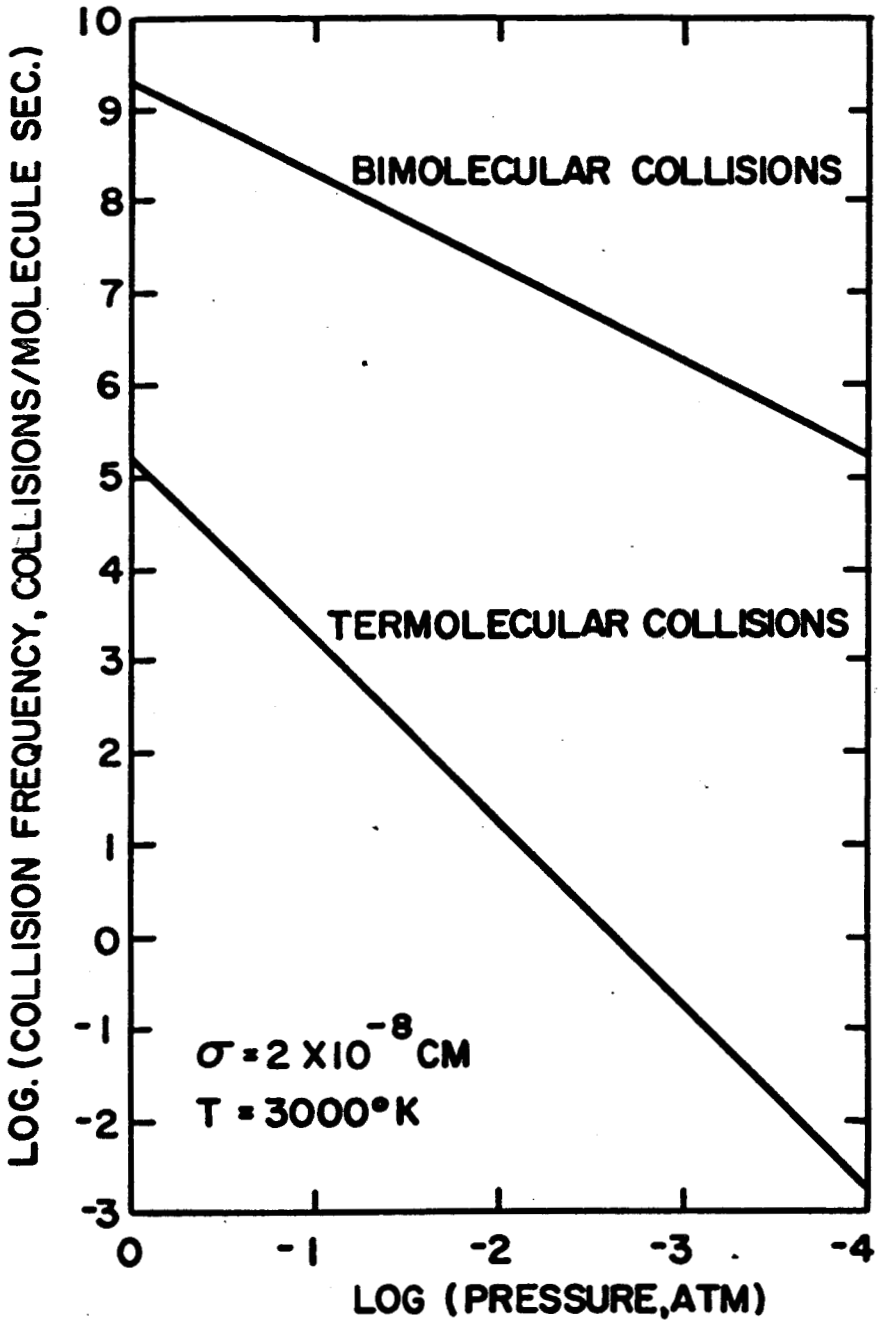

FIG. 3: HYDROGEN ATOM COLLISION FREQUENCY VERSUS PRESSURE.

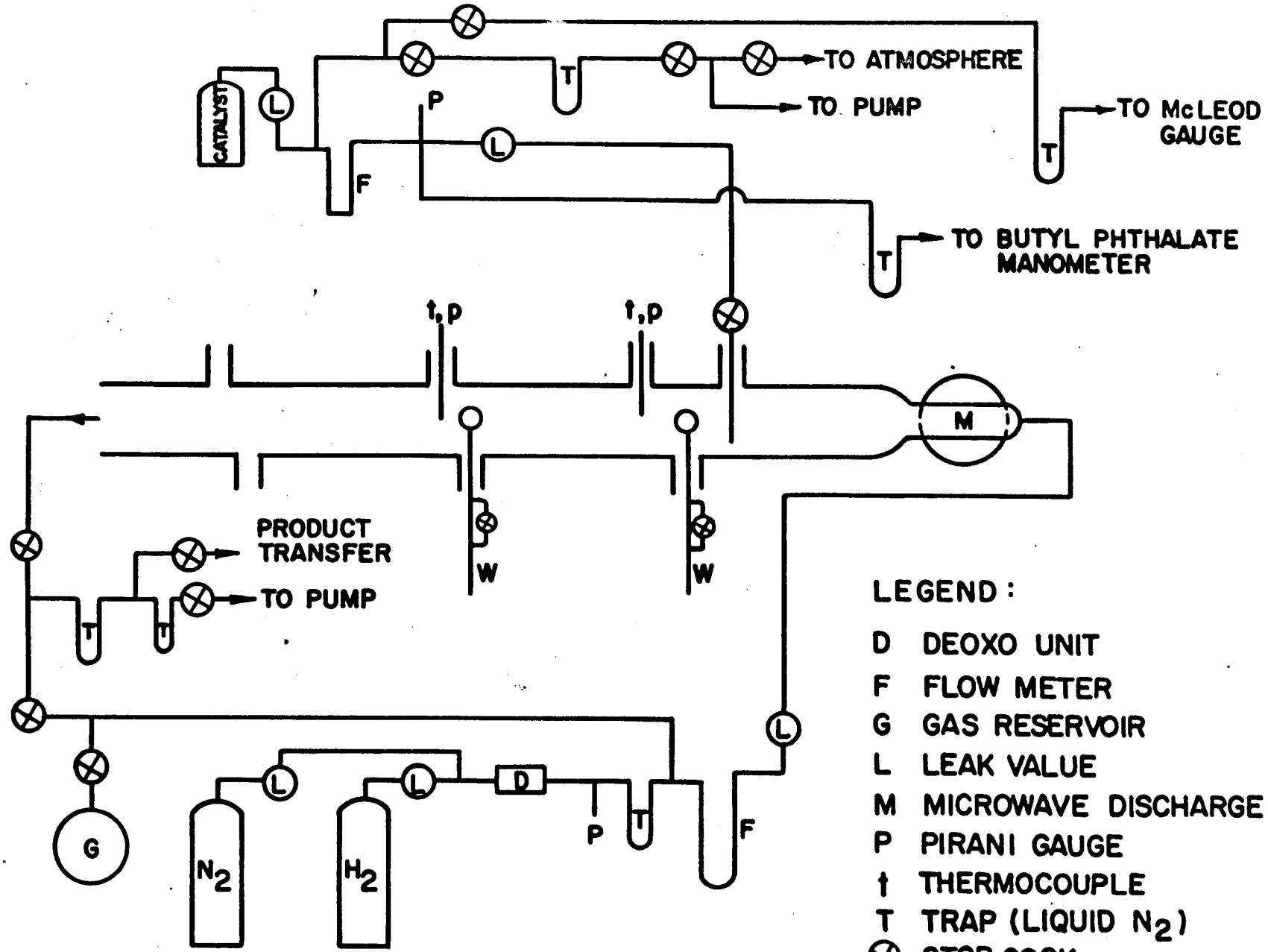
TO ATMOSPHERE
TO PUMP
TO McLEOD GAUGE
TO BUTYL PHTHALATE MANOMETER
CATALYST
L
P
F
T
t, p
M
W
PRODUCT TRANSFER
TO PUMP
G
N_2
H_2
D
LEGEND :
D DEOXO UNIT
F FLOW METER
G GAS RESERVOIR
L LEAK VALUE
M MICROWAVE DISCHARGE
P PIRANI GAUGE
t THERMOCOUPLE
T TRAP (LIQUID N_2)
STOP COCK
W WREDE GAUGE

FIG. 4

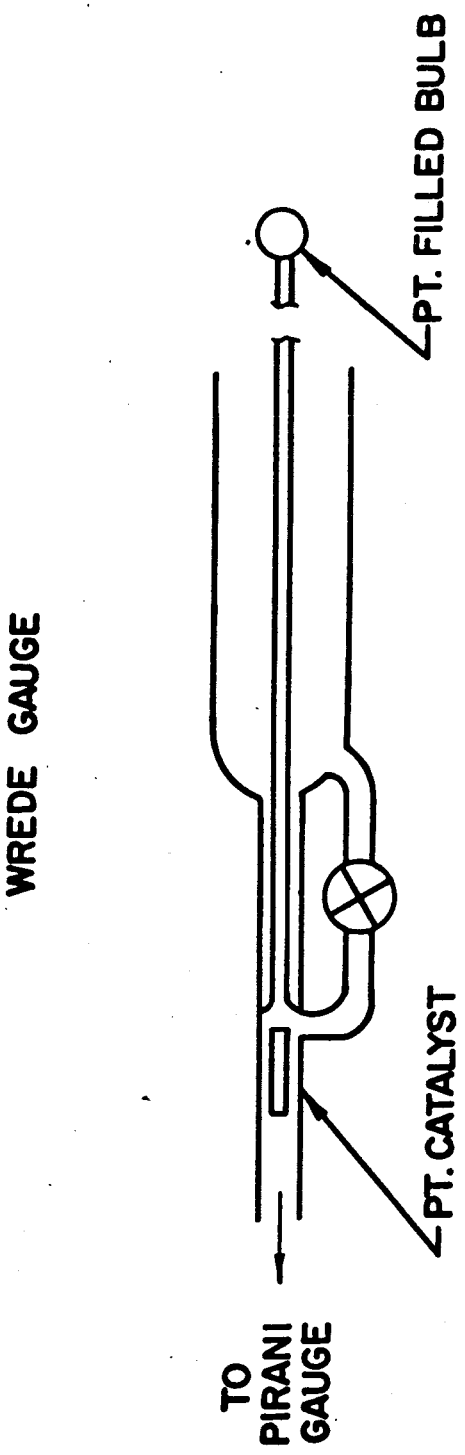

FIG. 5

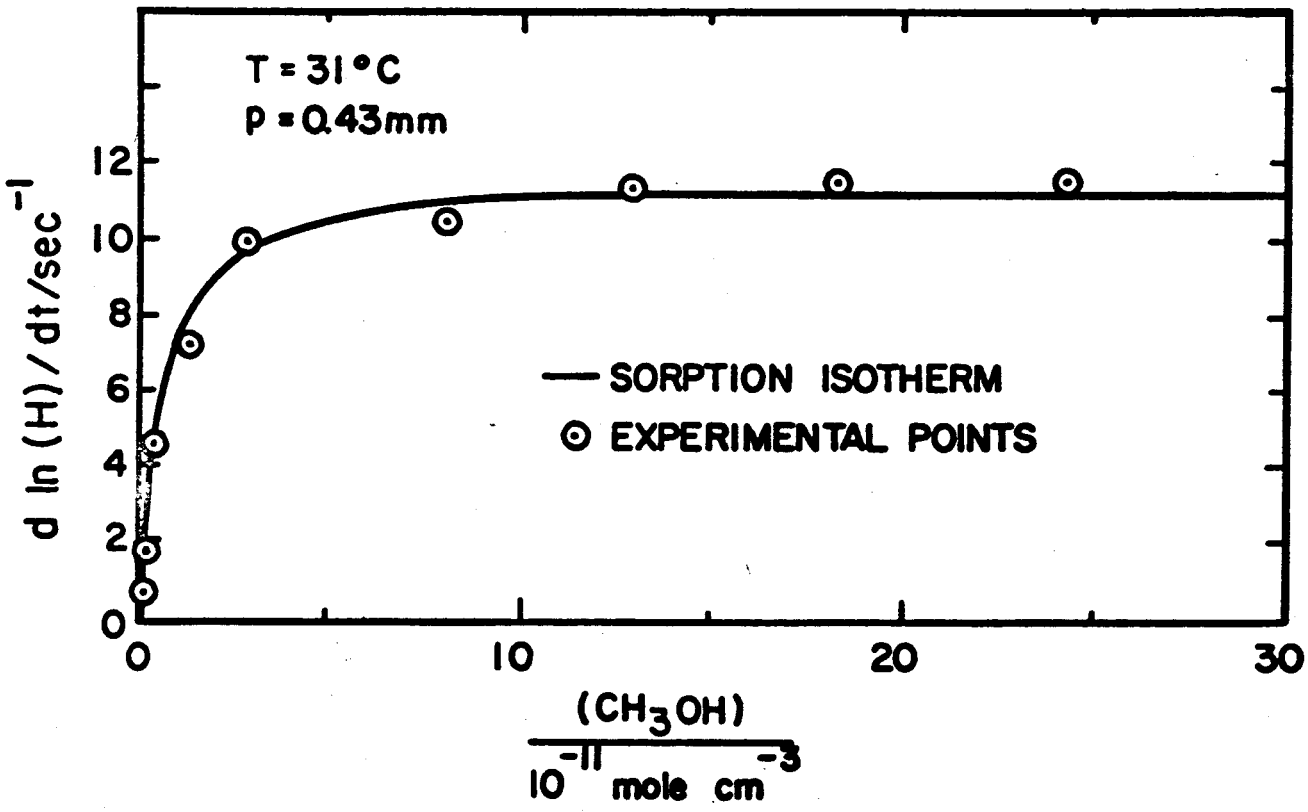

FIG. 6 : METHYL ALCOHOL EXPERIMENT.

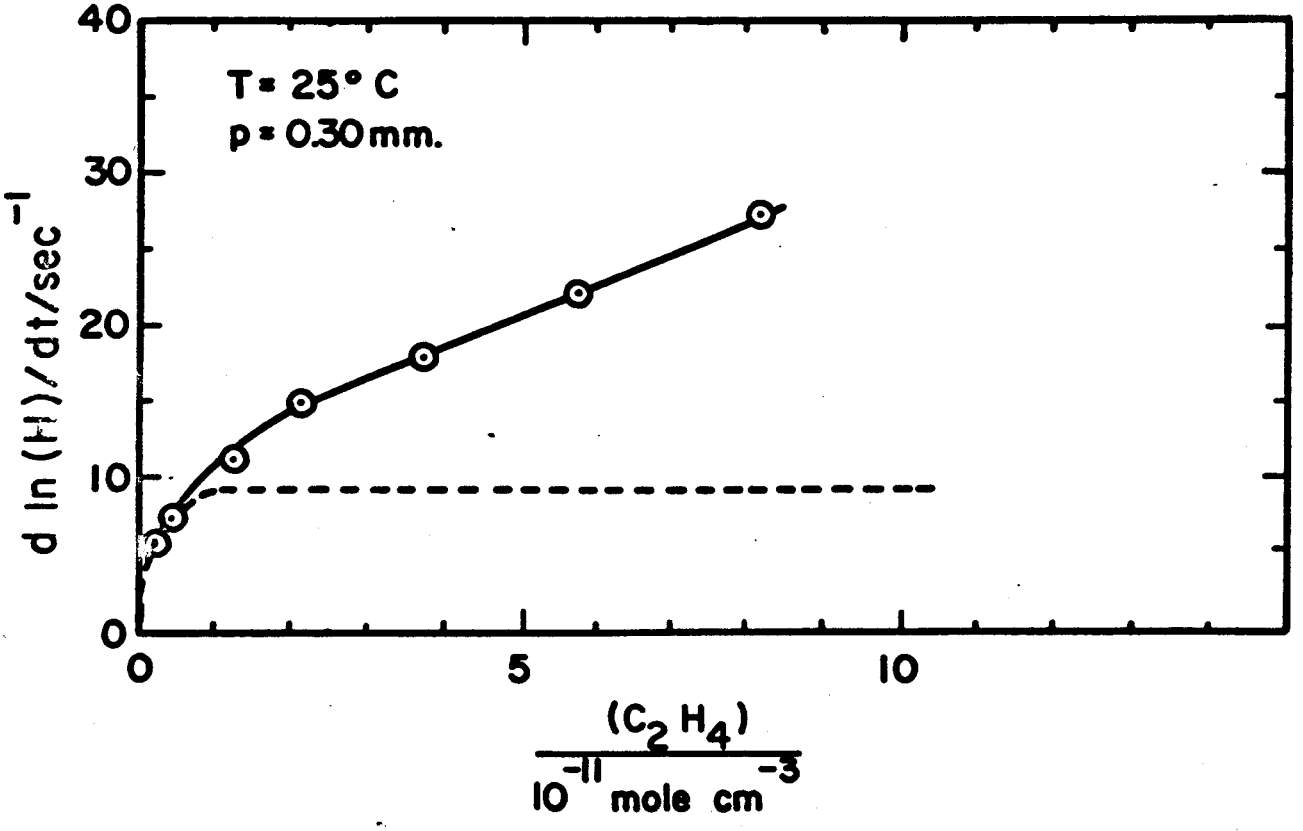

FIG. 7 : ETHYLENE EXPERIMENT.

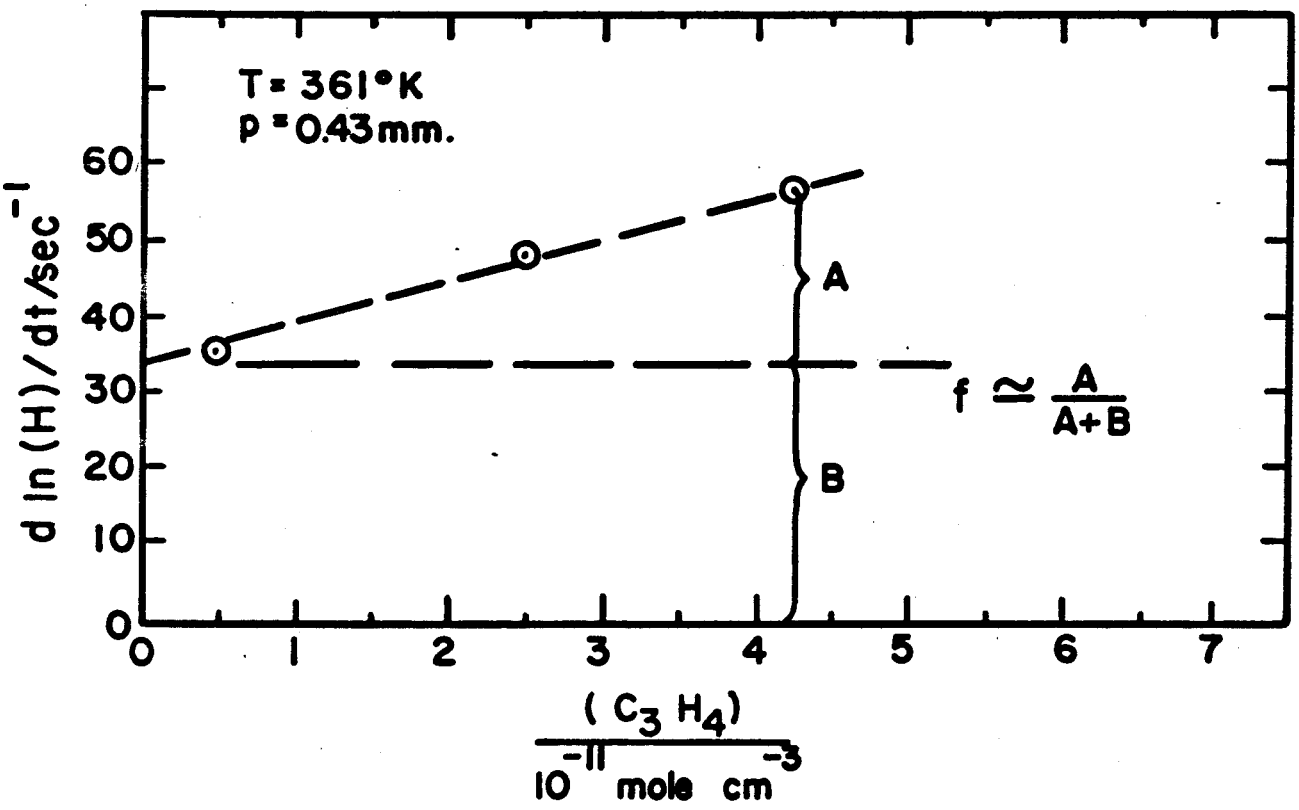

FIG. 8 : ALLENE EXPERIMENTS.

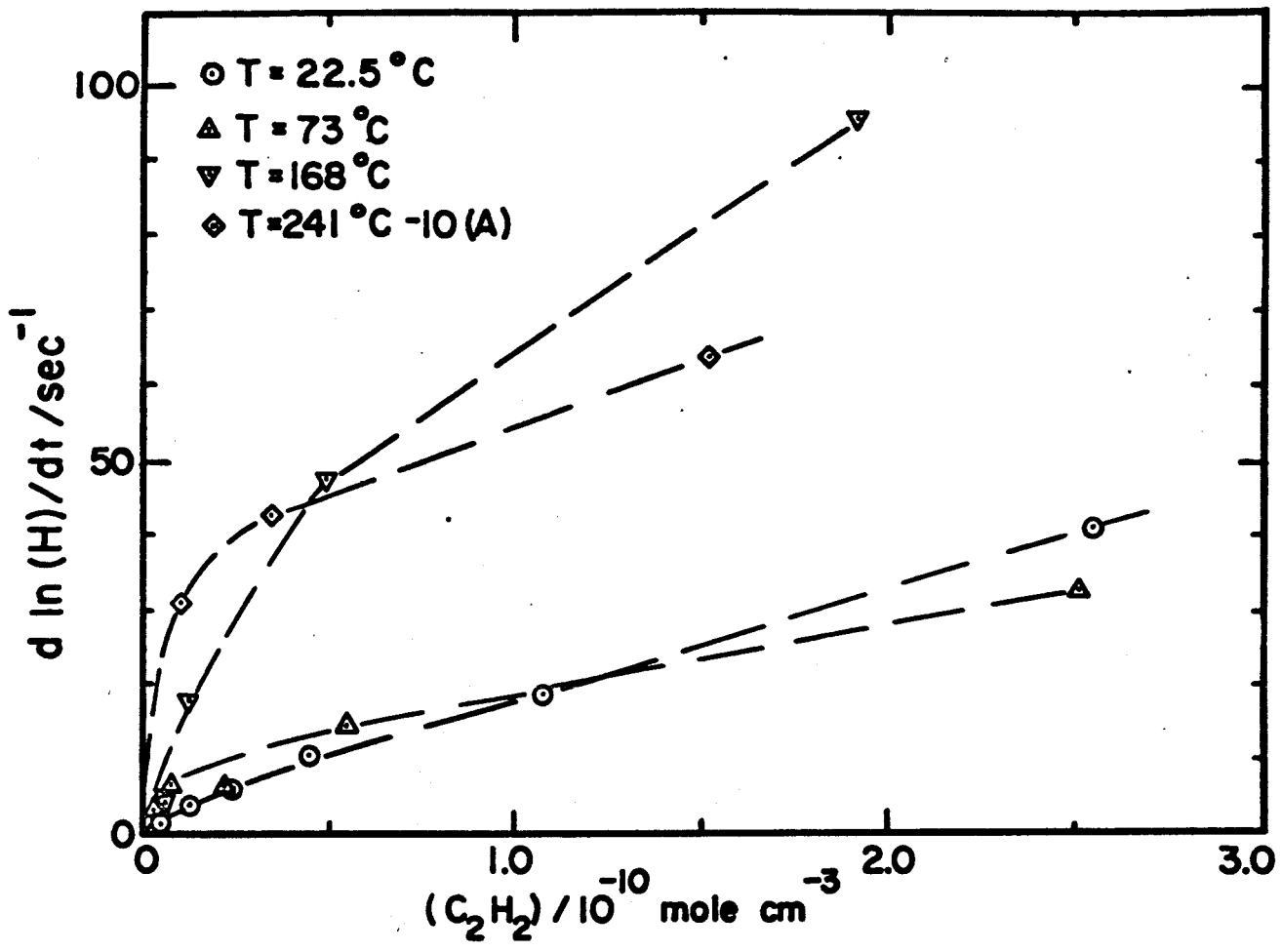

FIG. 9 : ACETYLENE EXPERIMENTS

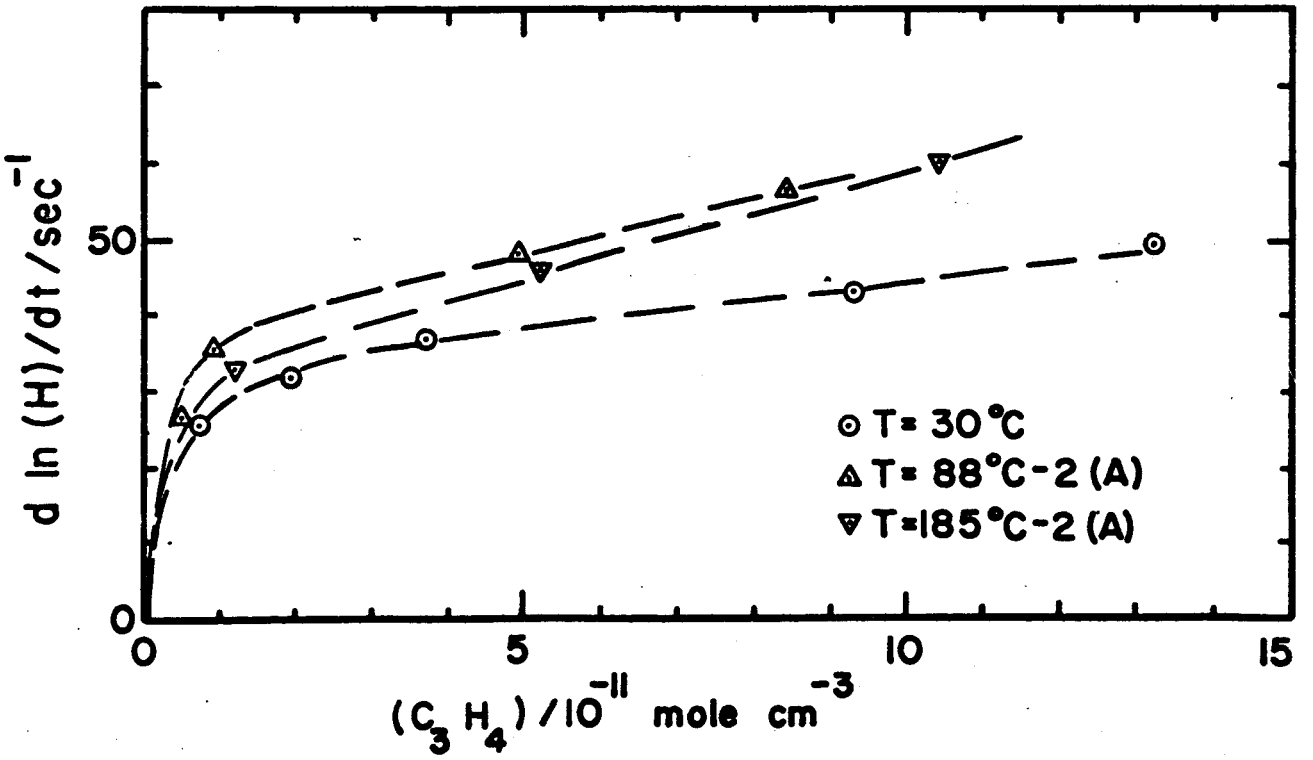

FIG. 10 : ALLENE EXPERIMENTS

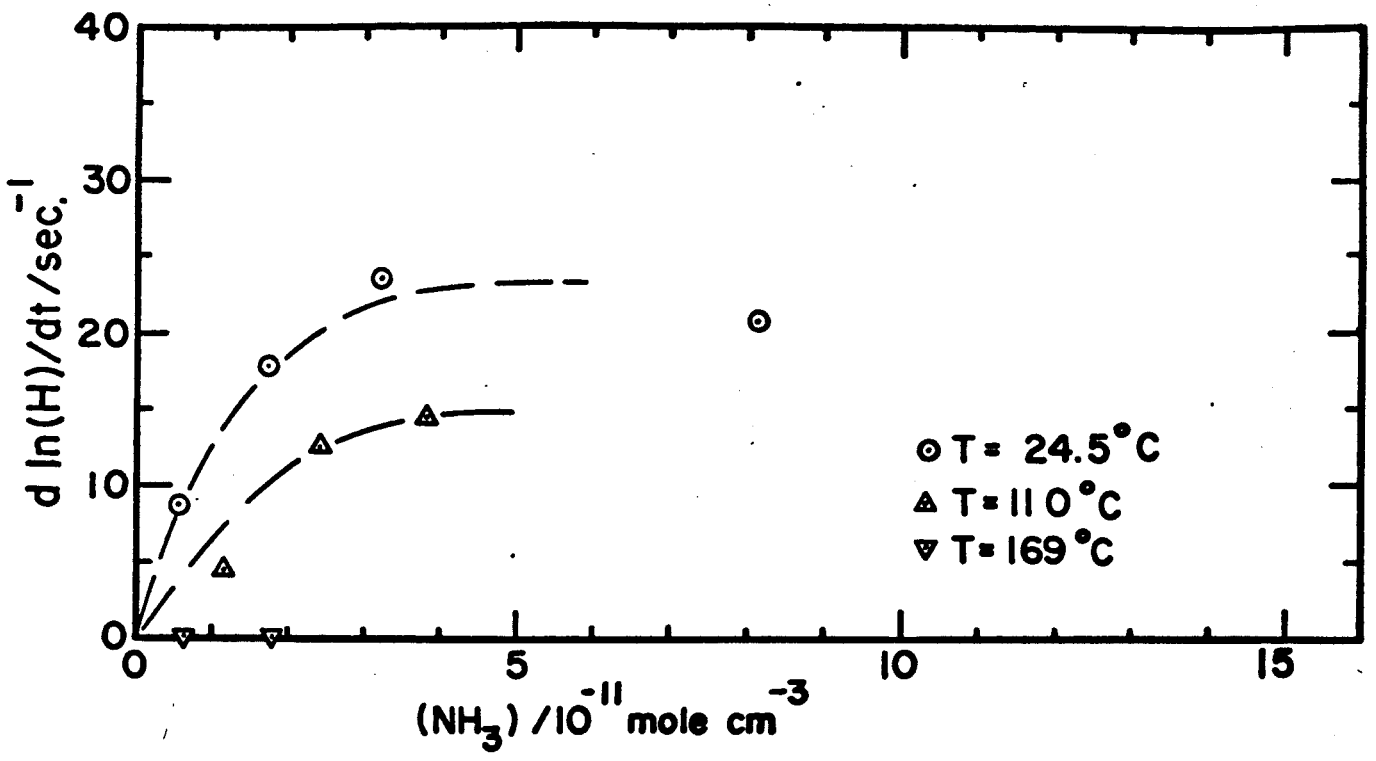

FIG. 11 : AMMONIA EXPERIMENTS.

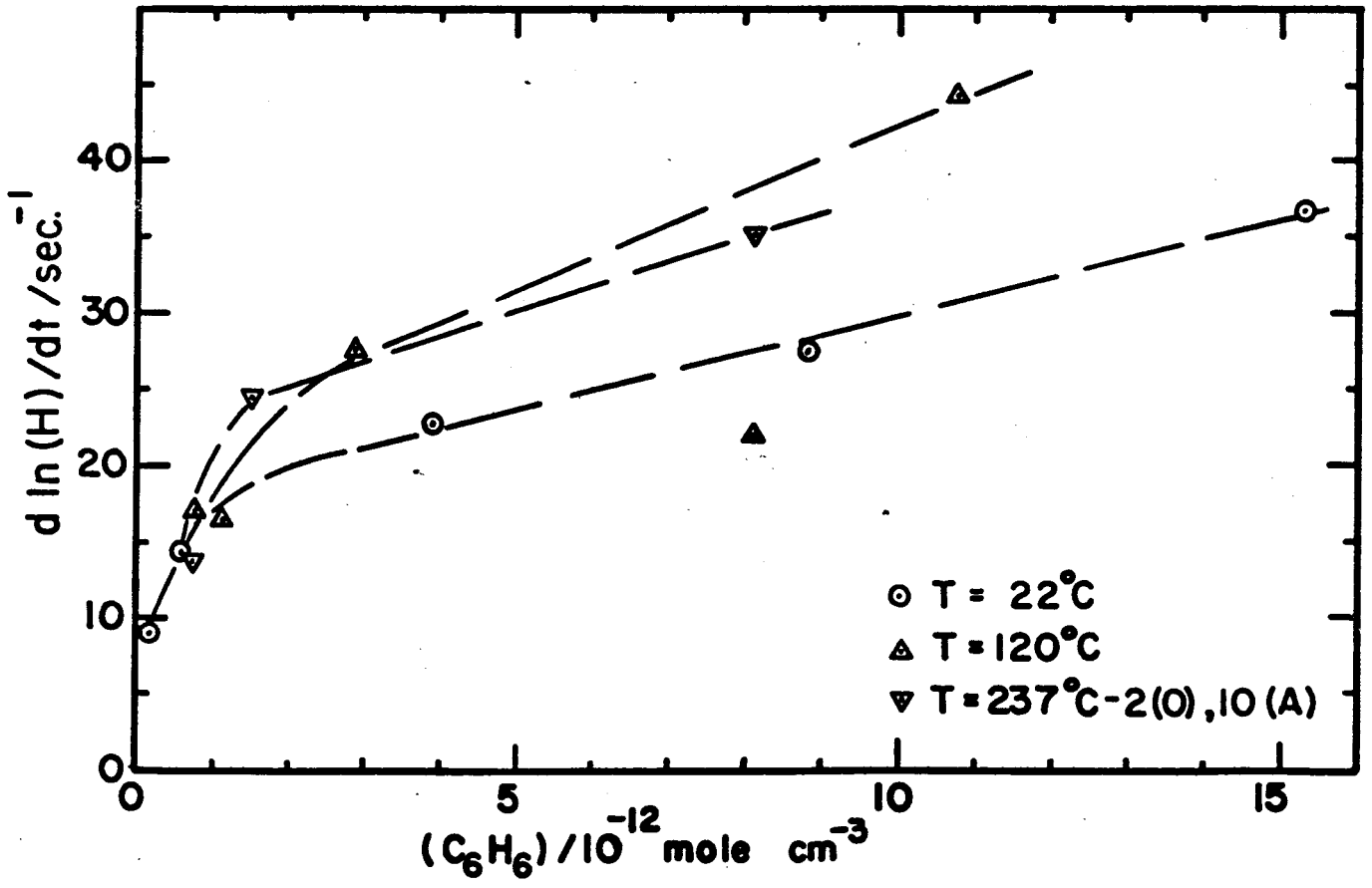

FIG. 12 : BENZENE EXPERIMENTS.

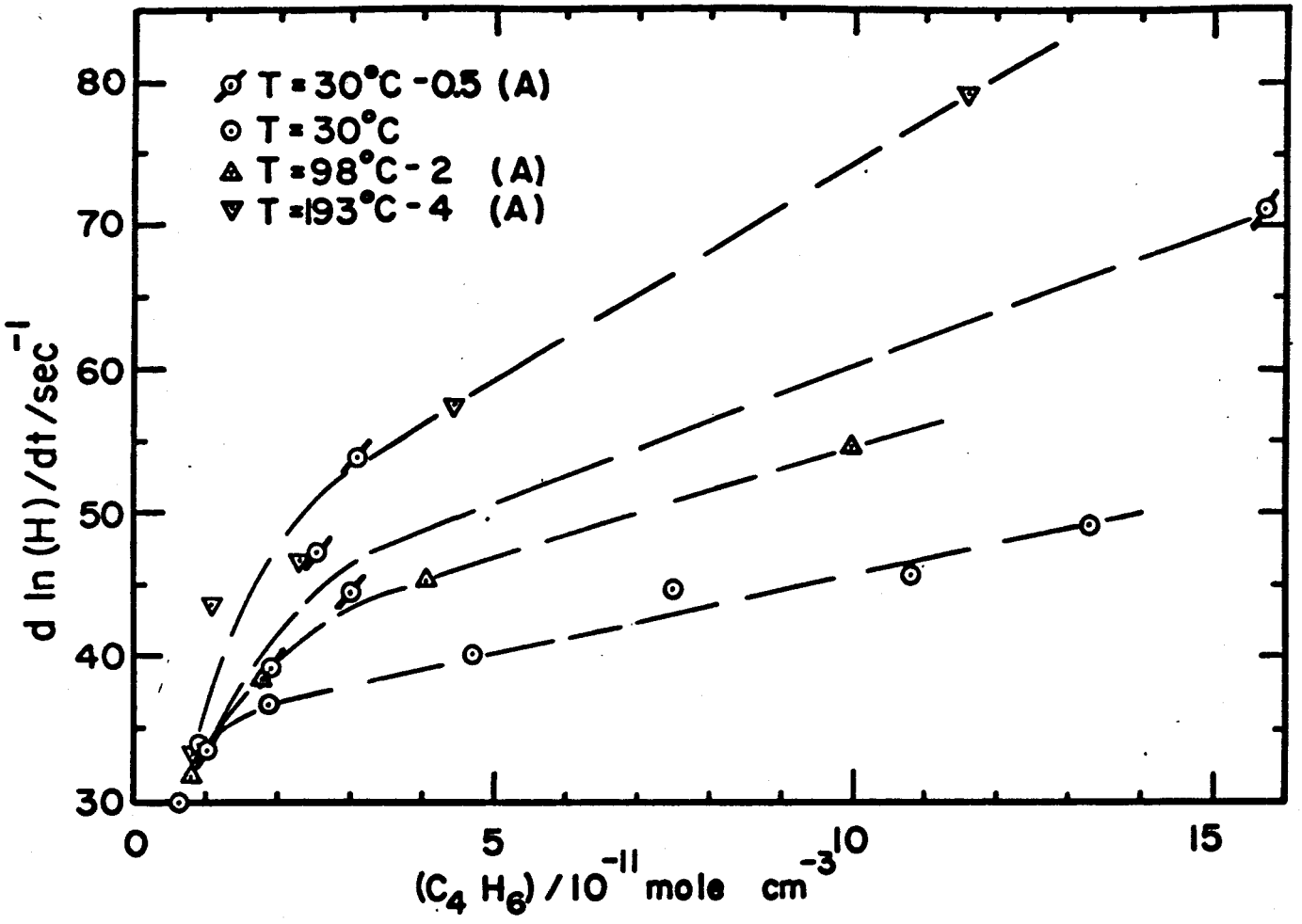

FIG. 13 : 1, 3- BUTADIENE EXPERIMENTS

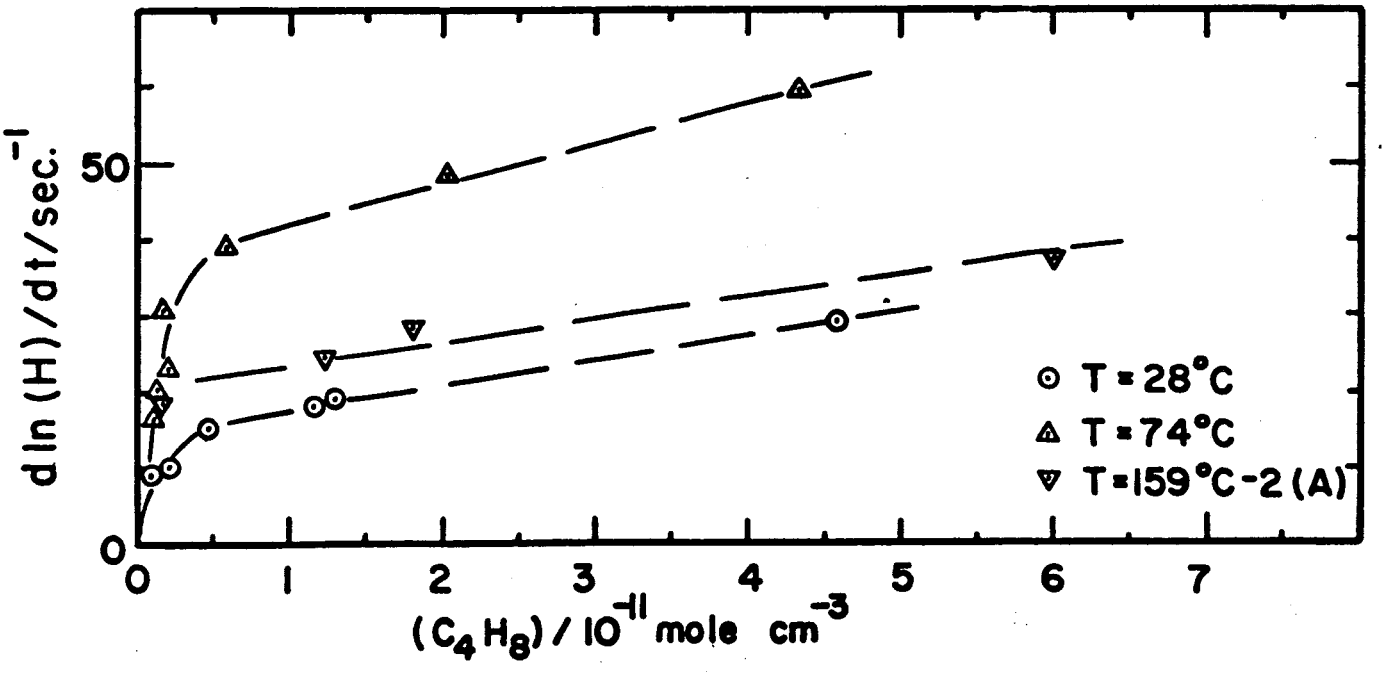

FIG. 14 : CIS - BUTENE - 2 EXPERIMENTS.

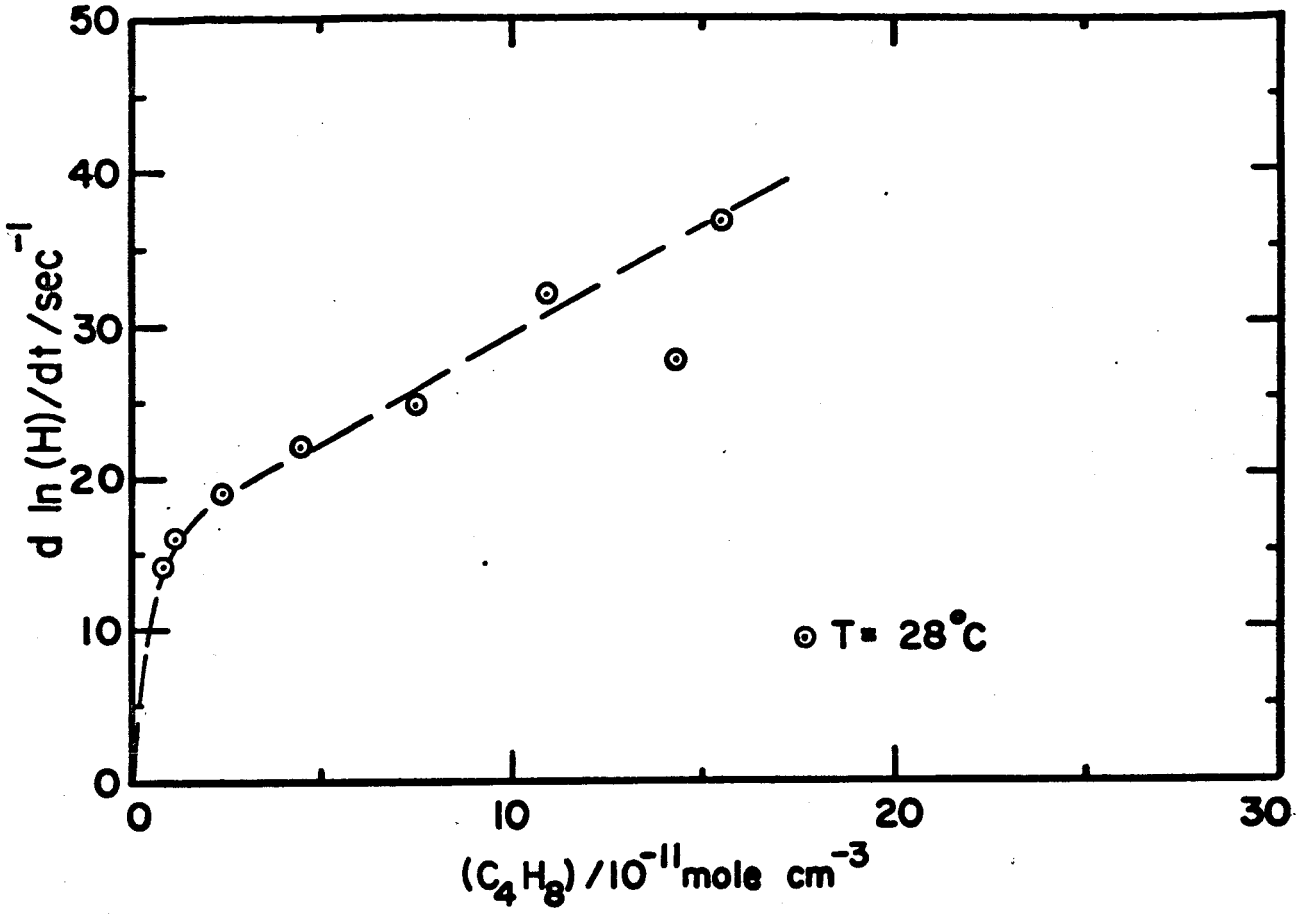

FIG. 15: TRANS-BUTENE-2 EXPERIMENTS.

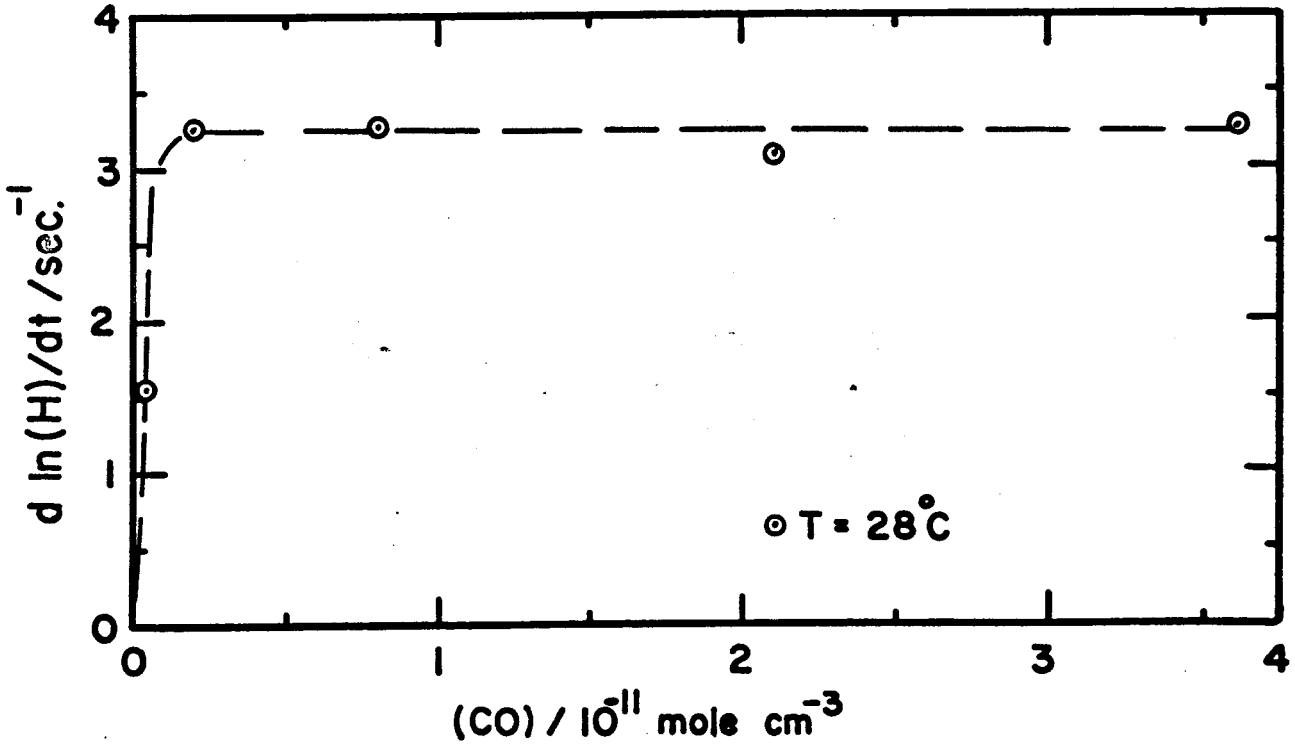

FIG. 16 : CARBON MONOXIDE EXPERIMENTS.

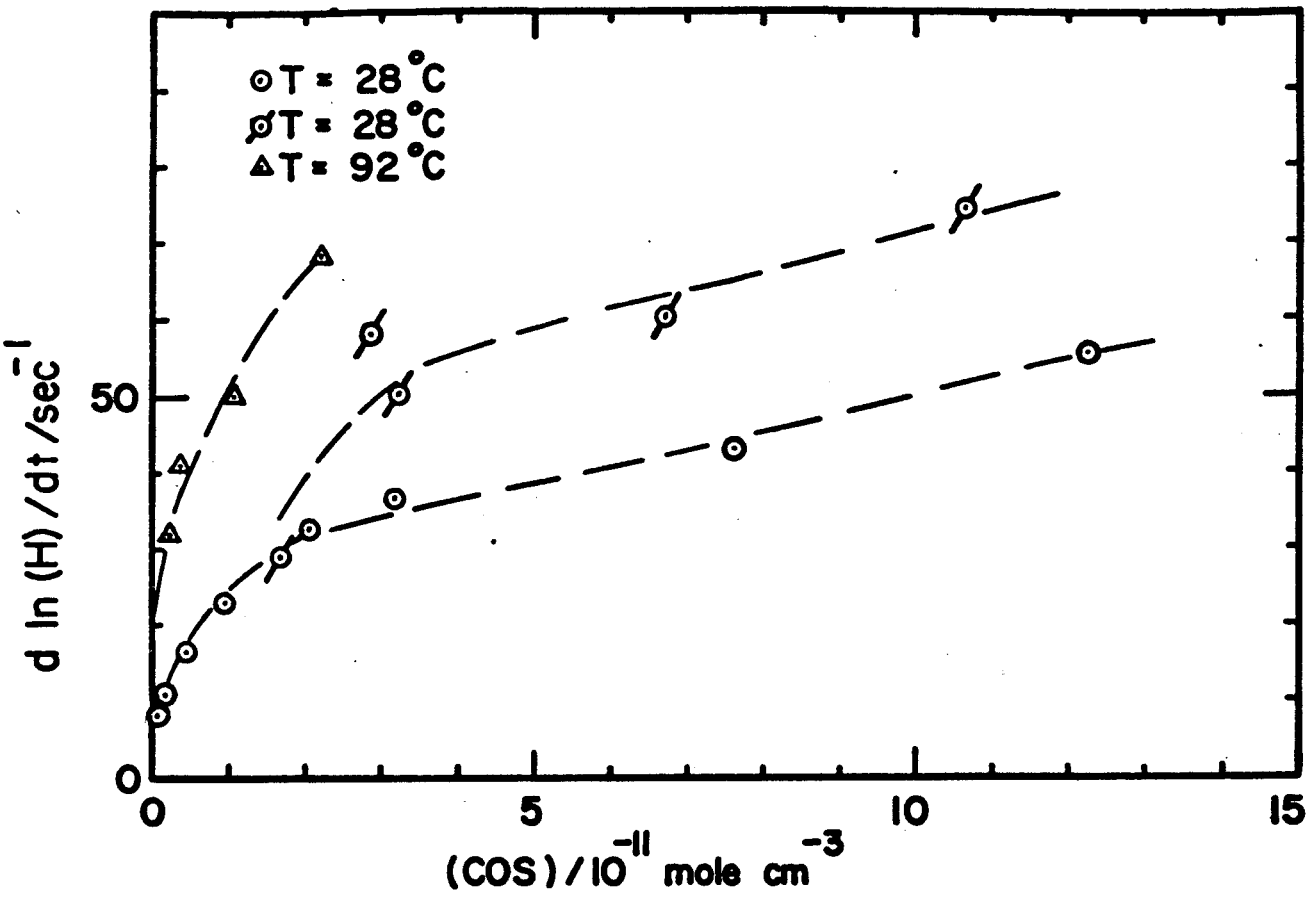

FIG. 17 : CARBONYL SULFIDE EXPERIMENTS.

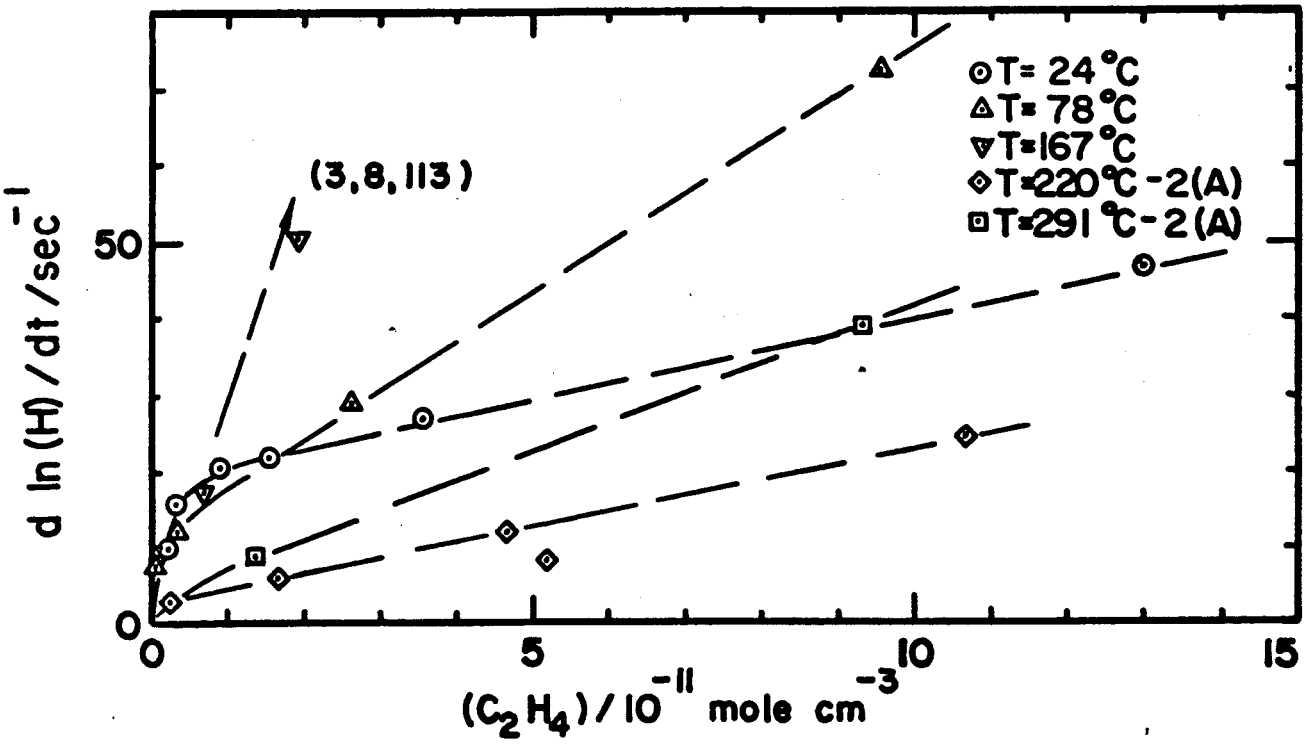

FIG. 18 : ETHYLENE EXPERIMENTS.

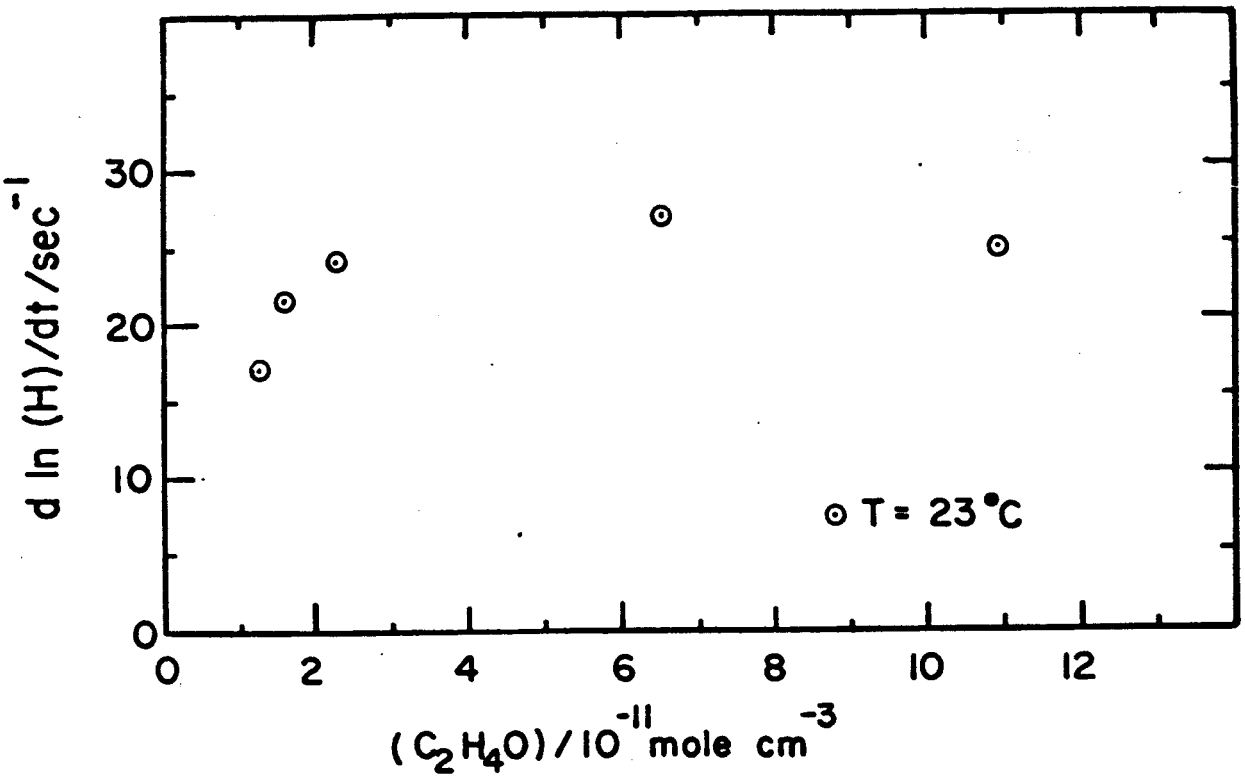

FIG. 19 : ETHYLENE OXIDE EXPERIMENTS.

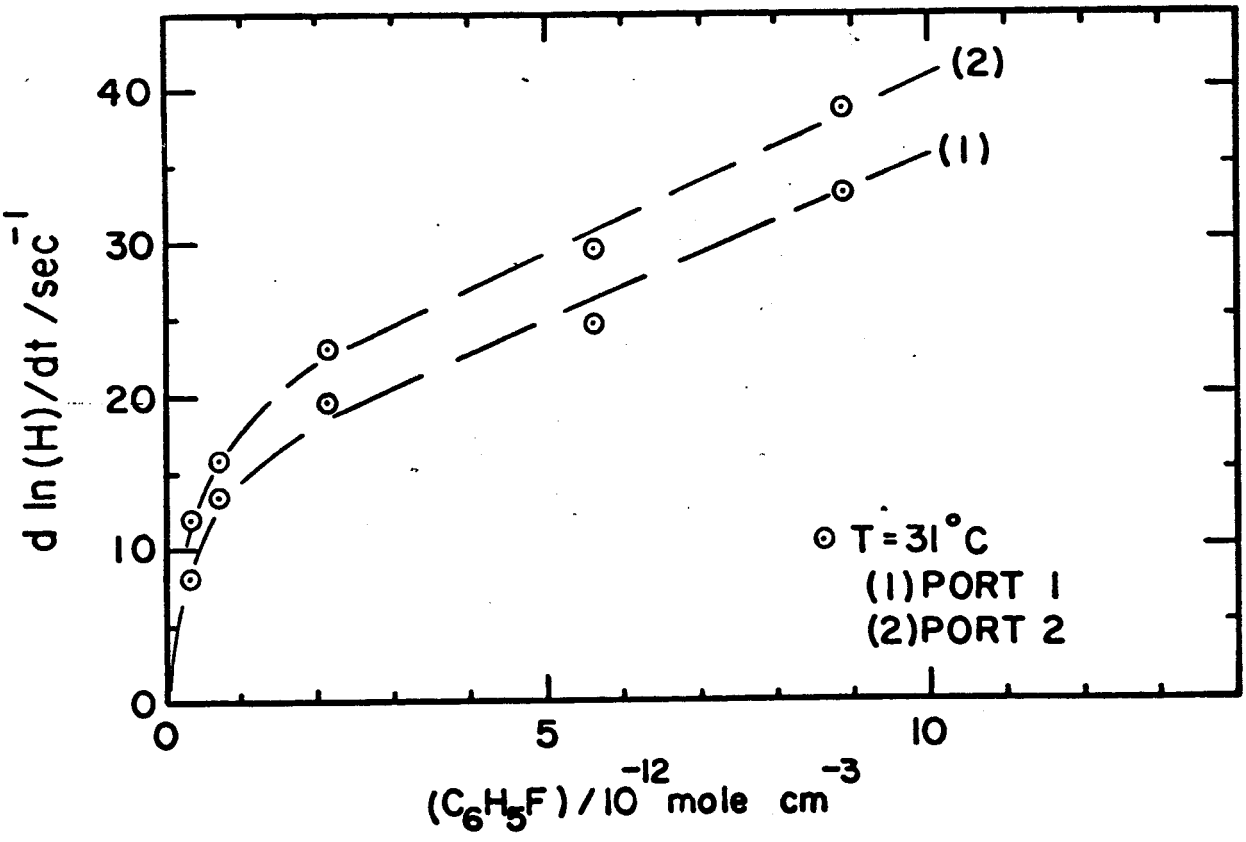

FIG. 20 : FLUOROBENZENE EXPERIMENTS.

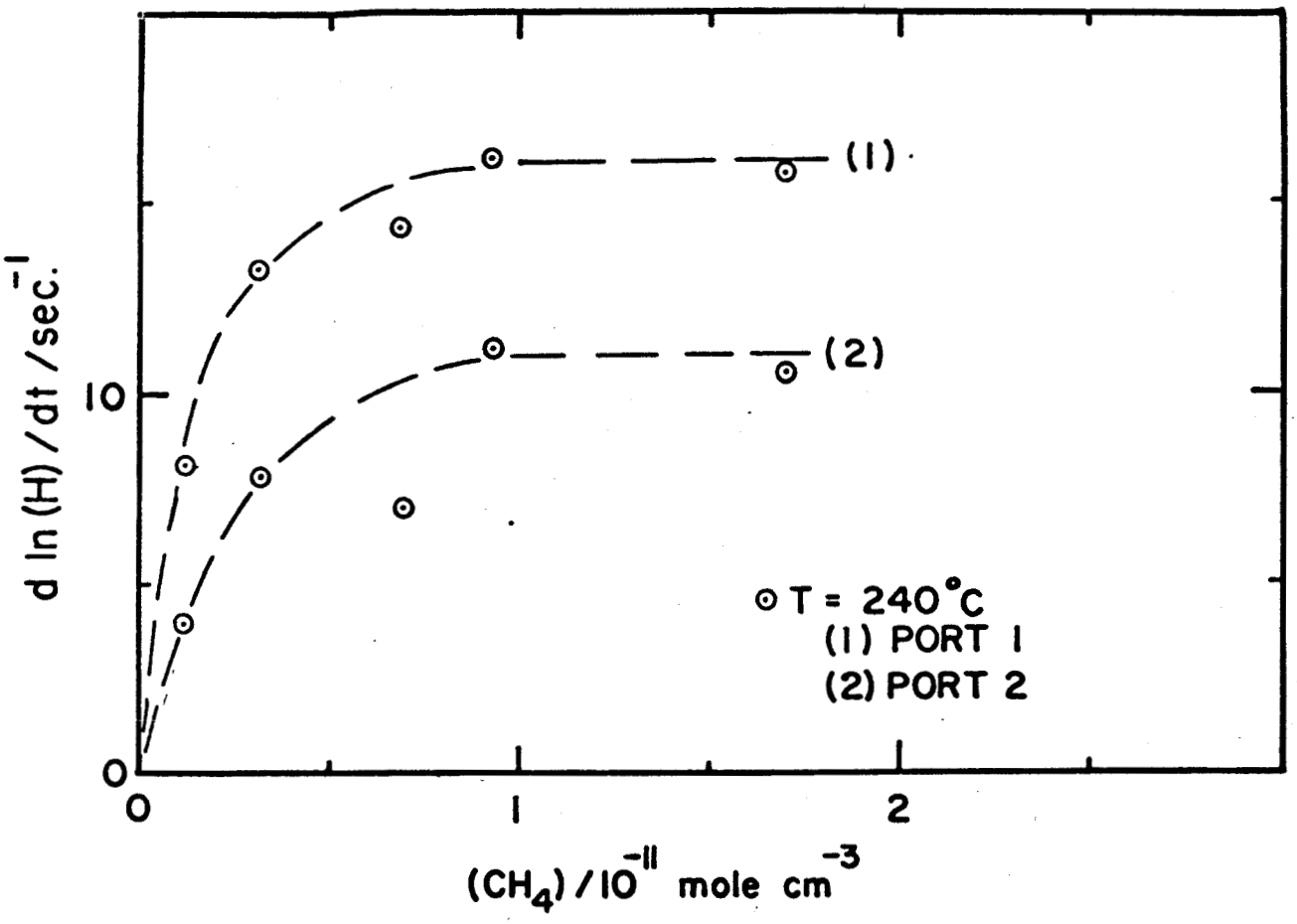

FIG. 21 : METHANE EXPERIMENTS.

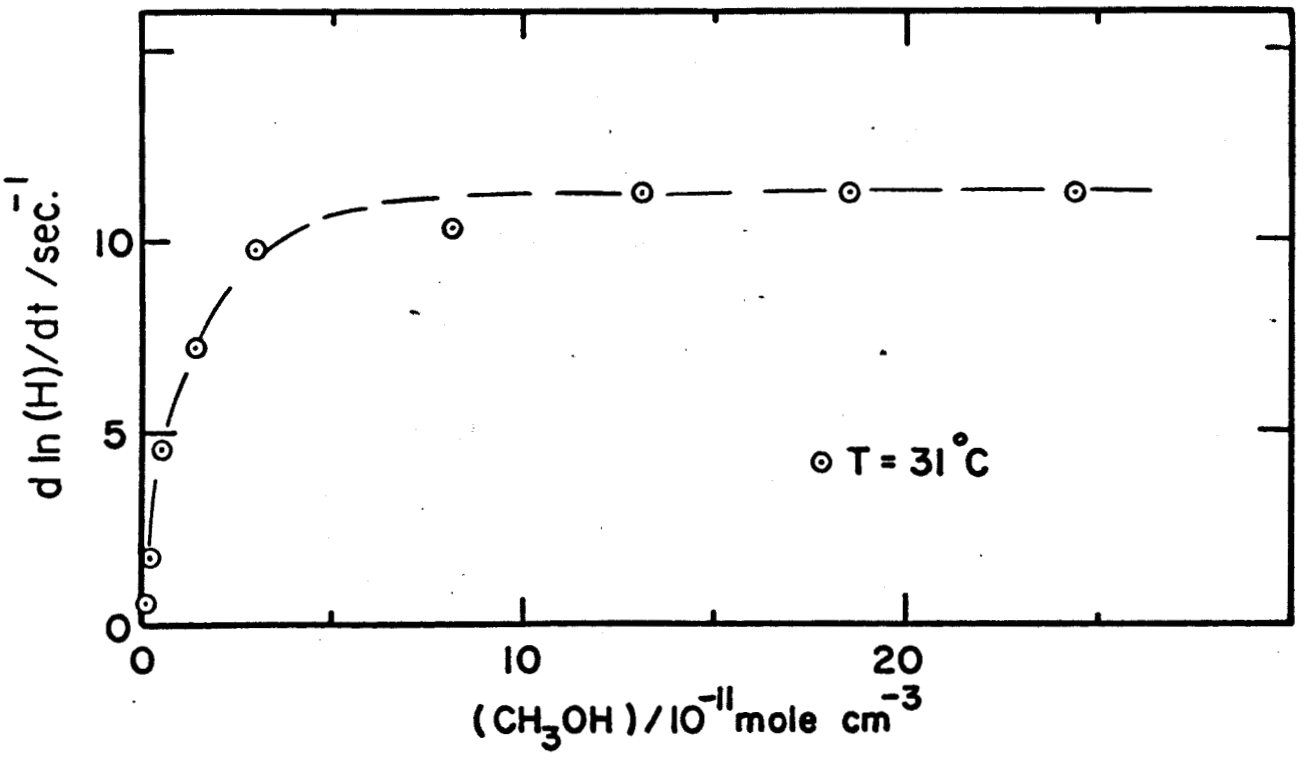

FIG. 22 : METHYL ALCOHOL EXPERIMENTS.

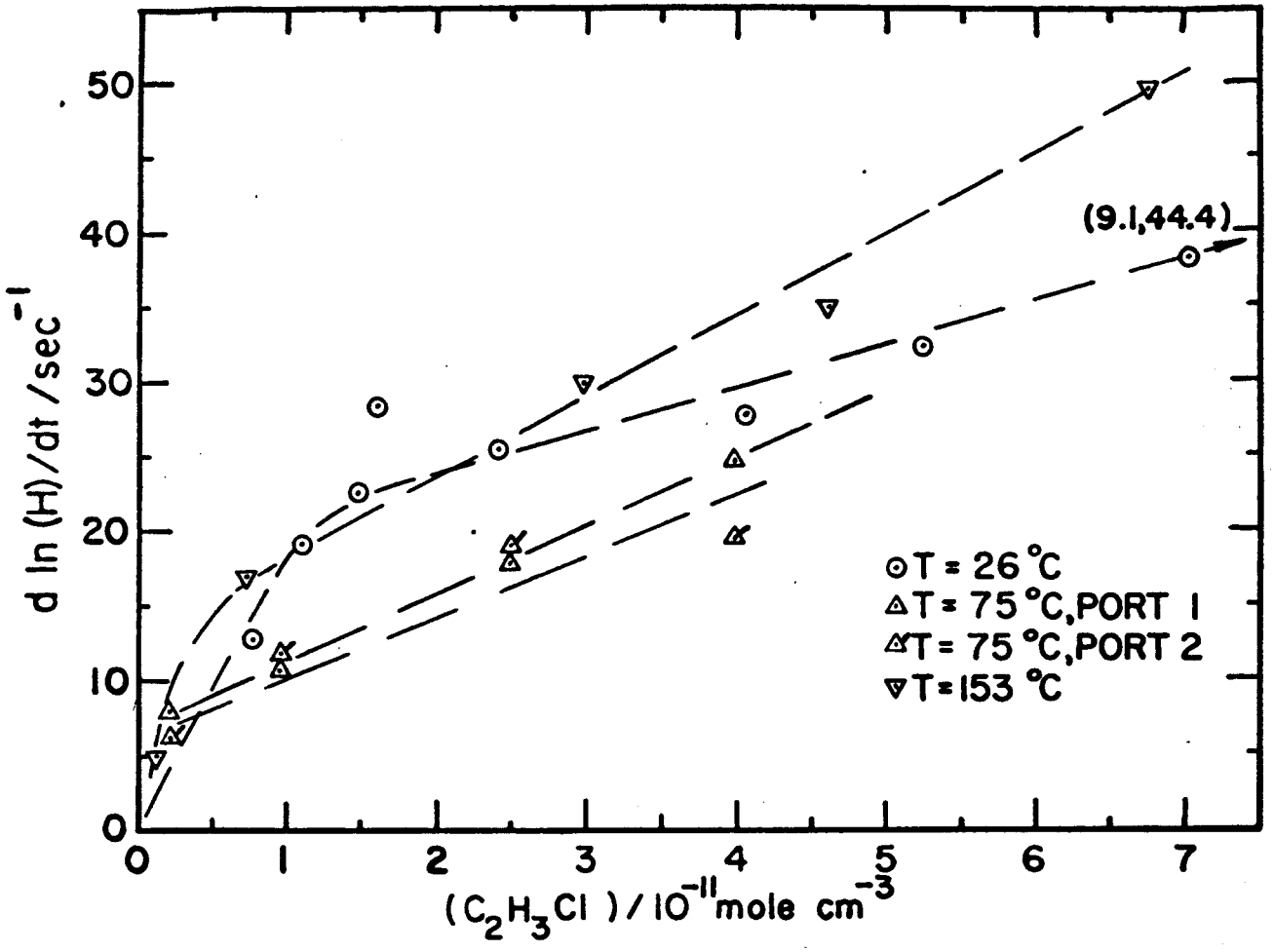

FIG. 23 : VINYL CHLORIDE EXPERIMENTS

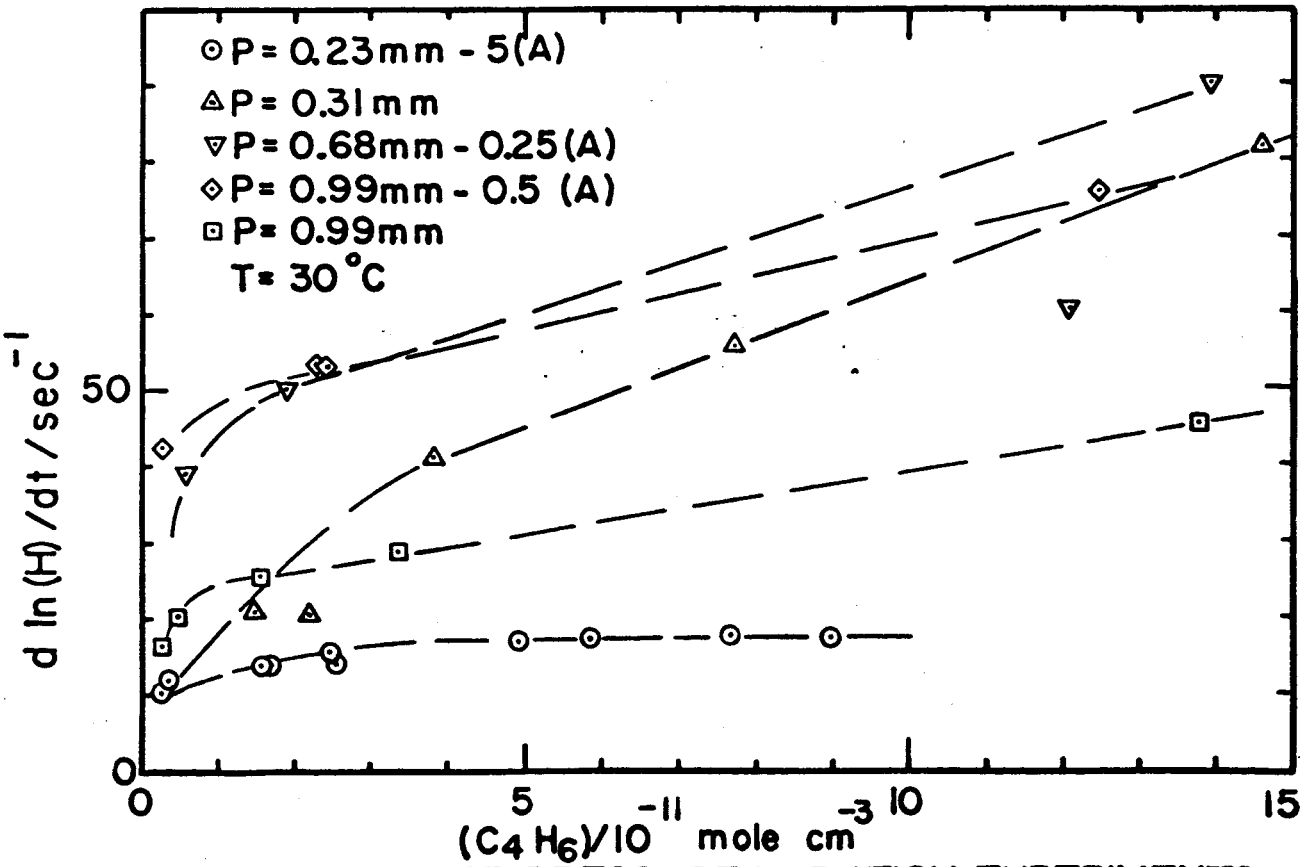

FIG. 24 : 1,3-BUTADIENE PRESSURE VARIATION EXPERIMENTS.

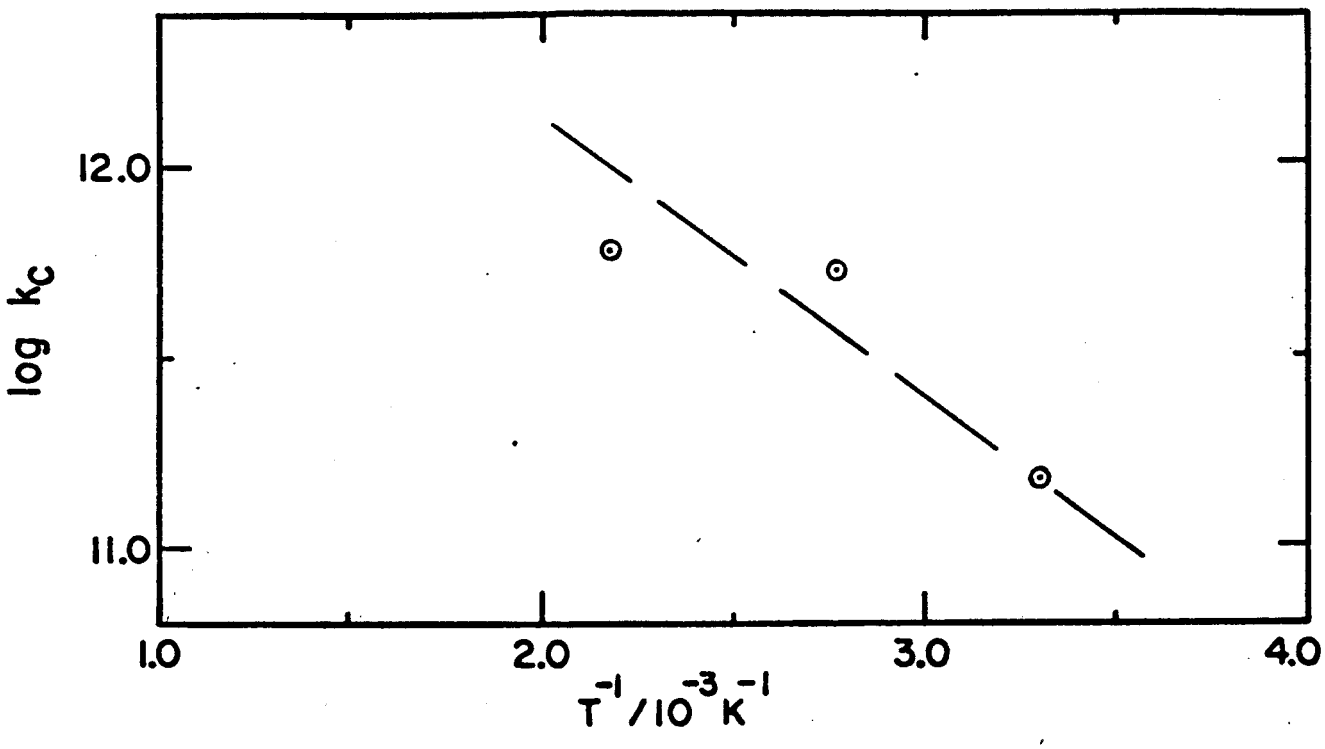

FIG. 29 : ALLENE DATA

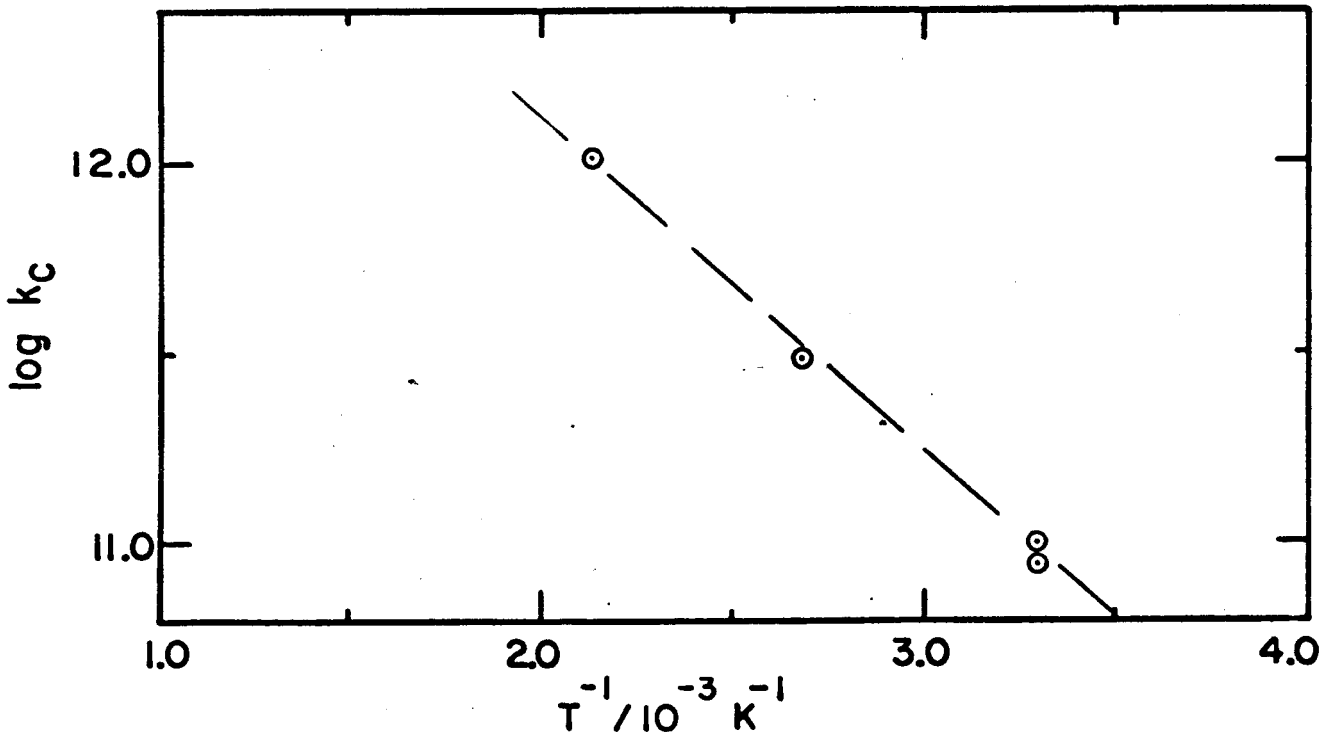

FIG. 30 : 1,3 - BUTADIENE DATA

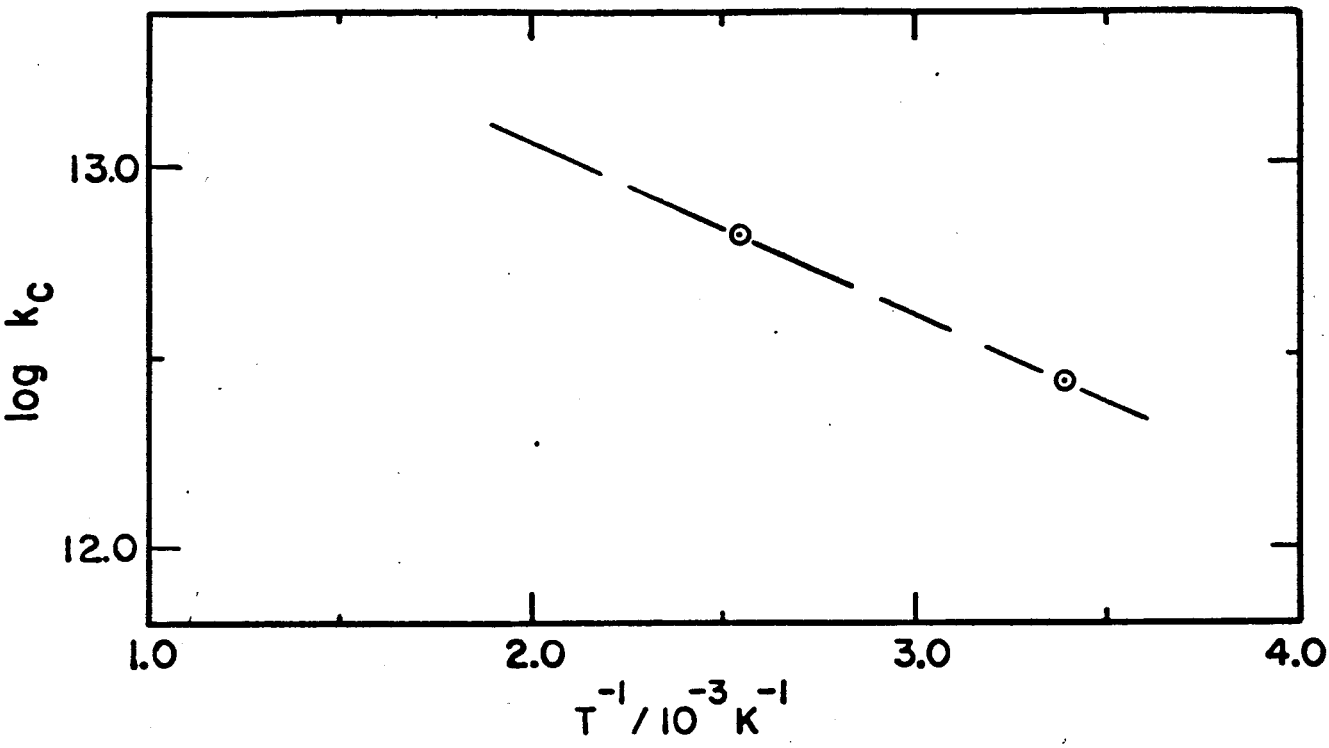

FIG.31: BENZENE DATA

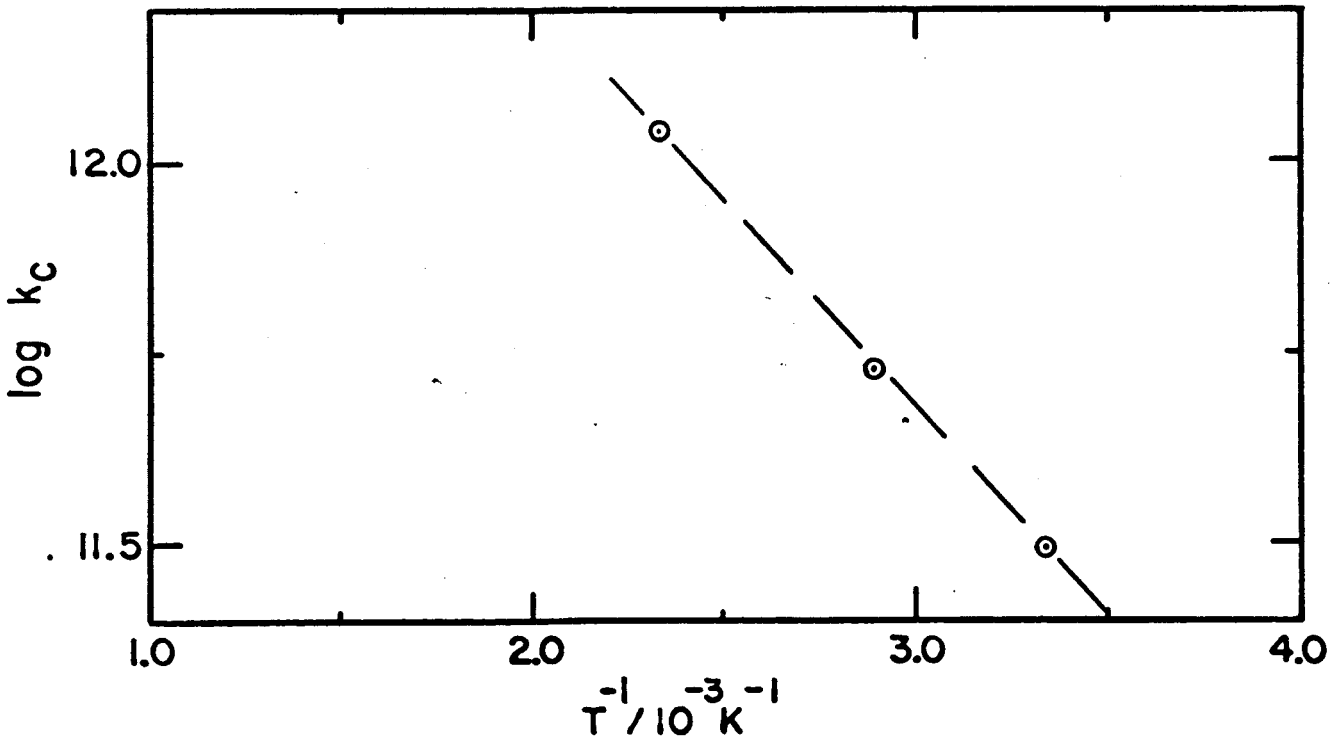

FIG. 32 : CIS-BUTENE-2 DATA

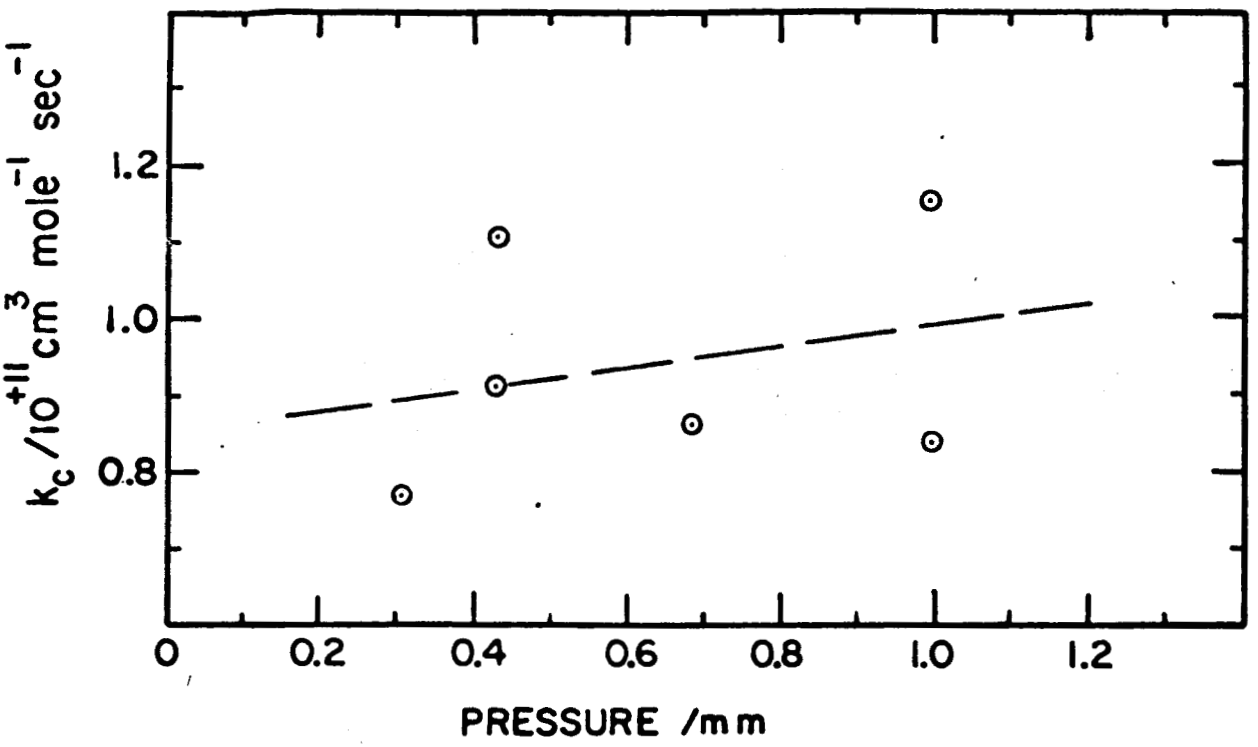

FIG. 25 : 1,3 BUTADIENE PRESSURE VARIATION EXPERIMENTS.

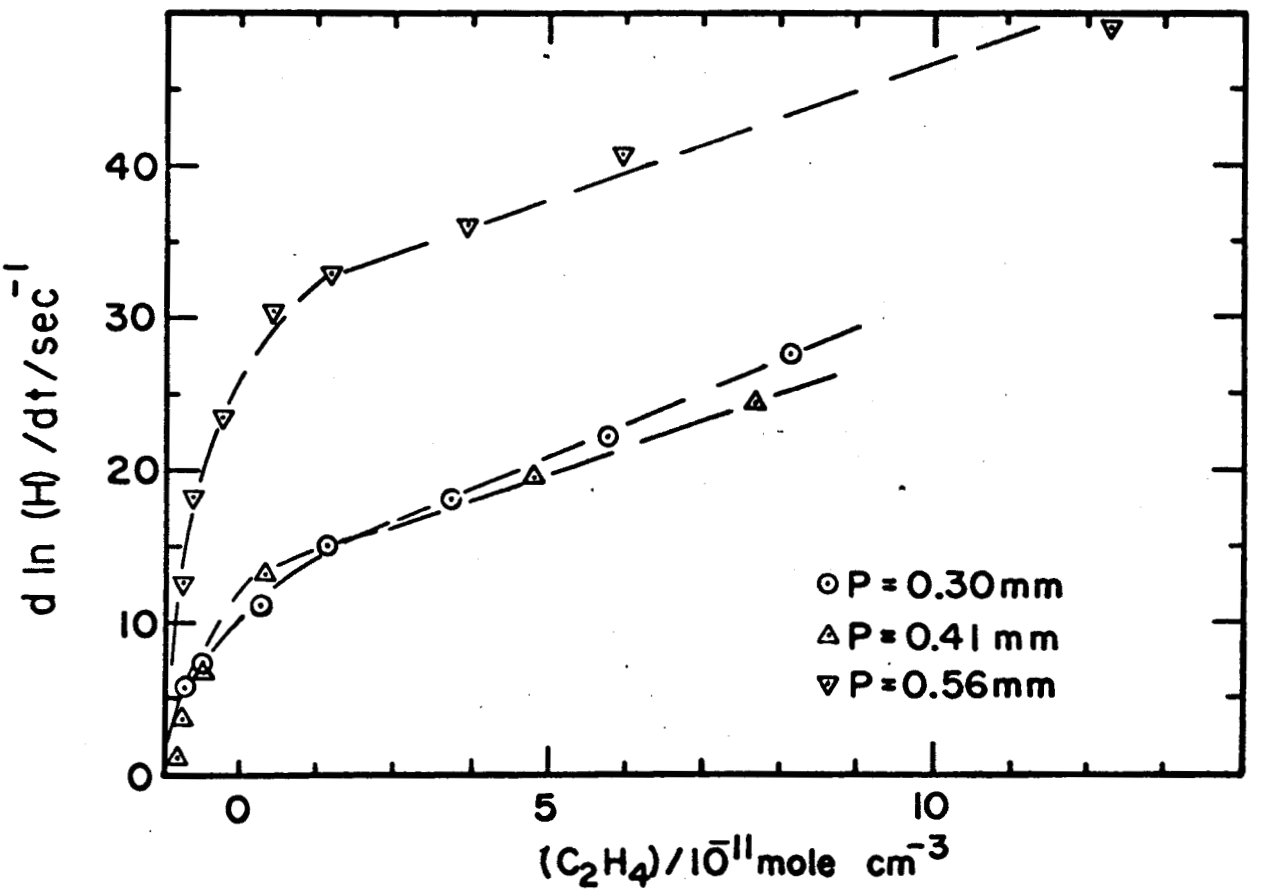

FIG. 26 : ETHYLENE PRESSURE VARIATION EXPERIMENTS.

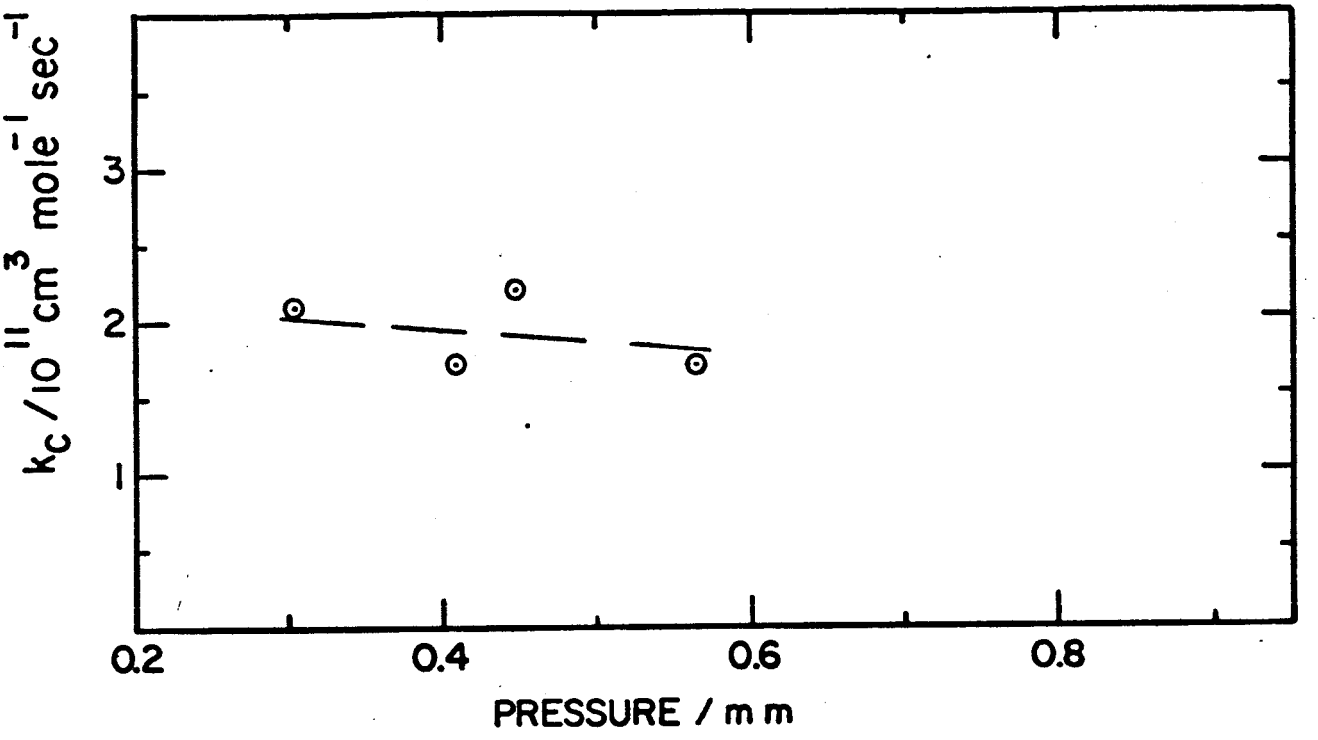

FIG. 27 : ETHYLENE PRESSURE VARIATION EXPERIMENTS.

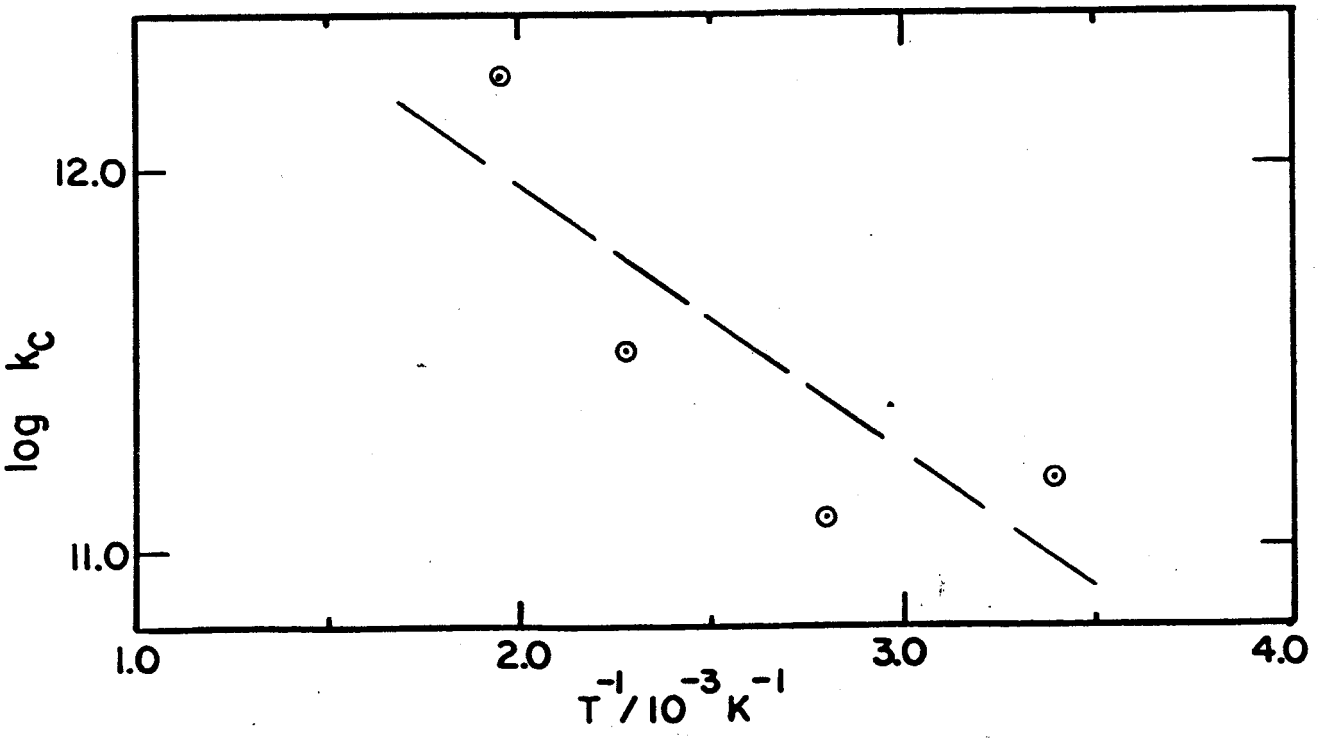

FIG. 28 : ACETYLENE DATA

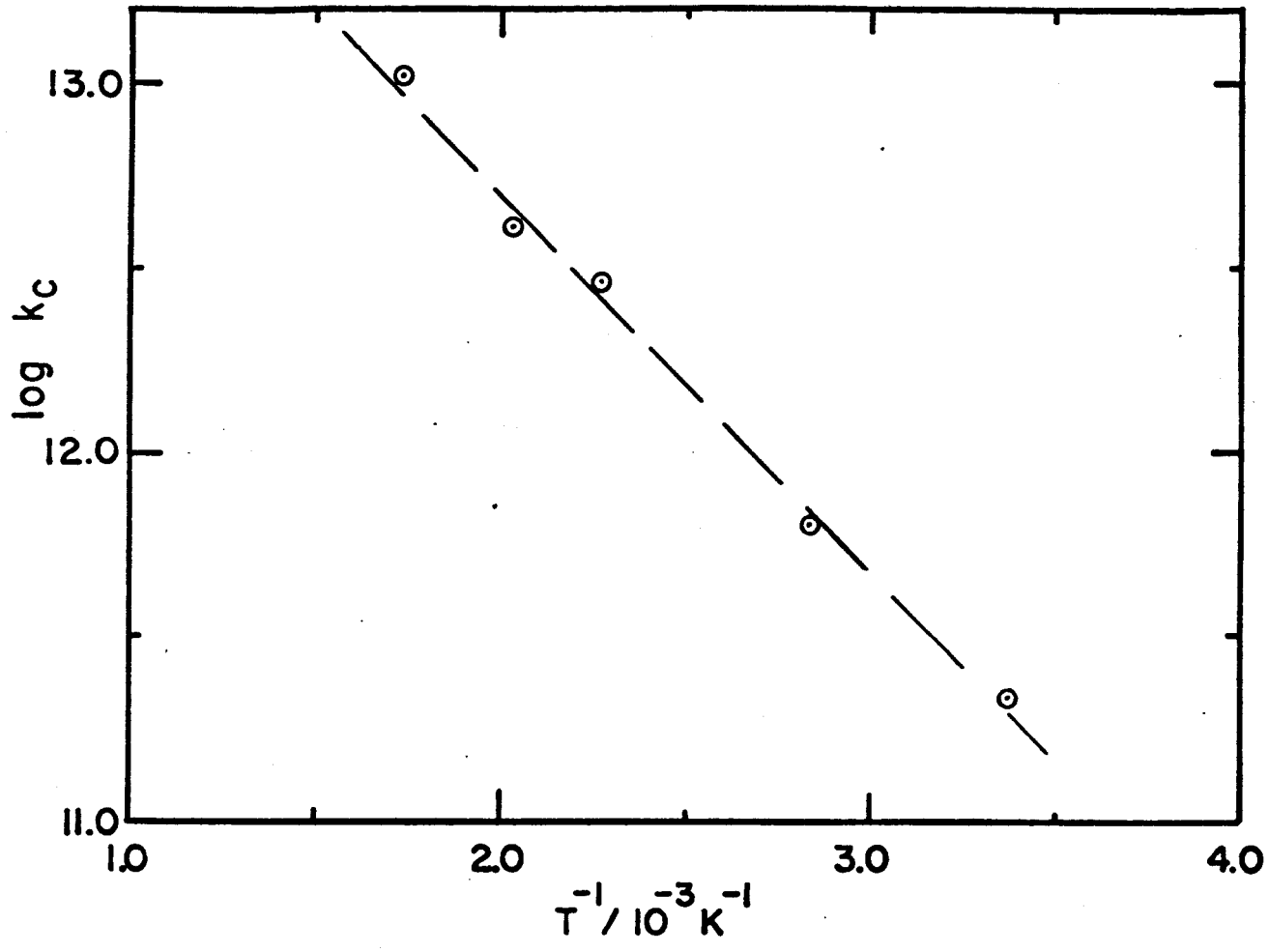

FIG. 33 : ETHYLENE DATA.

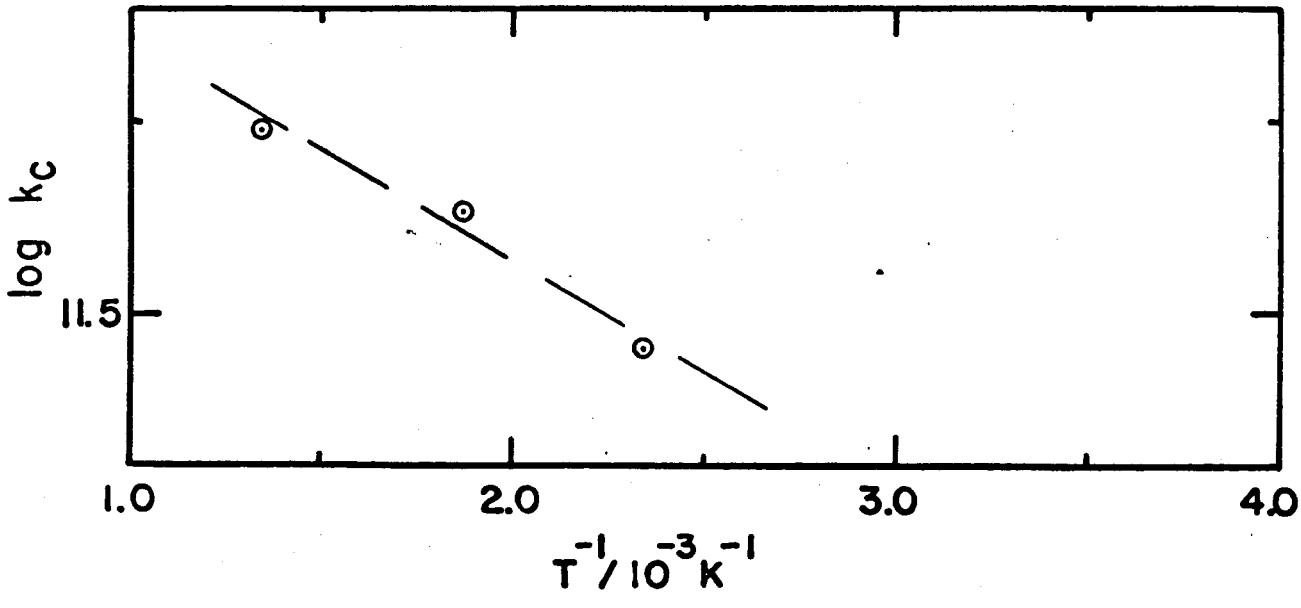

FIG. 34 : VINYL CHLORIDE DATA.

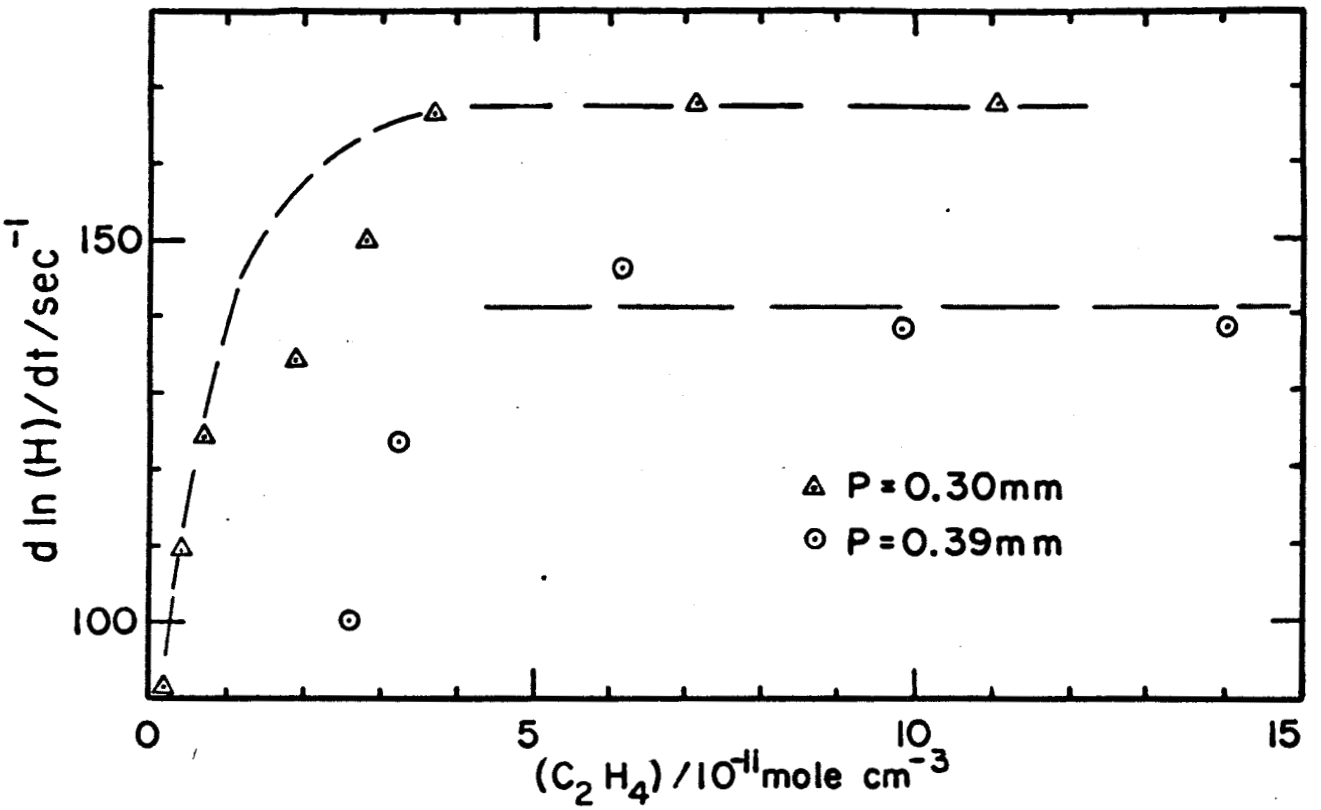

FIG. 35 : ETHYLENE EXPERIMENTS WITH SMALL DIAMETER FLOW TUBE.

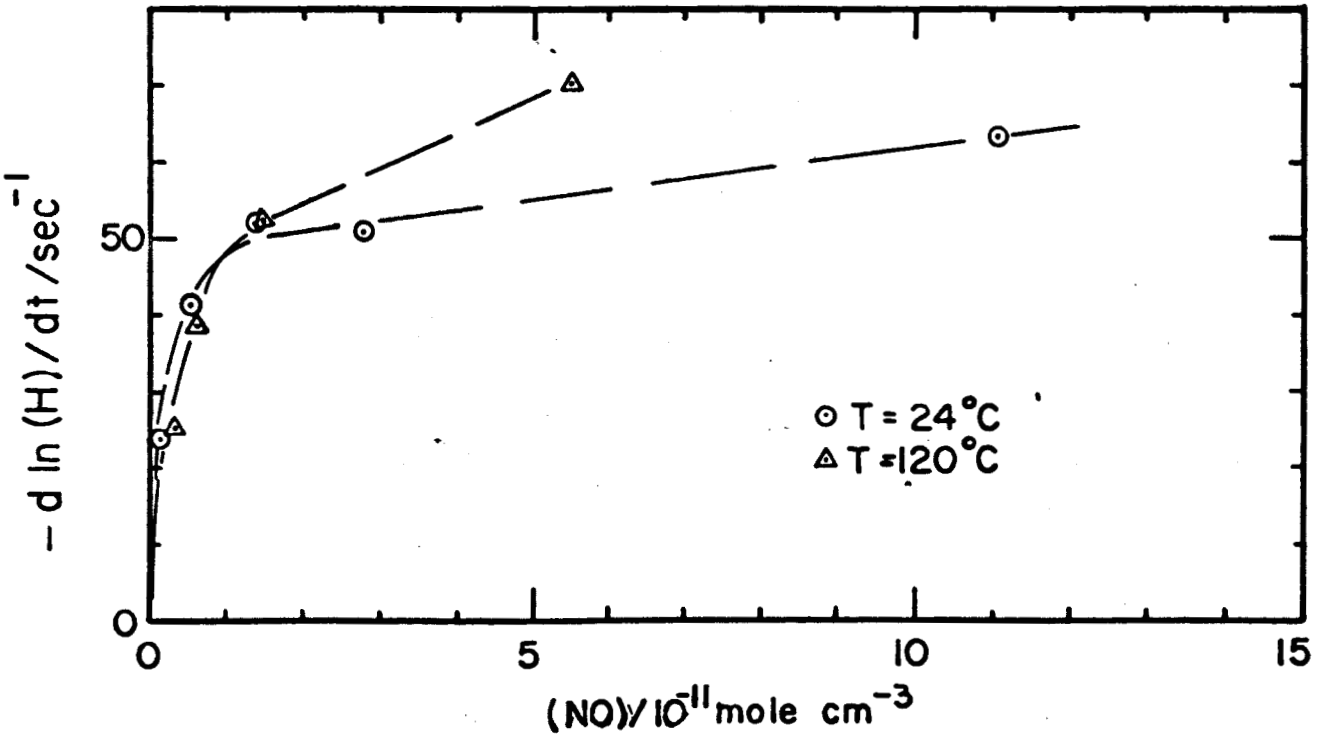

FIG. 36 : NITRIC OXIDE EXPERIMENTS

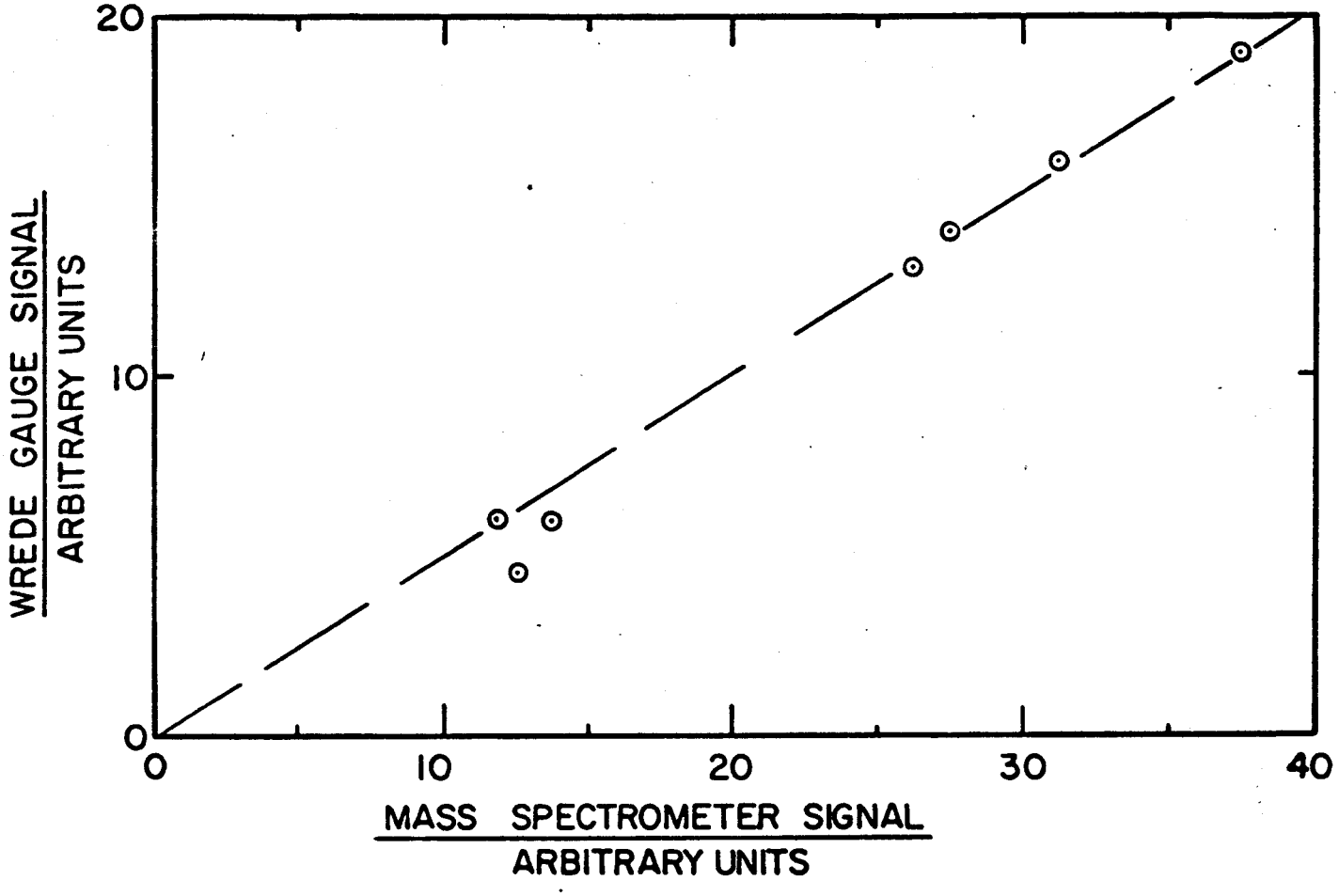

FIG. 37 : CORRELATION BETWEEN WREDE GAUGE AND MASS SPECTROMETER SIGNAL.